NASA TECHNICAL NOTE

NASA TN D-7762

NASA TN D-7762

THE CRYOGENIC WIND-TUNNEL CONCEPT FOR HIGH REYNOLDS NUMBER TESTING

by Robert A. Kilgore, Michael J. Goodyer, Jerry B. Adcock, and Edwin E. Davenport

Langley Research Center
Hampton, Va. 23665

NATIONAL AERONAUTICS AND SPACE ADMINISTRATION • WASHINGTON, D. C. • NOVEMBER 1974

1. Report No.	2. Government Accession No.	3. Recipient's Catalog No.
NASA TN D-7762		

4. Title and Subtitle	5. Report Date
THE CRYOGENIC WIND-TUNNEL CONCEPT FOR HIGH REYNOLDS NUMBER TESTING	November 1974
	6. Performing Organization Code

7. Author(s)	8. Performing Organization Report No.
Robert A. Kilgore, Michael J. Goodyer, Jerry B. Adcock, and Edwin E. Davenport	L-9396
	10. Work Unit No. 501-06-09-05
9. Performing Organization Name and Address	11. Contract or Grant No.
NASA Langley Research Center Hampton, Va. 23665	
	13. Type of Report and Period Covered
12. Sponsoring Agency Name and Address	Technical Note
National Aeronautics and Space Administration Washington, D.C. 20546	14. Sponsoring Agency Code

15. Supplementary Notes

Michael J. Goodyer is lecturer in the Department of Aeronautics and Astronautics, the University of Southampton, England.

16. Abstract

Theoretical considerations indicate that cooling the wind-tunnel test gas to cryogenic temperatures will provide a large increase in Reynolds number with no increase in dynamic pressure while reducing the tunnel drive-power requirements. Studies have been made to determine the expected variations of Reynolds number and other parameters over wide ranges of Mach number, pressure, and temperature, with due regard to avoiding liquefaction. The range of test conditions available in a cryogenic pressure tunnel will allow the independent determination of the effects of Reynolds number, aeroelasticity, and Mach number on the aerodynamic characteristics of a model. Practical operational procedures have been developed in a low-speed cryogenic tunnel. Aerodynamic experiments in the facility have demonstrated the theoretically predicted variations in Reynolds number and drive power. Whereas most types of wind tunnels could operate with advantage at cryogenic temperatures, the continuous-flow fan-driven tunnel is particularly well suited to take full advantage of operating at cryogenic temperatures.

17. Key Words (Suggested by Author(s))	18. Distribution Statement
Wind tunnels Reynolds number Cryogenic	Unclassified – Unlimited STAR Category 11

19. Security Classif. (of this report)	20. Security Classif. (of this page)	21. No. of Pages	22. Price*
Unclassified	Unclassified	94	$4.00

*For sale by the National Technical Information Service, Springfield, Virginia 22151

CONTENTS

THE CRYOGENIC WIND-TUNNEL CONCEPT FOR HIGH REYNOLDS NUMBER TESTING

By Robert A. Kilgore, Michael J. Goodyer,*
Jerry B. Adcock, and Edwin E. Davenport
Langley Research Center

SUMMARY

A theoretical investigation published by Smelt in 1945 indicated that the use of air at temperatures in the cryogenic range, that is, below about 172 K (-150° F), would permit large reductions of wind-tunnel size and power requirements in achieving a given Reynolds number. Lack of suitable cooling techniques and suitable structural materials precluded application of this cryogenic wind-tunnel concept at the time of Smelt's work. Because of the recent advances in cryogenic engineering and structural materials and the current interest, both in this country and in Europe, in the development of high Reynolds number transonic tunnels, a program has been initiated recently at the NASA Langley Research Center to extend the analysis of Smelt and to study the feasibility of the cryogenic wind-tunnel concept.

The results of this work indicate that cryogenic subsonic, transonic, and supersonic wind tunnels offer significant increases of test Reynolds number without increases of aerodynamic load. As a result of the decreased velocity of sound as temperature is lowered, the drive-power requirements for cryogenic tunnels are considerably lower than for normal tunnels. The range of test conditions available in a cryogenic pressure tunnel will allow the independent determination of the effects of Reynolds number, aeroelasticity, and Mach number on the aerodynamic characteristics of a model.

Experiments performed at the Langley Research Center in a low-speed continuous-flow cryogenic tunnel have demonstrated the predicted changes in Reynolds number, drive power, and fan speed with temperature, while operating with nitrogen as the test gas. The experiments have also demonstrated that cooling to cryogenic temperatures by spraying liquid nitrogen directly into the tunnel circuit is practical and that tunnel temperature can be controlled within close limits. A water-jacketed strain-gage balance has demonstrated satisfactory operation in the low-speed cryogenic tunnel.

Based on the current theoretical and low-speed experimental study, the cryogenic concept appears very promising. Since the most useful application presently envisioned

*Lecturer, Department of Aeronautics and Astronautics, The University of Southampton, England.

for the cryogenic concept is at transonic speeds, the experimental studies are being extended to include the design and operation of a modest-size cryogenic continuous-flow transonic tunnel capable of operating at moderate pressure to provide further firm design data and additional engineering and operational experience.

INTRODUCTION

The discovery during the development of high-speed subsonic transports that the flow simulation provided by existing wind tunnels was inadequate, coupled with present interest in the development of transports and maneuvering aircraft to operate efficiently in the transonic range, has resulted in a review of the problems of flow simulation in transonic wind tunnels. Among the more serious problems is that related to inadequate test Reynolds number, and it is this problem and an attractive solution to the problem that is the subject of this paper.

The need for increased testing capability in terms of Reynolds number has been well documented, for example, references 1 and 2. A major problem is that of scale effect on boundary-layer shock-wave interaction. Not only is aircraft performance affected by the interaction, but other characteristics such as loads and load distribution, stability, buffeting, and maneuverability are also affected.

The possibility of simulating high values of Reynolds number in existing wind tunnels has not been overlooked, and many devices for causing boundary-layer transition are in use in the various aeronautical laboratories. However, as noted in reference 3, fixing the location of boundary-layer transition is in itself seldom sufficient to duplicate the flow associated with full-scale Reynolds number.

Recognition of such problems has resulted in a consensus, both in the United States and in Europe, that there is an urgent need for wind tunnels having greatly increased Reynolds number capability. The need is especially acute at transonic speeds where, because of the large power requirements of transonic tunnels, economic forces have dictated the use of relatively small tunnels. With ever increasing aircraft size, the existing transonic tunnels are becoming even more inadequate in test Reynolds number capability.

The inadequate Reynolds number capability of existing tunnels was the underlying theme of many of the papers presented at a fluid dynamics panel specialists' meeting held at Göttingen, Germany in 1971. One of the fundamental difficulties is to define the level of Reynolds number which is required for valid transonic testing, and this was discussed in several papers during that meeting (see refs. 4 and 5). As a result of these studies, several proposals (refs. 3, 6, and 7) were made at the Göttingen meeting for new wind-tunnel facilities which would be capable of providing a Reynolds number at transonic

speeds of at least 40×10^6, based on the mean geometric chord of a typical swept-wing aircraft, which is considerably greater than existing wind-tunnel capability.

At a given Mach number, the Reynolds number may be increased by using a heavy gas rather than air as the test gas, by increasing the size of the tunnel and model, by increasing the operating pressure of the tunnel, and by reducing the test temperature. The method chosen to increase Reynolds number will, in general, also affect dynamic pressure, mass flow rate, and the power consumption of the tunnel per unit of run time. The use of a heavy gas is a well-known method of achieving high Reynolds number. Freon-12 is one of the most suitable of the heavy gases for use in a wind tunnel (see ref. 8). However, as reported in reference 9, the differences in the ratio of specific heats become important when compressibility effects become significant, thus making Freon-12 a questionable transonic test medium. The more common approaches of increased size and increased stagnation pressures involve serious problems related to such questions as construction and operating costs, model and support loads (see ref. 10), and the possibility of providing continuous-flow capability. The fourth method, that of reduced test temperature, appears to offer an attractive solution to the preceding problems and is the subject of this paper.

In reference 11, a theoretical investigation by Smelt in 1945 indicated that the use of air at temperatures in the cryogenic range, that is, below about 172 K (-150° F), would permit large reductions of wind-tunnel size and power requirements in comparison with a wind tunnel operated at normal temperature and at the same pressure, Mach number, and Reynolds number. The lack of a practical means of cooling a wind tunnel to cryogenic temperatures and the unavailability of suitable structural materials precluded application of this cryogenic wind-tunnel concept at the time of Smelt's work. The first practical application of the cryogenic concept appears to be a low temperature test rig for centrifugal compressors, as reported by Rush in reference 12, which used an air–liquid-nitrogen heat exchanger. The advances which have been made in recent years in the field of cryogenic engineering and structural materials have been such that a cryogenic wind tunnel now appears practical and should be given serious consideration. Therefore, following a theoretical investigation started in October 1971 and aimed at extending the analysis of Smelt, an experimental program was initiated at the Langley Research Center with the objective of verifying some of the theoretical predictions and of exposing and solving the practical problems associated with the use of a cryogenic wind tunnel. Limited portions of the theoretical and experimental results of this program, as well as suggestions for the exploitation of the benefits afforded by the cryogenic wind-tunnel concept, were reported in reference 13. The present report contains much of the basic material presented in reference 13, corrected, however, to account properly for the real-gas characteristics of the test gas at cryogenic temperatures. This report also contains some additional low-speed experimental results and additional information

with respect to the expanded testing capability which can be realized in a pressure tunnel capable of cryogenic as well as normal temperature operation.

SYMBOLS

Measurements and calculations were made in the U.S. Customary Units; however, with the exception of pressure, they are presented herein in the International System of Units (SI). Details concerning the use of SI units, together with physical constants and conversion factors, are given in reference 14.

a	speed of sound, m/s
A	cross-sectional area of test section, m^2
c,k	constants
$\bar{c}$	mean geometric chord, m
C	any aerodynamic coefficient
C_D	drag coefficient, $\frac{\text{Drag}}{qS}$
C_L	lift coefficient, $\frac{\text{Lift}}{qS}$
C_m	pitching-moment coefficient, $\frac{\text{Pitching moment}}{qS\bar{c}}$
ℓ	linear dimension of model or test section, m
m	molecular weight
$\dot{m}$	mass flow rate, kg/s
M	Mach number
M_L	local Mach number
p	pressure, atm (1 atm = 101.3 kN/m^2)

P	drive power, W
q	dynamic pressure, $\rho V^2/2$, N/m^2
Q	ratio defined in equation (12)
R	Reynolds number, $\rho V \ell / \mu$
$R_{\bar{c}}$	Reynolds number based on $\bar{c}$
$\mathcal{R}$	universal gas constant, $J\text{-}mol^{-1}\text{-}K^{-1}$
S	reference wing area, m^2
t	time
T	temperature, K
u	local velocity in boundary layer at height y, m/s
V	velocity, m/s
x	distance from leading edge of flat plate, m
y	height above surface of flat plate, m
Z	compressibility factor
α	angle of incidence, deg
γ	ratio of specific heats
δ	total thickness of boundary layer, m
η	tunnel power factor
η'	efficiency of drive motor
μ	viscosity, $N\text{-}s/m^2$

ρ density, kg/m^3

σ mass of liquid nitrogen required to cool unit mass of material through given temperature range

Subscripts:

a air

BL boundary layer

e effective

F Freon-12

max maximum

min minimum

t stagnation conditions

TS test section

x based on x

1 upstream

2 downstream

∞ free stream

METHODS FOR INCREASING REYNOLDS NUMBER

In comparison of methods for increasing test Reynolds number, in all cases except perhaps in tests at low subsonic speeds, it is proper to adopt a value of test Mach number which is representative of the range required from the tunnel. For transonic testing, therefore, any proposed method of increasing Reynolds number has to exclude contributions from a change of Mach number. At a fixed but representative Mach number, the Reynolds number of model tests in a wind tunnel may be increased, relative to some datum value in air, either by using a heavy test gas or mixtures of gases other than air,

by increasing the size of the tunnel and model, by increasing the operating pressure of the tunnel, or by reducing the test temperature. The method chosen to increase Reynolds number will, in general, also affect dynamic pressure, mass flow rate, and drive power. Expressions are presented for Reynolds number, dynamic pressure, mass flow rate, and drive power which allow comparisons to be made between the various methods of increasing Reynolds number. Although simplifying assumptions have been used in the analysis, the resulting expressions represent, with reasonable fidelity, the trends in Reynolds number, dynamic pressure, mass flow rate, and drive power which result from changes in tunnel size or the properties of the test gas. Comparisons are made between the various methods of increasing Reynolds number, but with the assumption of a constant temperature of the test gas. Additional comparisons are made in a later section where the use of low test temperature is introduced as a method for increasing test Reynolds number.

BASIC RELATIONS

Reynolds Number

Reynolds number R is defined as

$$R = \frac{\rho V \ell}{\mu} \tag{1}$$

The equation of state for a perfect gas is $\rho = \frac{mp}{\mathcal{R}T}$. The Mach number M is given by $M = \frac{V}{a}$. For a perfect gas,

$$V = Ma = M\sqrt{\gamma \frac{\mathcal{R}}{m} T}$$

Upon substitution of V and ρ into equation (1),

$$R = \frac{pM\ell}{\mu}\sqrt{\frac{m\gamma}{\mathcal{R}T}} \tag{2}$$

It is convenient to compare the various techniques in terms of stagnation rather than static values; therefore, equation (2) is now modified to allow stagnation values to appear by first invoking the usual static-to-stagnation temperature and pressure expressions for isentropic flow of a perfect gas

$$\frac{T}{T_t} = \frac{2}{2 + (\gamma - 1)M^2}$$

and

$$\frac{p}{p_t} = \left[\frac{2}{2 + (\gamma - 1)M^2}\right]^{\frac{\gamma}{\gamma-1}}$$

where the subscript t denotes stagnation conditions. For the range of M and γ under consideration, these ratios are relatively weak functions of γ; therefore, for simplicity without appreciable error, $\frac{p}{p_t}$ and $\frac{T}{T_t}$ are assumed constant for a given Mach number. Also, for any given gas, μ is a function of temperature alone, to the first order. Since μ has been found to vary as a power of T, little error is introduced in the following analysis by making the simplifying assumption that $\mu \propto \mu_t$ for a given Mach number. This simplifying assumption is used only in developing the approximate functional relationships which follow. Later calculations presented in this paper use more exact relations for viscosity which take into account the variation of viscosity with pressure as well as temperature. Hence, following the assumption of constant Mach number for the purposes of comparison, equation (2) may be rewritten in the form

$$R \propto \frac{p_t \ell}{\mu_t}\sqrt{\frac{m\gamma}{T_t}} \tag{3}$$

Dynamic Pressure

Dynamic pressure is defined as

$$q = \frac{1}{2}\rho V^2 \tag{4}$$

Upon substitution of ρ and V for constant Mach number, equation (4) becomes

$$q \propto \gamma p_t \tag{5}$$

Mass Flow

The mass flow rate is given in terms of flow conditions in the test section by

$$\dot{m} = \rho V A_e$$

where A_e is the stream tube area required to pass the mass flow at test-section values of ρ and V. At constant Mach number, it is assumed that the ratio of effective area

A_e to the geometrical flow area A remains sensibly constant. Thus, the expression for mass flow rate can be written

$$\dot{m} \propto p_t A \sqrt{\frac{m\gamma}{T_t}} \tag{6}$$

Drive Power

The ratio of the power input to the fan to the rate of flow of kinetic energy in the test-section free stream is usually defined as the power factor η. Thus,

$$P = \eta q V A \tag{7}$$

For a given tunnel geometry, η is primarily a function of Mach number and a weak function of Reynolds number. For constant Mach number and neglecting as insignificant the variation of η with Reynolds number, equation (7) becomes

$$P \propto \gamma^{3/2} A p_t \sqrt{\frac{T_t}{m}} \tag{8}$$

The expressions derived for Reynolds number (eq. (3)), dynamic pressure (eq. (5)), mass flow rate (eq. (6)), and power (eq. (8)) are given in table I which shows the terms through which these parameters are influenced by changes in test gas, tunnel size, stagnation pressure, and stagnation temperature; constant Mach number is assumed. For the case where stagnation temperature is the independent variable, the simplifying assumption is made that, for any given gas over the limited range of temperatures of interest, $\mu \propto \mu_t \propto T_t^{0.9}$. For the case where tunnel size is the variable, it is assumed that $A \propto \ell^2$.

TABLE I.- INFLUENCE OF TEST GAS, TUNNEL SIZE, STAGNATION PRESSURE, AND STAGNATION TEMPERATURE ON REYNOLDS NUMBER, DYNAMIC PRESSURE, MASS FLOW RATE, AND DRIVE POWER WITH CONSTANT TEST MACH NUMBER

Property / Variable	$R \propto \frac{p_t \ell}{\mu_t}\sqrt{\frac{m\gamma}{T_t}}$	$q \propto \gamma p_t$	$\dot{m} \propto p_t A \sqrt{\frac{m\gamma}{T_t}}$	$P \propto \gamma^{3/2} A p_t \sqrt{\frac{T_t}{m}}$
Test gas	$\frac{\sqrt{m\gamma}}{\mu_t}$	γ	$\sqrt{m\gamma}$	$\frac{\gamma^{3/2}}{\sqrt{m}}$
Tunnel size, ℓ	ℓ	---	ℓ^2	ℓ^2
Stagnation pressure, p_t	p_t	p_t	p_t	p_t
Stagnation temperature, T_t	$\frac{1}{T_t^{1.4}}$	---	$\frac{1}{\sqrt{T_t}}$	$\sqrt{T_t}$

USING A HEAVY GAS

The use of a heavy gas is a well-known method of achieving high Reynolds number. After toxic gases and gases having high condensation temperatures have been eliminated, one of the most suitable of those remaining is Freon-12 (CCl_2F_2) which has been used with good results in subsonic tests. The relations in table I may be used to assess the changes in R, q, $\dot{m}$, and P when Freon-12 rather than air is used as the test gas. The relevant properties of Freon-12 compared with those of air are as follows:

Molecular weight,

$$m_F \approx 4.17 m_a$$

Ratio of specific heats,

$$\gamma_F \approx 0.81 \gamma_a$$

Viscosity,

$$\mu_F \approx 0.69 \mu_a$$

If tunnel size, stagnation pressure, and stagnation temperature are assumed constant, these values, when used with the expressions of table I, give the following:

$$R_F \approx 2.66 R_a$$

$$q_F \approx 0.81 q_a$$

$$\dot{m}_F \approx 1.84 \dot{m}_a$$

$$P_F \approx 0.36 P_a$$

Thus, the use of Freon-12, rather than air, as a test gas can result in a significant increase in test Reynolds number while reducing both dynamic pressure and drive power. However, the ratio of specific heats γ for Freon-12 is considerably different from that for air ($\gamma = 1.40$ and $\gamma = 1.13$ for air and Freon-12, respectively, at standard conditions). Apparently, the consequences of this are small in subsonic flow; and where effects do exist, there are techniques for correcting wind-tunnel data. However, as reported in reference 9, data obtained in Freon-12 do not agree with data obtained in air when compressibility effects become significant.

An important example of the differences between the behavior of Freon-12 and air is the pressure change in a shock wave. The relation between the static pressure upstream and downstream of a shock wave normal to the stream is given by

$$\frac{p_2}{p_1} = \frac{2\gamma}{\gamma + 1} M_1^2 - \frac{\gamma - 1}{\gamma + 1}$$

The ratio of the pressure rise across the shock, $\Delta p = p_2 - p_1$, to upstream static pressure is

$$\frac{\Delta p}{p_1} = \frac{p_2 - p_1}{p_1} = \frac{p_2}{p_1} - 1$$

or

$$\frac{\Delta p}{p_1} = \frac{2\gamma}{\gamma + 1}\left(M_1^2 - 1\right)$$

For the same values of upstream Mach number and static pressure, the ratio $\frac{\Delta p}{p_1}$ is 10 percent higher in air than in Freon-12 because of the difference in γ. In flow fields in which the stability of the position of the shock is sensitive to the interaction between the shock wave and boundary layer, significant differences could exist in the shock position and, hence, in the aerodynamic data between tests made in air and Freon-12.

Mixtures of gases can be chosen which offer advantages over air, while maintaining γ for the mixture close to that for air; one such mixture is Freon-12 with argon. But, it has been shown in reference 15 that the advantages in wind-tunnel design that would result from the use of this mixture would be relatively small.

INCREASING SIZE

One of the most straightforward methods of increasing test Reynolds number is to increase the size of the model. However, if ℓ is taken to be a measure of model linear dimension, the test-section area A must increase as ℓ^2 if tunnel-wall interference effects are to be kept constant. Assuming a given test gas and holding stagnation pressure and stagnation temperature constant, the expressions of table I show that Reynolds number increases linearly with increasing size, dynamic pressure is independent of size, and both mass flow rate and drive power increase as the square of the size.

The increases in capital investment and operating cost are serious problems associated with this method of increasing Reynolds number. In addition, the cost of models as well as the cost of modifying models during a test program increases with model size.

INCREASING PRESSURE

From the relations shown in table I it can be seen that Reynolds number, dynamic pressure, mass flow rate, and power all increase linearly with increasing pressure. From the point of view of capital and operating cost, it is therefore better to increase Reynolds number by increasing pressure rather than by increasing size. However, the accompanying increase in dynamic pressure will produce, in relation to a low pressure

tunnel, increases in balance and model loads and stresses, reductions in test lift-coefficient capability, increases in support sting interference and aft fuselage distortion, and a reduced stress margin for use in aeroelastic matching. At transonic speeds, as noted in reference 10, stagnation pressures in excess of about 5 atm are not practical for development type testing of large aspect-ratio models due to excessive wing deformation. If in the order of 5 atm is a practical upper limit on stagnation pressure, then a test section about 6 by 6 m (20 by 20 ft) will be required to provide a Reynolds number at Mach 1 of 40×10^6. Thus, even at a stagnation pressure of 5 atm, a very large tunnel is required to meet current Reynolds number requirements. The combination of high pressures and large size would make such a tunnel very costly to build and to operate.

REDUCING TEST TEMPERATURE

As can be seen from the expressions given in table I, Reynolds number, mass flow rate, and drive power are all functions of stagnation temperature. Based on these simple relationships, it is seen that Reynolds number can be increased by reducing stagnation temperature while actually reducing the drive-power requirement. In the following section, the implications and limitations of increasing Reynolds number by reducing test temperature are examined and the use of low test temperatures in tunnels of modest size and operating at modest pressure is studied as an alternative approach to the traditional methods of increasing Reynolds number.

DISCUSSION OF CRYOGENIC WIND-TUNNEL CONCEPT

The use of low temperatures in wind tunnels was first proposed by Smelt in reference 11 as a means of reducing tunnel drive-power requirements at constant values of test Mach number, Reynolds number, and pressure. Studies have been made which show that a significant increase in Reynolds number may be realized at Mach numbers up to about 3 by operating at cryogenic temperatures. In this section the changes in Reynolds number, dynamic pressure, test-section mass flow rate, and tunnel drive power due to changes in temperature are described. Consideration is then given to the limits on the minimum operating temperatures which may be set by condensation and by real-gas effects. Finally, in relation to the alternative methods which are available, some of the advantages of increasing Reynolds number by the use of low test temperatures are described.

EFFECTS OF REDUCING TEMPERATURE

The relations presented in table I are again used to illustrate the effect of reducing test temperature in a given gas with constant values of tunnel size, stagnation pressure, and Mach number.

For comparison purposes, it is assumed that the test gas is air. A stagnation temperature for normal tunnels of 322 K (120° F) is here assumed as a datum. Figure 1 shows the variation of several flow parameters in the tunnel test section as the stagnation temperature is reduced from this datum. For this figure, values of viscosity over the range of temperatures were obtained from reference 16. With decreasing temperature, viscosity is reduced and density is increased; because of a reduction in the speed of sound with decreasing temperature and the assumption of constant test-section Mach number, the velocity is reduced.

Reynolds Number

The effect of the changes in the flow parameters is a variation in Reynolds number approximately in accordance with the relation

$$R \propto \frac{1}{T_t^{1.4}}$$

Even though the more precise values of viscosity from reference 16 were used instead of the exponential approximation, figure 1 shows that the relative variation of viscosity with stagnation temperature T_t is a weak function of the assumed Mach number and, therefore, the relative change of Reynolds number with temperature is also a weak function of Mach number. Curves are shown for several free-stream Mach numbers.

Dynamic Pressure

At a fixed Mach number the aerodynamic loads on the model are a strong function of dynamic pressure but, in general, only a weak function of Reynolds number. Under these conditions, the stresses and deflections within a model, as noted in reference 17, vary in direct proportion to dynamic pressure. From table I it is seen that as the test temperature is reduced there is no change in dynamic pressure. Therefore, by reducing temperature, an increase in Reynolds number is achieved without increase in aerodynamic loads except as introduced by the effect of Reynolds number on the aerodynamic coefficient. Note that changes of aerodynamic loading from this source are common, by

definition, to all methods of increasing Reynolds number and are normally second-order effects. Problems that might arise from aeroelastic distortion of the model or its supports due to increase of dynamic pressure therefore do not arise, in contrast with the case of increasing Reynolds number by increasing stagnation pressure. This constant dynamic pressure feature of the cryogenic tunnel is extremely important, particularly with regard to isolating Reynolds number effects from aeroelastic effects as will be discussed more fully in the section entitled "Operating Envelopes." An increase in Reynolds number is therefore achieved with lower aerodynamic loads compared with the same increase achieved by increasing pressure. Some advantages associated with the reduced loads include reduced support interference and a reduction in the severity of afterbody modification, both of which arise from the need for a smaller size of sting.

Alternatively, or additionally, the reduced loads could allow an increase in the load-limited maximum lift coefficient or allow the model to be designed for improved aeroelastic matching.

Mass Flow

For constant values of tunnel size, stagnation pressure, and Mach number, test-section mass flow rate increases with decreasing temperature in accordance with the relation

$$\dot{m} \propto \sqrt{\frac{1}{T_t}}$$

Thus, for example, when operating at temperatures near 100 K, the mass flow rate is increased by a factor of about 1.8 over the mass flow rate at ambient conditions. For certain modes of cryogenic operation of blowdown or injector-driven tunnels considered in appendix A, the increase in mass flow rate will reduce run time when operating from a fixed size of air storage tank. In general, however, the increase of mass flow rate is of no consequence.

Drive Power

For constant values of tunnel size and stagnation pressure, the relation between drive power and temperature is

$$P \propto \sqrt{T_t}$$

The variations of drive power, as Reynolds number is increased from the datum (322 K), is shown in figure 2 for the three methods of increasing Reynolds number in air. If Reynolds number is increased just by enlarging the wind tunnel and model, power will increase as the square of the size, curve A. If Reynolds number is increased just by increasing the stagnation pressure, power will increase in direct proportion to the

increase in pressure, curve B. However, as Reynolds number is increased by means of a reduction of test temperature in a particular size of wind tunnel, the drive power is reduced, curve C.

OPERATIONAL LIMITS SET BY SATURATION AND OTHER REAL-GAS EFFECTS

Saturation Boundary

The minimum stagnation temperature which can conceivably be used in a cryogenic wind tunnel depends on several factors. It has been assumed that liquefaction must be avoided under the most adverse conditions to be met on the model. The test gas is most likely to begin to condense in localized low-pressure regions adjacent to the model. The local pressures, in turn, depend on the shape and orientation of the model and on the test Mach number and stagnation pressure. In order to compute likely conditions in these regions, variations of maximum local Mach number $M_{L,max}$ with free-stream Mach number M_∞ have been assumed and are shown in figure 3. The curves shown in this figure were constructed from inspections of pressure distributions over typical wing sections. In order to compute the minimum temperatures that may be utilized, the assumptions have been made that the test gas expands isentropically as an ideal gas from the tunnel settling chamber through to the localized high Mach number regions and that the saturation boundary for the test gas should not be crossed. It is believed that some of these assumptions are biased toward the conservative. In addition, the maximum local Mach numbers shown in figure 3 may be higher than those realized in many tests.

Testing in Air

Using the saturated vapor pressure data for air from reference 16, the minimum usable stagnation temperatures have been calculated for a range of Mach numbers and stagnation pressures. The minimum stagnation temperature is assumed to be that value which results in the gas just reaching the saturation boundary at the local static conditions at $M_{L,max}$. The results are shown in figure 4 for Mach number $M_{L,max}$ up to 2 and stagnation pressures up to 7 atm.

Figure 5 illustrates the restrictions which are imposed on stagnation temperature when testing in a sonic free stream. The restrictions are set by the gas reaching the saturation boundary at three different values of local Mach number M_L for various values of stagnation pressure. At a given stagnation pressure, the Reynolds number which can be obtained is reduced as the maximum local Mach number $M_{L,max}$ is increased since the saturation boundary and thus the possibility of liquefaction is determined by the local values of temperature and pressure rather than the free-stream values. The range of local Mach number shown in this figure covers the range of maximum

values likely to be met on any model at $M_\infty = 1.0$. With a knowledge of the maximum local Mach number expected or achieved during a test, the permissible test conditions are well defined and any possibility of liquefaction of the test gas can easily be avoided.

For sonic tests in a cryogenic wind tunnel using air as the test gas, the permissible minimum stagnation temperature T_t and the Reynolds number relative to datum (T_t = 322 K (120° F)) are given in the following table for stagnation pressures p_t up to 5 atm. (The stagnation temperatures have been chosen such that the saturation boundary is reached at $M_{L,max} = 1.4$.)

p_t, atm	T_t, K	R relative to datum
1	98.7	5.33
2	107.3	4.71
3	112.3	4.40
4	116.0	4.20
5	119.0	4.04

As can be seen, cryogenic operation is effective in increasing Reynolds number even at elevated pressures. Thus, where tunnel size is restricted or where economies in drive power are required, Reynolds number can be increased by combining the advantages of cryogenic operation with moderate increases in pressure.

Testing in Nitrogen

Using the vapor pressure data for nitrogen from reference 18, the minimum stagnation temperatures which can be used to avoid condensation by the same criteria but with nitrogen as the test gas have been calculated. The results are shown in figure 6 for maximum local Mach numbers up to 2 and stagnation pressures up to 7 atm.

The following table for sonic test in nitrogen (based on the same assumptions as the table for air) shows the permissible minimum operating temperatures and relative Reynolds number in nitrogen:

p_t, atm	T_t, K	R relative to datum
1	95.7	5.59
2	102.5	5.05
3	107.0	4.75
4	110.4	4.53
5	113.3	4.37

As can be seen by comparing these two tables, lower test temperatures can be used for nitrogen than for air because the saturation temperature of nitrogen is lower than that for air. In addition to the increased Reynolds number available in nitrogen, there are other advantages to using nitrogen rather than air as the test gas.

Real-Gas Effects

At cryogenic temperatures, the test gas can no longer be considered to be an ideal gas even at moderate pressures because both thermal and caloric imperfections are present. For example, at 4 atm and 100 K the compressibility factor $Z = \frac{pm}{\rho \mathcal{R} T}$ for air is about 0.915 and the ratio of specific heats γ is about 1.53, rather than the constant ideal gas values of $Z = 1$ and $\gamma = 1.4$. Thus, in considering the increase of Reynolds number by the use of reduced temperatures, the consequence of these departures of the test gas from ideal-gas behavior must be considered.

In reference 13 some tentative restrictions were placed on the lowest temperature which might be used in testing because γ departed from the ideal diatomic gas value of 1.4 and this departure was expected to affect the static pressure rise across a shock. However, subsequent studies have been made which show that the restrictions of reference 13 are not necessary and that, for operating pressures up to 5 atm, the lowest operating temperatures are determined only by liquefaction considerations.

The present study examined the consequence of real-gas effects on both isentropic flow and the flow across a normal shock for nitrogen over a wide range of temperatures and pressures. The various ratios which describe the flows were calculated using the real-gas properties of nitrogen and were compared with ratios derived by using ideal-gas equations and by using constant (ideal) values of $Z = 1.0$ and $\gamma = 1.4$. The results show that for stagnation pressures up to about 5 atm, the real-gas ratios differ from the ideal-gas ratios by a maximum of about 0.4 percent. For example, for $M_\infty = 1.7$, the static pressure rise across a shock in cryogenic nitrogen relative to the ideal diatomic gas static pressure rise for $p_t = 1.0$ atm and $T_t = 103$ K is 0.9990 while for $p_t = 5.0$ atm and $T_t = 123$ K the ratio is 0.9963.

Thus, for most purposes, it would appear satisfactory to adopt ideal-gas equations in the analysis of wind-tunnel test data taken in a cryogenic nitrogen wind tunnel at any stagnation pressure up to about 5 atm.

NITROGEN AS COOLANT AND TEST GAS

Recent advances in cryogenic technology and the availability of liquid nitrogen in large quantities at low cost have eliminated many of the problems of cooling the tunnel and test gas to cryogenic temperatures which formerly existed. Evaporating liquid

nitrogen offers an attractive alternative to mechanical refrigeration of the tunnel and test gas. Once the use of nitrogen as the test gas is accepted, the particularly simple cooling technique is available of injecting and evaporating liquid nitrogen inside the tunnel circuit. As might be expected, the properties of air and nitrogen are similar since air is about 78-percent nitrogen by volume.

The increased Reynolds number capability of the cryogenic nitrogen tunnel over tunnels using air at conventional temperatures is illustrated by use of figures 7 and 8. Figure 7 shows the operating temperatures that have been assumed for the tunnels. For the cryogenic nitrogen tunnel, the temperature has been set by the saturation boundary based on the operating pressure and the typical local maximum Mach number curve of figure 3. The Reynolds number increase due to the lower temperatures is shown in figure 8. From subsonic to near sonic Mach numbers, the Reynolds number of the cryogenic tunnel is from 4 to 6 times greater, depending on the total pressure. At a supersonic Mach number of 3, this increase factor has dropped to about 2. If supersaturation is permissible, the operating temperatures shown in figure 7 can be lowered with corresponding increase in the test Reynolds number.

CRYOGENIC OPERATION OF VARIOUS TYPES OF TUNNELS

As far as can be seen at this time, cryogenic operation might be used with advantage in most types of wind tunnels with the obvious exceptions of tunnels operating at hypersonic speeds. Brief comments are given in appendix A concerning the application of the cryogenic concept to several types of intermittent nonfan-driven tunnels. In this section, consideration is given to the cryogenic operation of continuous-flow fan-driven tunnels.

When run times greater than those available in intermittent tunnels are required for a particular testing procedure, some form of continuous or semicontinuous tunnel must be used. Also, where the amount of testing is large, the high productivity of a continuous-flow tunnel is essential even for those types of test capable of being made in intermittent tunnels. As previously noted, high Reynolds number tunnels capable of continuous running at normal temperatures and moderate pressures are large, and thereby costly, and make heavy demands on power. Because of the large reduction in tunnel size (and thereby cost) and drive power made possible by operating at cryogenic temperatures, the feasibility of a high Reynolds number continuous-flow fan-driven tunnel, with all of its attendant advantages, is enhanced.

As with any wind-tunnel concept, details of tunnel design and operating capability will vary greatly depending upon the main purpose for which a particular tunnel is built. For the purpose of this brief illustration, two possible continuous-flow fan-driven

cryogenic nitrogen tunnels are compared with their noncryogenic counterparts at the same Reynolds number and Mach number in order to illustrate the impact of cryogenic operation on tunnel size and drive-power requirements.

Low-Speed Testing ($M_\infty = 0.35$)

At a stagnation pressure of 1 atm, the cryogenic tunnel would be 20 percent of the size and would require 2 percent of the drive power of a conventional tunnel.

Sonic Testing ($M_\infty = 1.00$)

At a stagnation pressure of 3 atm, the cryogenic tunnel would be 23 percent of the size and would require 3 percent of the drive power of a conventional tunnel.

The reduction of capital outlay which is implied by the preceding figures, coupled with the avoidance of problems associated with high model loads, convenience, high productivity, and the low operating cost per data point of such continuous-flow tunnels, has prompted further consideration of the closed-circuit continuous-flow cryogenic tunnel for the attainment of high Reynolds number. Therefore, a low-speed continuous-flow cryogenic tunnel has been constructed at the NASA Langley Research Center and will be described in the following sections.

LOW-SPEED CRYOGENIC TUNNEL EXPERIMENT

DESCRIPTION OF THE LOW-SPEED TUNNEL AND GENERAL OPERATING CHARACTERISTICS

The low-speed tunnel was a single-return fan-driven tunnel with a 17.8- by 27.9-cm (7- by 11-in.) closed-throat test section. The atmospheric tunnel could be operated at Mach number from near 0 to 0.2 over a temperature range from 333 K (140° F) to 80 K (-316° F). The low-speed tunnel was adapted from an existing $\frac{1}{24}$-scale model of the Langley V/STOL tunnel and was therefore aerodynamically representative of modern low-speed tunnel practice.

A sketch of the low-speed tunnel circuit is shown in figure 9. A photograph of the tunnel being insulated is shown in figure 10, and a photograph of the insulated tunnel and test apparatus is shown in figure 11. Materials of construction included wood, plywood, Plexiglas, mild and stainless steels, aluminum, brass, copper, and fiber glass reinforced plastic. The fan blades were made of laminated wood.

Viewing ports were provided to allow inspection of key areas of the tunnel circuit including the test section, spray zones, corner vanes, screen section, and contraction

section. The viewing ports consisted of either three or four layers of Plexiglas separated by air gaps. Thermal insulation for the remainder of the circuit was a 7.6-cm to 10.2-cm (3-in. to 4-in.) layer of expanded polystyrene applied to the outside of the tunnel structure with a 0.0127-cm-thick (0.005-in.) polyethylene vapor barrier on the outside. Some details of a typical section of insulation and a viewing port are shown in figure 12.

The expanded polystyrene thermal insulation proved adequate and kept the outside of the tunnel warm and dry even in areas of minimum thickness (7.6 cm). The viewing ports as originally designed consisted of only two layers of Plexiglas and would fog over after a few minutes of tunnel operation at cryogenic temperatures. A second design added a third piece of Plexiglas and allowed a continuous flow of ambient-temperature nitrogen between the two outer layers. While this approach proved satisfactory for the smaller viewing ports, a very high nitrogen flow rate was needed to keep the larger viewing ports clear for even 5 or 10 minutes of cryogenic operation. The final design, illustrated in figure 12, consisted of four layers of Plexiglas separated by air gaps. This system, which was completely passive in that no ambient-temperature nitrogen was used, allowed clear viewing even after as much as an hour of cryogenic operation except under very humid room air conditions when moisture would condense on the outer Plexiglas surface.

Prior to cooling the tunnel, it was necessary to remove any moisture from the tunnel circuit in order to avoid the formation of frost on the model and those parts of the tunnel which cooled down first such as the screens and turning vanes. Most of the moisture was removed during a prerun purging of the tunnel at ambient temperature. The drive fan was used during the prerun purge to keep a slight circulation in the tunnel while gaseous nitrogen was injected into the tunnel. The nitrogen gas displaced the oxygen, water vapor, and other gases which were exhausted along with the excess nitrogen gas to the atmosphere through a duct leading from the tunnel circuit. The test gas was therefore nitrogen. Any moisture remaining in the circuit was removed by freezing it out of the stream on a cryopanel located against the tunnel wall in the low-speed end of the return leg of the circuit. The cryopanel was a 0.28 m^2 (3.0 ft^2) sheet of copper to which was brazed a coil of 1.27-cm-diameter (0.5-in.) copper tubing. By passing liquid nitrogen through the tubing, the temperature of the cryopanel was held near 77 K (-320° F) which caused any moisture in the tunnel circuit to condense and remain on the cryopanel as frost.

The tunnel was cooled and the heat of compression added to the stream by the drive fan was removed by spraying liquid nitrogen at about 77 K (-320° F) directly into the tunnel circuit in either of the two locations shown in figure 9. Complete evaporation of the liquid nitrogen was achieved down to the lowest temperature explored of 80 K (-316° F).

The liquid nitrogen was injected into the tunnel circuit through very simple spray bars consisting of copper pipes with narrow slots. Two of the types used are sketched in figure 13. The liquid pressure was measured near the spray bars. The differential injection pressure ranged from near zero at the low flow rates to about 0.70 atm at the high flow rates.

The rate of cooling of the tunnel circuit was such that, for example, a temperature of 116 K (-250° F) could be stabilized within 10 minutes of the initiation of cooling from room temperature. The tunnel was operated at temperatures from 333 K (140° F) to 80 K (-316° F). The lower temperature is very close to the saturation temperature of nitrogen of 77.4 K (-320.4° F) at 1 atm. At 80 K the Reynolds number is increased by a factor of about 7 over that achieved at normal tunnel temperatures and the same Mach number. Approximately 40 hr of tunnel operation were at cryogenic temperatures, that is, below 172 K (-150° F). At the reference station in the test section, the test temperature was held to within about ±1 K (±2° F) by automatic on-off control of one or more of the nitrogen injection nozzles. Much closer temperature control was achieved by injecting a slight excess of liquid nitrogen and establishing temperature equilibrium at the desired test temperature by modulating the heat input from a simple wire-grid electrical heater which was built into the tunnel in the low-speed end of the return leg of the circuit. Using this technique, test temperatures within about ±0.2 K (±0.4° F) of the mean could be maintained.

The gas temperature in the test section was measured with an aspirated copper-constantan thermocouple probe. The probe was mounted such that it could be traversed along a horizontal line passing across the test section and through its center line. The thermocouple and its recording meter were carefully calibrated at the tunnel site between room temperature and liquid-nitrogen temperature and could resolve about 0.2 K at liquid-nitrogen temperature. With this system it was not possible to detect any temperature variation across the test section at any operating temperature.

The tunnel was instrumented to measure temperatures and pressure around the circuit, dewpoint (or frost point) of the test gas, oxygen content of the test gas, and drive-motor speed and power.

EXPERIMENTAL RESULTS

Drive Power and Fan Speed

The low-speed tunnel was powered by a water-jacketed fan motor which was mounted in a nacelle in the return leg of the circuit. The fan motor was rated at 10 hp, but due to frequency limitations of the generating system which powered the fan motor, the maximum power was limited to about 2.46 kW (3.3 hp).

No practical problems were encountered with the drive motor or fan blades. The theoretical variation of drive power with increase of Reynolds number above the value at room temperature for constant Mach number previously presented in figure 2 is shown in figure 14 along with the measured power variations taken with nitrogen in the cryogenic tunnel at $M_\infty \approx 0.1$. The different coefficients of expansion of the materials used to build the low-speed tunnel caused gaps to open up around the tunnel circuit as the operating temperature was reduced. At the lowest operating temperatures many of the gaps were as wide as 1.27 cm (0.5 in.). The additional circuit losses caused by these gaps are thought to have caused the measured values of drive power to be greater than the predicted values.

The velocities of the gas around the circuit are a function of test-section Mach number and temperature. Fan rotational speed is roughly proportional to gas velocity, and at a particular Mach number the gas velocity is proportional to the speed of sound which, in turn, is proportional to the square root of the gas temperature. The theoretical and measured variations of fan speed with Mach number and temperature are shown in figure 15. The fan speed varied roughly as predicted by theory, that is, proportional to Mach number at constant temperature and proportional to the square root of temperature at constant Mach number. The higher than theoretically predicted fan speeds observed at lower temperatures might also have been caused by demands for higher values of drive power and fan pressure ratio caused by the gaps which opened up around the tunnel circuit at the lower operating temperatures.

Boundary-Layer Experiment

An experiment was devised to demonstrate the changes of Reynolds number that accompany changes of conditions in the test section. Clearly, an aerodynamic experiment was required in which there would be a change in some measurable aerodynamic parameter solely due to change of Reynolds number. Further, the change in the measured parameter should be reasonably sensitive to and vary predictably with Reynolds number. It was decided to install a simple boundary-layer experiment in which the variation of a measure of boundary-layer thickness with Reynolds number would be compared with theory. It was decided to make measurements in a laminar boundary layer since boundary-layer thickness δ varies as $R_x^{-1/2}$ for a laminar boundary layer but only approximately as $R_x^{-1/5}$ for a turbulent boundary layer.

A small diameter pitot tube (0.0330-cm o.d. and 0.0165-cm i.d.) was mounted as a Preston tube against a flat plate in the test section. The pitot tube was mounted at a fixed position 3.261 cm (1.284 in.) from the rounded leading edge of the plate. The longitudinal location of the pitot tube was such that it would lie in the laminar portion of

the boundary layer over a wide range of conditions in the test section. A sketch of the experimental arrangement is shown in figure 16.

In the tunnel, Reynolds number was varied by temperature or by M_∞. Changes in the ratio of the dynamic head at the pitot tube to the free-stream dynamic head indicate changes in boundary-layer thickness and Reynolds number. The zero pressure gradient form of the Pohlhausen laminar boundary-layer velocity profile (see ref. 19) was adopted in order to allow a curve to be fitted to data taken with the tunnel running warm which eliminated the need to estimate effective values for x and y from the geometry of the plate and pitot tube. The form is

$$\frac{u}{u_\infty} = 2\frac{y}{\delta}\left[1 - \left(\frac{y}{\delta}\right)^2 + \frac{1}{2}\left(\frac{y}{\delta}\right)^3\right] \tag{9}$$

where

$$\delta = \frac{cx}{\sqrt{R_x}} \tag{10}$$

$$R_x = \frac{\rho u_\infty x}{\mu} \tag{11}$$

All of the tests were carried out at low Mach number; hence

$$\frac{q_{BL}}{q_\infty} = Q = \left(\frac{u}{u_\infty}\right)^2 \tag{12}$$

where q_{BL} is the dynamic pressure in the boundary layer and q_∞ is the free-stream dynamic pressure. From equation (9),

$$Q = 4\left(\frac{y}{\delta}\right)^2\left[1 - 2\left(\frac{y}{\delta}\right)^2 + \left(\frac{y}{\delta}\right)^3 + \left(\frac{y}{\delta}\right)^4 - \left(\frac{y}{\delta}\right)^5 + \frac{1}{4}\left(\frac{y}{\delta}\right)^6\right] \tag{13}$$

where

$$\frac{y}{\delta} = \frac{y}{cx}\sqrt{R_x} \tag{14}$$

For the present experiment, x, y, and c are constant, thus Q depends only on unit Reynolds number. Therefore Q should be the same for all combinations of Mach number and temperature for which unit Reynolds number is constant. Equation (14) can be rewritten as

$$\frac{y}{\delta} = \frac{y}{c\sqrt{x}}\sqrt{\frac{\rho a}{\mu}}\sqrt{M} = \sqrt{kM} \tag{15}$$

where, for the present experiment at low M and constant stagnation pressure, k is a function only of T_t. From equations (15) and (13),

$$Q = 4kM\left[1 - 2kM + (kM)^{1.5} + (kM)^2 - (kM)^{2.5} + \frac{1}{4}(kM)^3\right] \tag{16}$$

With this expression the independent effects of M and T_t on Q can be readily predicted since k is proportional to $\frac{\rho a}{\mu}$. The value of k for which equation (16) produced a best fit to the data taken at $T_t = 322$ K was found to be 0.64. Predicted variations of Q with M for other temperatures were then obtained from equation (16) using

$$k = 0.64 \frac{\left(\frac{\rho a}{\mu}\right)_{T_t}}{\left(\frac{\rho a}{\mu}\right)_{T=322\ K}}$$

and the curves thus obtained are plotted in figure 17.

The experimental data at 227.6 K are in good agreement with the theoretical curve, and the data at the two lower temperatures are in fair agreement. The experimental data were a confirmation of the magnitude of the theoretical predictions of the increase of Reynolds number with M_∞ at constant temperature, but, more importantly, a first experimental confirmation of the increases of Reynolds number with decreasing temperature at constant M_∞.

Strain-Gage Balance Experiment

In order to determine if conventional techniques might be used to make force and moment measurements at cryogenic temperatures, a 11.4-cm (4.5-in.) span sharp leading-edge 74° delta-wing model was tested on an existing water-jacketed strain-gage balance in the cryogenic tunnel. Since the purpose of this test was to investigate any possible adverse effects of temperature on the measuring techniques rather than the effects of Reynolds number on the model, a sharp leading-edge 74° delta-wing model was chosen since it is known that, except for the usual effects of friction drag, the aerodynamic characteristics of this shape are relatively insensitive to Reynolds number. A sketch of the model is shown in figure 18 and a photograph of the model, balance, and supporting sting is presented in figure 19. The strain-gage elements of the balance were heated and insulated from the cryogenic environment by a water jacket through which was circulated water at approximately 294 K (70° F). A quadrant allowed model incidence to be changed from -4° to 22°. A sketch of the model support mechanism is shown in figure 20.

Some of the aerodynamic test results are presented in figure 21 as the variation of C_m, C_L, and C_D with α for various test conditions. As can be seen, there is good

agreement between the data obtained at stagnation temperatures from 322 K (120° F) to 111 K (-260° F). Based on the results of these tests, there appear to be no fundamental or practical difficulties in obtaining force and moment data in a cryogenic tunnel using conventional strain-gage balance techniques.

ANTICIPATED CHARACTERISTICS OF CONTINUOUS-FLOW FAN-DRIVEN HIGH REYNOLDS NUMBER CRYOGENIC TUNNELS

As noted in the introduction, it is widely recognized both in the United States and in Europe that there is an urgent need for wind tunnels capable of testing models at near full-scale Reynolds number. Because of the large power requirements of transonic tunnels, economic forces have dictated the use of relatively small transonic tunnels. With ever increasing aircraft size, existing transonic tunnels are becoming even more inadequate in test Reynolds number capability. Because of this, a high Reynolds number transonic tunnel is at present generally considered to be one of the most urgent needs. Therefore, in this section, performance charts, anticipated design features, and anticipated operational characterisitics are presented for continuous-flow fan-driven closed-circuit pressure tunnels capable of transonic operation at cryogenic temperatures. Although the information was produced specifically for low speed and transonic fan-driven tunnels, much of the material is general in nature and is therefore applicable to supersonic cryogenic fan-driven tunnels as well as to nonfan-driven tunnels such as those described in appendix A.

PERFORMANCE CHARTS

Performance charts for continuous-flow cryogenic tunnels using nitrogen as the test gas have been prepared which show the variation of Reynolds number and drive power with test-section size and stagnation pressure for free-stream Mach numbers of 0.35, 0.70, 1.00, and 1.20.

Basic Assumptions

Reynolds Number

Reynolds number is based on mean geometric chord $\bar{c}$, where $\bar{c}$ is taken to be one-tenth of the square root of the test-section area. The Reynolds number calculations were based on the real-gas properties of the test gas. However, certain simplifying assumptions were made so that the majority of the calculations could be made on a relatively small digital computer. Comparisons with calculations made by using exact

relations show the errors introduced by the simplifying assumptions to be generally less than two-tenths of 1 percent and are considered to be negligible.

Minimum Stagnation Temperature

As previously discussed, the values of minimum stagnation temperatures were dictated by consideration of avoiding liquefaction of the test gas under the local conditions of temperature and pressure determined by isentropic expansion to an assumed maximum local Mach number, $M_{L,max}$. Three values assumed were:

(1) $M_{L,max}$ = Free-stream Mach number M_∞

(2) $M_{L,max}$ = Typical maximum local Mach number (see fig. 3)

(3) $M_{L,max}$ = High maximum local Mach number (see fig. 3)

The minimum stagnation temperatures dictated by these assumed restrictions on $M_{L,max}$ can be found from the curves presented in figure 6.

Drive Power

Drive power was calculated from the equation

$$P = \frac{qVA\eta}{\eta'}$$

where q is the dynamic pressure in the test section, V is the velocity in the test section, A is the cross-sectional area of the test section, η is the tunnel power factor, and η' is the efficiency of the drive motor. The values of η and η' used for these calculations are based on measured values in some typical transonic tunnels at the Langley Research Center. The values used in the following examples are

M_∞	η	η'
0.35	0.150	0.59
.70	.124	.80
1.00	.130	.90
1.20	.113	.90

The values given for drive power represent the power input to the fan drive motor in a transonic tunnel utilizing an auxiliary plenum-air removal system at supersonic speeds. The values given for $M_\infty = 1.20$ do not include any power which might be required for plenum-air removal since the amount of power used for this purpose is a strong function of tunnel design.

As an example of the additional power which must be allowed for plenum-air removal at $M_\infty = 1.20$, the case of a tunnel design requiring the removal of 3 percent of the total mass flow $\dot{m}_{TS}$ has been considered. With an assumed stagnation pressure of 2.5 atm, about 1.6 percent of $\dot{m}_{TS}$ must be vented to the atmosphere because this amount is continuously added to the tunnel circuit to absorb the heat added to the circuit by the drive fan and plenum-air removal system. The remaining 1.4 percent of $\dot{m}_{TS}$ is pumped back into the tunnel circuit. Under the conditions assumed, the power required for this plenum pumping amounts to about 17 percent of the power allowed for the main drive fan.

The performance charts for free-stream Mach numbers of 0.35, 0.70, 1.00, and 1.20 are presented in figures 22 to 25.

Tabulated values of minimum stagnation temperature and other conditions relating to the performance charts are given in tables II to V.

Examples of Use of Performance Charts

Examples for free-stream Mach numbers of 0.35 and 1.00 are presented in the following sections in order to illustrate the use of the charts and to illustrate the reduction in size and drive power made possible by operation at cryogenic temperatures.

Low-Speed Testing ($M_\infty = 0.35$)

The charts for a Mach number of 0.35 are presented in figure 22. For subsonic wind-tunnel research, operation at less than full-scale Reynolds numbers often appears adequate, as suggested, for example, in reference 20. For the purposes of this example, therefore, it is assumed that a fairly modest Reynolds number of 15×10^6 based on $\bar{c}$ is desired in a 3- by 3-m (9.84- by 9.84-ft) test section. The maximum local Mach number on the model is assumed to be equal to the typical maximum value of 0.88 (see fig. 3). At these local conditions the gas-liquid saturation boundary is just reached. In figure 22(b) the value of a 3- by 3-m test section intersects $R_{\bar{c}} = 15 \times 10^6$ to indicate operation at a stagnation pressure of about 1.16 atm for a drive power of 1.37 MW (1830 hp). At these test conditions, table II indicates operation with nitrogen at a stagnation temperature of about 85.9 K (-305° F). In comparison it should be noted that a conventional tunnel operating at 300 K (80° F) and at the same stagnation pressure, 1.16 atm, and the same Reynolds number, $R_{\bar{c}} = 15 \times 10^6$, would require a 17.4- by 17.4-m (57.2- by 57.2-ft) test section with a drive power of about 88 MW (118 000 hp). Alternatively, in a conventional tunnel operating at 300 K with the same size test section (3- by 3-m), the same Reynolds number would require operation at a stagnation pressure of 6.8 atm with a drive power of about 15 MW (20 000 hp).

TABLE II.- ASSUMED OPERATING CONDITIONS RELATED TO A CRYOGENIC NITROGEN TUNNEL AT A FREE-STREAM MACH NUMBER OF 0.35

Stagnation pressure, p_t, atm	Minimum stagnation temperature, $T_{t,min}$, K	Reynolds number per meter, millions	Reynolds number factor (a)	Dynamic pressure, q, kN/m^2	Free-stream static pressure, p_∞, atm	Free-stream static temperature, T_∞, K	Compressibility factor under free-stream conditions, Z_∞	Ratio of specific heats under free-stream conditions, γ_∞
Maximum local Mach number = 0.35								
1.00	78.5	49.3	6.5	8.0	.92	76.6	.958	1.452
1.25	80.5	59.4	6.5	10.0	1.15	78.6	.951	1.462
1.50	82.2	69.2	6.2	12.0	1.38	80.2	.944	1.472
1.75	83.6	78.7	6.2	14.0	1.61	81.6	.938	1.481
2.00	85.0	87.8	6.0	16.0	1.84	83.0	.932	1.490
2.50	87.3	105.6	5.8	20.0	2.30	85.2	.920	1.508
3.00	89.3	122.6	5.6	23.9	2.76	87.2	.910	1.526
3.50	91.0	139.2	5.4	27.9	3.22	88.8	.900	1.543
4.00	92.6	155.1	5.3	31.9	3.68	90.4	.891	1.560
5.00	95.4	185.7	5.1	39.9	4.59	93.1	.874	1.593
Maximum local Mach number = 0.88								
1.00	84.6	44.0	5.8	8.0	.92	82.6	.967	1.442
1.25	86.6	53.1	5.8	10.0	1.15	84.5	.961	1.450
1.50	88.3	61.9	5.5	12.0	1.38	86.2	.956	1.458
1.75	89.8	70.4	5.5	14.0	1.61	87.7	.951	1.465
2.00	91.2	78.7	5.3	16.0	1.84	89.0	.946	1.473
2.50	93.5	94.8	5.1	20.0	2.30	91.3	.937	1.487
3.00	95.5	110.2	5.0	23.9	2.76	93.2	.928	1.501
3.50	97.3	125.1	4.8	27.9	3.22	95.0	.920	1.515
4.00	98.9	139.6	4.7	31.9	3.68	96.5	.913	1.529
5.00	101.7	167.4	4.5	39.9	4.59	99.3	.899	1.555
Maximum local Mach number = 1.42								
1.00	96.2	36.2	4.8	8.0	.92	93.9	.978	1.428
1.25	98.2	43.9	4.8	10.0	1.15	95.9	.974	1.434
1.50	100.0	51.3	4.6	12.0	1.38	97.6	.970	1.439
1.75	101.6	58.4	4.6	14.0	1.61	99.2	.967	1.445
2.00	102.9	65.5	4.4	16.0	1.84	100.4	.963	1.450
2.50	105.4	79.0	4.3	20.0	2.30	102.9	.957	1.460
3.00	107.4	92.1	4.2	23.9	2.76	104.8	.951	1.470
3.50	109.3	104.7	4.0	27.9	3.22	106.7	.946	1.479
4.00	110.9	117.1	4.0	31.9	3.68	108.2	.940	1.488
5.00	113.8	140.7	3.8	39.9	4.59	111.1	.930	1.507

[a]Reynolds number obtained at minimum stagnation temperature divided by Reynolds number obtained at typical stagnation temperature of 300 K (80° F).

TABLE III.- ASSUMED OPERATING CONDITIONS RELATED TO A CRYOGENIC NITROGEN TUNNEL AT A FREE-STREAM MACH NUMBER OF 0.70

Stagnation pressure, p_t, atm	Minimum stagnation temperature, $T_{t,min}$, K	Reynolds number per meter, millions	Reynolds number factor (a)	Dynamic pressure, q, kN/m^2	Free-stream static pressure, p_∞, atm	Free-stream static temperature, T_∞, K	Compressibility factor under free-stream conditions, Z_∞	Ratio of specific heats under free-stream conditions, γ_∞
Maximum local Mach number = 0.70								
1.00	82.1	80.2	6.6	25.1	.72	74.8	.965	1.443
1.25	84.0	97.0	6.4	31.3	.90	76.5	.959	1.452
1.50	85.7	113.0	6.3	37.6	1.08	78.1	.953	1.459
1.75	87.2	128.5	6.0	43.8	1.26	79.4	.948	1.467
2.00	88.5	143.7	5.9	50.1	1.44	80.6	.942	1.475
2.50	90.8	173.1	5.7	62.6	1.80	82.7	.933	1.489
3.00	92.9	200.9	5.5	75.2	2.16	84.6	.924	1.503
3.50	94.6	228.3	5.4	87.7	2.52	86.2	.915	1.517
4.00	96.3	254.2	5.3	100.2	2.88	87.7	.907	1.530
5.00	99.0	305.3	5.1	125.3	3.61	90.2	.892	1.557
Maximum local Mach number = 1.14								
1.00	89.5	70.3	5.8	25.1	.72	81.5	.973	1.433
1.25	91.5	85.0	5.6	31.3	.90	83.4	.969	1.440
1.50	93.3	99.2	5.5	37.6	1.08	84.9	.964	1.446
1.75	94.8	113.0	5.3	43.8	1.26	86.3	.960	1.452
2.00	96.1	126.5	5.2	50.1	1.44	87.6	.956	1.458
2.50	98.5	152.5	5.0	62.6	1.80	89.7	.948	1.469
3.00	100.6	177.5	4.8	75.2	2.16	91.6	.941	1.480
3.50	102.4	201.7	4.7	87.7	2.52	93.2	.935	1.491
4.00	104.0	225.2	4.6	100.2	2.88	94.6	.928	1.502
5.00	106.8	270.6	4.5	125.3	3.61	97.3	.917	1.523
Maximum local Mach number = 1.52								
1.00	98.8	60.6	5.0	25.1	.72	90.0	.980	1.425
1.25	101.0	73.3	4.8	31.3	.90	92.0	.977	1.430
1.50	102.7	85.7	4.7	37.6	1.08	93.5	.974	1.434
1.75	104.3	97.8	4.6	43.8	1.26	95.0	.970	1.439
2.00	105.7	109.5	4.5	50.1	1.44	96.3	.967	1.443
2.50	108.2	132.2	4.4	62.6	1.80	98.5	.962	1.452
3.00	110.3	154.2	4.2	75.2	2.16	100.5	.956	1.460
3.50	112.1	175.6	4.1	87.7	2.52	102.1	.951	1.468
4.00	113.7	196.4	4.1	100.2	2.88	103.6	.947	1.476
5.00	116.6	236.4	3.9	125.3	3.61	106.2	.938	1.492

[a]Reynolds number obtained at minimum stagnation temperature divided by Reynolds number obtained at typical stagnation temperature of 311 K (100° F).

TABLE IV.- ASSUMED OPERATING CONDITIONS RELATED TO A CRYOGENIC NITROGEN TUNNEL AT A FREE-STREAM MACH NUMBER OF 1.00

Stagnation pressure, p_t, atm	Minimum stagnation temperature, $T_{t,min}$, K	Reynolds number per meter, millions	Reynolds number factor (a)	Dynamic pressure, q, kN/m^2	Free-stream static pressure, p_∞, atm	Free-stream static temperature, T_∞, K	Compressibility factor under free-stream conditions, Z_∞	Ratio of specific heats under free-stream conditions, γ_∞
Maximum local Mach number = 1.00								
1.00	86.7	88.4	6.6	37.5	.53	72.3	.972	1.434
1.25	88.8	106.6	6.3	46.8	.66	74.0	.967	1.441
1.50	90.5	124.4	6.1	56.2	.79	75.4	.962	1.447
1.75	92.0	141.7	5.9	65.6	.92	76.7	.958	1.453
2.00	93.4	158.4	5.8	74.9	1.06	77.8	.954	1.458
2.50	95.7	191.1	5.6	93.7	1.32	79.8	.946	1.470
3.00	97.7	222.4	5.5	112.4	1.59	81.4	.938	1.481
3.50	99.6	252.3	5.3	131.1	1.85	82.0	.932	1.491
4.00	101.2	281.7	5.2	149.9	2.11	84.3	.925	1.501
5.00	104.0	338.5	5.0	187.3	2.64	86.7	.912	1.522
Maximum local Mach number = 1.40								
1.00	95.7	76.0	5.7	37.5	.53	79.7	.979	1.426
1.25	97.8	92.0	5.4	46.8	.66	81.5	.976	1.431
1.50	99.5	107.5	5.3	56.2	.79	82.9	.972	1.435
1.75	101.1	122.6	5.1	65.6	.92	84.2	.969	1.440
2.00	102.5	137.3	5.0	74.9	1.06	85.4	.966	1.444
2.50	104.9	165.8	4.9	93.7	1.32	87.4	.960	1.453
3.00	107.0	193.3	4.8	112.4	1.59	89.1	.954	1.461
3.50	108.8	220.0	4.6	131.1	1.85	90.7	.949	1.469
4.00	110.4	245.9	4.5	149.9	2.11	92.0	.944	1.477
5.00	113.3	295.9	4.4	187.3	2.64	94.4	.934	1.492
Maximum local Mach number = 1.70								
1.00	104.2	66.8	5.0	37.5	.53	86.8	.984	1.420
1.25	106.4	81.0	4.8	46.8	.66	88.7	.981	1.424
1.50	108.2	94.8	4.7	56.2	.79	90.2	.978	1.427
1.75	109.7	108.4	4.5	65.6	.92	91.4	.976	1.431
2.00	111.2	121.4	4.5	74.9	1.06	92.7	.973	1.434
2.50	113.7	146.8	4.3	93.7	1.32	94.8	.969	1.441
3.00	115.8	171.4	4.2	112.4	1.59	96.5	.964	1.448
3.50	117.7	195.2	4.1	131.1	1.85	98.1	.960	1.454
4.00	119.4	218.3	4.0	149.9	2.11	99.5	.956	1.460
5.00	122.3	263.2	3.9	187.3	2.64	101.9	.949	1.472

[a]Reynolds number obtained at minimum stagnation temperature divided by Reynolds number obtained at typical stagnation temperature of 322 K (120° F).

TABLE V.- ASSUMED OPERATING CONDITIONS RELATED TO A CRYOGENIC NITROGEN TUNNEL AT A FREE-STREAM MACH NUMBER OF 1.20

Stagnation pressure, p_t, atm	Minimum stagnation temperature, $T_{t,min}$, K	Reynolds number per meter, millions	Reynolds number factor (a)	Dynamic pressure, q, kN/m^2	Free-stream static pressure, p_∞, atm	Free-stream static temperature, T_∞, K	Compressibility factor under free-stream conditions, Z_∞	Ratio of specific heats under free-stream conditions, γ_∞
Maximum local Mach number = 1.20								
1.00	90.7	86.0	6.1	42.1	.41	70.4	.977	1.428
1.25	92.8	103.9	6.0	52.6	.52	72.1	.973	1.434
1.50	94.6	121.2	5.8	63.2	.62	73.4	.969	1.439
1.75	96.2	137.9	5.6	73.7	.72	74.7	.965	1.443
2.00	97.5	154.5	5.5	84.2	.83	75.7	.961	1.448
2.50	99.9	186.4	5.3	105.3	1.03	77.6	.955	1.457
3.00	102.0	217.0	5.2	126.3	1.24	79.2	.948	1.466
3.50	103.7	247.1	5.2	147.4	1.44	80.5	.942	1.475
4.00	105.4	275.8	4.9	168.5	1.65	81.8	.937	1.483
5.00	108.2	331.8	4.8	210.6	2.06	84.0	.926	1.500
Maximum local Mach number = 1.59								
1.00	100.8	73.2	5.2	42.1	.41	78.4	.983	1.421
1.25	103.0	88.6	5.1	52.6	.52	80.1	.980	1.425
1.50	104.8	103.6	4.9	63.2	.62	81.5	.977	1.429
1.75	106.4	118.3	4.8	73.7	.72	82.8	.974	1.432
2.00	107.8	132.5	4.7	84.2	.83	83.9	.972	1.436
2.50	110.2	160.2	4.6	105.3	1.03	85.8	.967	1.443
3.00	112.4	186.9	4.4	126.3	1.24	87.5	.962	1.449
3.50	114.2	212.9	4.3	147.4	1.44	88.9	.958	1.456
4.00	115.9	238.2	4.3	168.5	1.65	90.2	.953	1.462
5.00	118.7	287.0	4.1	210.6	2.06	92.5	.946	1.474
Maximum local Mach number = 1.85								
1.00	108.9	65.1	4.6	42.1	.41	84.6	.987	1.417
1.25	111.0	79.1	4.5	52.6	.52	86.2	.984	1.420
1.50	113.0	92.5	4.4	63.2	.62	87.7	.982	1.423
1.75	114.5	105.8	4.3	73.7	.72	88.9	.980	1.425
2.00	116.0	118.6	4.3	84.2	.83	90.1	.978	1.429
2.50	118.5	143.6	4.1	105.3	1.03	92.0	.973	1.434
3.00	120.7	167.7	4.0	126.3	1.24	93.7	.970	1.440
3.50	122.6	191.2	3.9	147.4	1.44	95.2	.966	1.445
4.00	124.5	213.5	3.8	168.5	1.65	96.7	.963	1.450
5.00	127.2	258.5	3.7	210.6	2.06	98.8	.956	1.460

[a]Reynolds number obtained at minimum stagnation temperature divided by Reynolds number obtained at typical stagnation temperature of 322 K (120° F).

Sonic Testing ($M_\infty = 1.00$)

The performance charts for a Mach number of 1.00 are given in figure 24. For the purposes of this example it is assumed that a Reynolds number of 40×10^6 based on $\bar{c}$ is desired in a 3- by 3-m test section. The maximum local Mach number on the model is assumed to correspond to the typical maximum value of 1.40 (see fig. 3). It can be seen from figure 24(b) that a stagnation pressure of about 1.93 atm is required in a cryogenic tunnel with a drive power of about 17 MW (23 000 hp). At these test conditions, table IV indicates operation with nitrogen at a stagnation temperature of about 102 K (-276° F).

While a stagnation temperature of 300 K is typical of low-speed testing, most conventional fan-driven transonic pressure tunnels operate at higher temperatures so that smaller heat exchangers can be used in the circuit for cooling. Thus a stagnation temperature of 322 K (120° F) is now assumed for a conventional pressure tunnel to compare with the cryogenic pressure tunnel. At the same stagnation pressure, 1.93 atm, and same Reynolds number, $R_{\bar{c}} = 40 \times 10^6$, a conventional tunnel operating at 322 K would require a 15.2- by 15.2-m (49.9- by 49.9-ft) test section with a drive power of about 805 MW (1 080 000 hp). Alternatively, with a stagnation temperature of 322 K and a 3- by 3-m test section, a Reynolds number of 40×10^6 would require a stagnation pressure of about 9.9 atm and a drive power of about 160 MW (214 000 hp).

From the foregoing examples, it is apparent that operating at cryogenic temperature can significantly decrease the size or operating pressure and drive-power requirements such that a continuous-flow fan-driven tunnel should be given serious consideration for subsonic and transonic high Reynolds number testing. This claim is supported by the existence of many fan-driven transonic tunnels absorbing powers greater than those required by the cryogenic tunnel. The operating cost of the cryogenic tunnel, including the cost of liquid nitrogen to cool down and hold the tunnel cool during a run, is considered in a subsequent section.

ANTICIPATED DESIGN FEATURES AND OPERATIONAL CHARACTERISTICS

The material which is presented in this section is based partly on experience gained with the low-speed cryogenic tunnel and is partly speculative. The techniques are not necessarily the best that can be devised but are included in order to show that such a facility is feasible at this time. Since the most useful application presently envisioned for the cryogenic concept is at transonic speeds, the experimental studies are being extended to include construction and operation of a modest-size cryogenic continuous-flow fan-driven transonic tunnel capable of operating at moderate pressures

to provide further firm design data and additional operational experience. There is much still to be learned, and during the further exploration and development of the cryogenic tunnel concept, new and better ideas will undoubtedly materialize.

Tunnel Circuit

Choice of Structural Material

As reported in reference 21, some common structural materials such as carbon steel have severely reduced impact strength at low temperatures. It is anticipated, therefore, that the cryogenic tunnel circuit would be fabricated from materials such as 9-percent nickel steel or 5058 aluminum alloy that have acceptable structural properties down to 77.4 K (-320.4° F), the temperature of boiling liquid nitrogen at 1 atm. Many different aspects must be considered in deciding on the material of construction. For example, the cool-down requirements are approximately 30 percent less for a tunnel constructed of 9-percent nickel steel compared with a tunnel constructed of aluminum alloy.

Provision must be made for an increased range of thermal expansion depending upon the choice of structural material. The worst case might be operation of the whole of the tunnel pressure vessel at the minimum temperature of the test-gas stream. The change of linear dimension for a 9-percent nickel-steel cryogenic tunnel being operated over a temperature range from a normal operating temperature for fan-driven transonic tunnels of 322 K (120° F) to the minimum temperature of about 77 K (-320° F) would be about 3 times the change of linear dimension for a conventional carbon-steel tunnel subjected to a temperature change from a low winter ambient of 255 K (0° F) to a normal operating temperature of 322 K.

Thermal Insulation

Of the many types of insulation which might be used for a cryogenic tunnel, the expanded foams are perhaps best suited. They are low in initial cost, can be foamed in place or applied in precut shapes, and require no rigid vacuum jacket. Although expanded foams have a higher thermal conductivity than some other insulations, the use of the more effective and costly types of insulation is rarely justified for large ground-based systems operating at liquid-nitrogen temperatures.

The optimum type and location of thermal insulation will vary with the size of the tunnel and the way a particular tunnel will be used. One method which would be suitable for relatively small tunnels would be to place the entire tunnel circuit in an insulated room or building. The main advantages of this technique are that it is simple and allows easy access to the interior and exterior of the tunnel for inspection or modification.

However, for larger tunnels the increase in surface area of the building as the size of the tunnel increases may result in unacceptable liquid-nitrogen usage if the tunnel and building are kept at cryogenic temperatures for extended periods.

A relatively thin layer of insulation might be applied to the inside of a tunnel circuit in the low velocity regions in order to reduce the mass of the tunnel structure to be cooled. Internal insulation would be particularly advantageous for the type of testing which would require several cool-down and warm-up operations each day since both cool-down and warm-up times, as well as liquid-nitrogen consumption, are reduced. An additional nontrivial advantage of certain types of internal insulation would be a reduction in noise within the tunnel circuit. In particular, the inner surface of the plenum surrounding the transonic test section is an ideal location for a combination thermal-insulation sound-absorbing material. Also, control valve and/or compressor noise could be considerably attenuated in tunnels using either passive or active plenum-air removal systems if the pipes were lined on the inside with a suitable insulating sound-absorbing material.

Although the use of internal insulation offers the advantages of reduced cool-down and warm-up times and costs and of reduced circuit noise, there are several disadvantages to internal insulation which must also be considered. One disadvantage is that the size of the pressure shell must be increased if the insulation is internal rather than external. Another disadvantage is related to the desire, if not the requirement, to periodically inspect the tunnel pressure shell. If only a thin layer of internal insulation is used to reduce the cool-down and warm-up times, it may be necessary to have additional external insulation to reduce the heat conduction through the tunnel walls to acceptable levels for tests requiring very long periods at cryogenic temperatures. Inspection of the tunnel pressure shell would be difficult in the areas where insulation was on both sides of the tunnel shell. Another disadvantage to internal insulation in a fan-driven tunnel is the possibility of damage to the fan or other parts of the tunnel as a consequence of some insulation breaking away.

Fan Design

An analysis has been made which indicates that the aerodynamic matching of the drive fan with a wind tunnel operating over a range of temperatures into the cryogenic range is no more involved than for a conventional tunnel. The analysis is presented in appendix B.

Liquid-Nitrogen Injection

Experience with the low-speed tunnel has demonstrated that simple and straightforward liquid-nitrogen injection systems work well. Specifically, neither the location

of the injector nozzles nor the detail design of the nozzles appears to be critical with respect to temperature control or distribution, within the bounds of current experience. The two injector locations which have been used, namely downstream of the test section and downstream of the fan, work equally well. The different types of nozzles which have been used seem to work equally well, and all produced satisfactory temperature distributions regardless of the spray pattern at the nozzle.

The required liquid-nitrogen supply pressure will be dictated by the tunnel operating pressure and by the particular injection scheme used. If a tunnel is to be operated over wide ranges of Mach number and pressure, it may be necessary to have control over separate banks of nozzles in order to have proper control over the wide range of liquid-nitrogen flow rate.

Where possible, a recirculating loop liquid-nitrogen supply system should be used since such a system would reduce supply pipe cool-down time and simplify the control of liquid-nitrogen flow rate by eliminating boiling in the supply pipe during tunnel operation.

Liquid-Nitrogen Requirements

Cool-Down Requirements

The amount of liquid nitrogen required to cool a cryogenic tunnel to its operating condition is a function of the cool-down procedure as well as the insulation and structural characteristics of the tunnel.

Under the idealized assumptions of zero heat conduction through the tunnel insulation and zero heat added to the stream by the fan during the cool-down process, the amount of liquid nitrogen required for cooling the tunnel structure is a minimum when the tunnel is cooled slowly and in such a way that the nitrogen gas leaves the tunnel circuit at a temperature equal to that of the warmest part of the structure being cooled. Again, with the same assumption of zero heat conduction through the tunnel insulation and zero heat added by the fan, and with the additional assumption that all of the liquid nitrogen does, in fact, vaporize, the amount of liquid nitrogen required for cool down is a maximum when only the latent heat of vaporization is used and the nitrogen gas leaves the tunnel circuit at the saturation temperature.

Let σ represent the mass of liquid nitrogen required to cool a unit mass of material through a given temperature range. An analysis using the method of reference 22 gave $\sigma_{min} = 0.26$ and $\sigma_{max} = 0.40$ for cooling a steel structure from 300 K (80° F) to 100 K (-280° F).

Cooling through this large temperature range would not necessarily be a regular occurrence since under some circumstances the tunnel circuit could be allowed to remain

cold between runs. Under these conditions, the heat to be removed before each run would equal the heat gained by the tunnel structure and test gas by conduction through the insulation. By proper design the heat conduction through the insulation can be kept to an acceptably low level.

Running Requirements

The heat to be removed while the tunnel is running consists of the heat conduction through the walls of the tunnel and the heat energy added to the tunnel circuit by the drive fan. As previously noted, the heat conduction can be made relatively small by using reasonable thicknesses of insulation either inside or outside the tunnel structure.

The conditions assumed for the two examples previously given to illustrate the use of the tunnel design charts will now be used to illustrate the amount of liquid nitrogen required to remove the heat added to the tunnel circuit by the drive fan and by conduction through the tunnel walls. The following assumptions are made:

Square test section, m (ft)	3	(9.84)
Tunnel surface area, m^2 (ft^2)	5400	(58 125)
Thermal conductivity of insulation, $\frac{W}{m^2\text{-K/m}}$ $\left(\frac{Btu}{hr\text{-}ft^2\text{-}^oF/ft}\right)$	0.0329	(0.0190)
Insulation thickness, cm (in.)	20	(7.9)

It is assumed that the inner surface of the tunnel is at a temperature equal to the stagnation temperature T_t, that there is zero temperature gradient through the metal pressure shell, and that the outside surface temperature is 300 K (80° F).

It is also assumed that the cooling thermal capacity of the nitrogen is equal to the latent heat together with the sensible heat of the gas phase between the saturation temperature and T_t. The cooling thermal capacity for nitrogen has been calculated based on the above assumptions and is given in figure 26 for a range of final gas conditions.

Low-speed testing ($M_\infty = 0.35$; $R_{\bar{c}} = 15 \times 10^6$).- The earlier low-speed example gave a drive-power requirement of 1.37 MW (1830 hp) and a value of T_t of 85.9 K (-305° F). Under these conditions, the liquid-nitrogen requirement is: 6.55 kg/sec (14.44 lbm/sec) to remove the heat added by the fan and 0.94 kg/sec (2.08 lbm/sec) to remove the heat conducted through the tunnel walls. For this low-speed example, the liquid nitrogen required to remove the heat conducted through the walls amounts to about 12.6 percent of the total running requirement. The total nitrogen requirement of 7.49 kg/sec (16.52 lbm/sec) would cost about 28 cents per second based on a cost of liquid nitrogen of $0.0375 per kilogram ($34 per short ton).

Sonic testing ($M_\infty = 1.00$; $R_{\bar{c}} = 40 \times 10^6$).- The previous sonic example gave a power requirement of 17 MW (23 000 hp) and $T_t = 102$ K (-276° F). Under these conditions the liquid-nitrogen requirements is: 77.23 kg/sec (170.27 lbm/sec) to remove the heat added by the fan and 0.81 kg/sec (1.78 lbm/sec) to remove the heat conducted through the tunnel walls. For this sonic example, the liquid nitrogen required to remove the heat conducted through the walls amounts to about 1 percent of the total running requirement. The total nitrogen requirement of 78.04 kg/sec (172.05 lbm/sec) would cost about $2.92 per second.

Liquid-nitrogen costs will obviously be a significant part of the cost of operating a cryogenic tunnel. However, when operating at the same values of Mach number, Reynolds number, and dynamic pressure, the total cost of operating a cryogenic tunnel could still be less than the cost of operating a conventional tunnel because of the large reduction in tunnel size and drive power made possible by operating at cryogenic temperatures.

Nitrogen Exhaust System

In order to hold stagnation pressure constant, the excess nitrogen gas, which amounts to about 1 percent of the test-section mass flow at sonic speeds, must be discharged from the tunnel circuit. If discharged from a large tunnel into the atmosphere, there would be potential problems associated with fogging, discharge noise, and possible freezing and asphyxiation of personnel and wildlife. Before being discharged, therefore, the excess nitrogen gas should be oxygenated and warmed to a safe level. Both oxygenation and warming can perhaps be achieved by discharging the nitrogen as the driver gas in an ejector which induces ambient air. The resultant mixture would be discharged through a muffler in order to reduce the noise associated with the discharge to an acceptable level. In the case of transonic testing at sufficiently high values of stagnation pressure, the major portion of the discharge might be taken from the test-section plenum chamber, but in other cases it might be taken from the low-speed section of the circuit.

The Model and Balance

It is recognized that incorrect flow simulation may occur if heat transfer takes place between the model and the stream during the test. As noted in reference 23, in wind tunnels where the flow is generated by expansion waves (Ludwieg tube driven tunnel and Evans clean tunnel), the model must be cooled to the expected recovery temperature if spurious scale effects due to heat transfer are to be avoided. Such problems are avoided in a continuous-flow tunnel regardless of the operating temperature since the model is never far from thermal equilibrium with the stream.

It would be desirable to make changes on the model or to rectify faults in the balance without bringing the gas in the tunnel or the tunnel structure up to room temper-

ature. For this purpose, the model and sting could be mechanically removed from the test section into an air lock for warming. The strain-gage balance and pressure transducers probably would be calibrated at room temperature and kept at room temperature by heating while in use in the cryogenic wind tunnel.

The effects of other error sources such as wall interference and model-support interference can often be as important as errors due to incorrect simulation of Reynolds number. Therefore, in order to take full advantage of the correct simulation of Reynolds number afforded by the cryogenic concept, advantage should also be taken in any high Reynolds number tunnel of the emerging technology in the areas of interference-free walls and magnetic model suspension and balance systems. For example, complete elimination of model-support interference and compromise of model shape which are inherent in conventional model-support schemes can be achieved by the use of magnetic model suspension and balance systems as described, for example, in reference 24. In addition, the demonstrated ease and rapidity with which the orientation of the model may be changed with the magnetic suspension system while keeping the model in the center of the test section will facilitate the rapid acquisition of aerodynamic data which may be a necessary feature of any high Reynolds number tunnel.

Operating Envelopes

In addition to the advantages of reduced dynamic pressures and reduced drive-power requirements, the cryogenic tunnel concept offers some unique operating envelopes. For a rigid model at a given orientation, any aerodynamic coefficient C is a function of Mach number M and a function of Reynolds number R. Since no model is truly rigid, the aeroelastic distortion of the model will vary with changing dynamic pressure q. Therefore, any aerodynamic coefficient measured in a wind tunnel is, in fact, a function of dynamic pressure as well as Mach number and Reynolds number; namely,

$$C = f(M,q,R)$$

In a cryogenic tunnel with independent control of temperature, pressure, and Mach number, it is possible to determine independently the effect of Reynolds number, dynamic pressure, and Mach number on the aerodynamic characteristics of the model. Expressed in terms of partial derivatives, this testing ability, which is unique to the pressurized cryogenic tunnel, allows the determination of the pure partial derivatives $\frac{\partial C}{\partial R}$, $\frac{\partial C}{\partial q}$, and $\frac{\partial C}{\partial M}$. In order to illustrate how this is accomplished, envelopes for several modes of operation are presented for a cryogenic transonic pressure tunnel having a 3- by 3-m test section. The main purpose of the envelopes is to illustrate the various modes of operation. However, the size of the tunnel as well as the ranges of temperature, pres-

sure, and Mach number have been selected with some care in order to represent the anticipated characteristics of a future high Reynolds number transonic tunnel.

Constant Mach Number Mode

A typical operating envelope showing the ranges of q and R available for sonic testing is presented in figure 27. The envelope is bounded by the maximum temperature boundary (taken in this example to be 350 K), the minimum temperature boundary (chosen to avoid saturation with $M_{L,max} = 1.40$), the maximum pressure boundary (4.0 atm), the minimum pressure boundary (0.2 atm), and a boundary determined by an assumed maximum available fan drive power (45 MW (60 300 hp)). The arrows indicate typical paths which might be used in determining $\frac{\partial C}{\partial R}$ and $\frac{\partial C}{\partial q}$. With such an operating capability, it is possible, for example, to determine at a constant Mach number the true effect of Reynolds number on the aerodynamic characteristics of the model, $\frac{\partial C}{\partial R}$, without having the results influenced by changes of model shape due to changing dynamic pressure, as is the case in a conventional pressure tunnel. This capability is of particular importance, for example, in research on critical shock boundary-layer interaction effects. Similar envelopes are, of course, available for other Mach numbers.

Constant Reynolds Number Mode

A typical operating envelope is presented in figure 28 which shows the ranges of q and M which are available when testing at a constant Reynolds number of 40×10^6. The same maximum temperature limits, maximum and minimum pressure limits, and fan drive power limits have been assumed as before. The minimum temperatures were never less than those consistent with avoiding saturation under local conditions where the maximum local Mach number corresponded to the typical local Mach number curve of figure 3. The arrows indicate typical paths which might be used to determine $\frac{\partial C}{\partial q}$ and $\frac{\partial C}{\partial M}$. The derivative $\frac{\partial C}{\partial q}$ has been discussed previously. The unique capability associated with $\frac{\partial C}{\partial M}$ allows true Mach number effects to be obtained by eliminating the usual problem introduced by changes of Reynolds number or aeroelastic effects.

Constant Dynamic Pressure Mode

Although the three derivatives have been illustrated previously, an additional form of the envelope is illustrated in figure 29 which shows the range of R and M available at a constant dynamic pressure of 100 kN/m^2 (2088.5 lb/ft^2). The arrows indicate typical paths which might be used in determining $\frac{\partial C}{\partial R}$ and $\frac{\partial C}{\partial M}$. With such an operating capability, it is possible to determine, for example, drag rise with Mach number $\frac{\partial C_D}{\partial M}$ without having the results influenced in any way by Reynolds number or aeroelastic effects.

CONCLUSIONS

A theoretical and experimental program has been initiated at the NASA Langley Research Center in order to study the feasibility of applying the cryogenic concept to a high Reynolds number wind tunnel. The results of this research to date and the conclusions drawn therefrom are as follows:

1. Cryogenic subsonic, transonic, and supersonic wind tunnels offer significant increases in test Reynolds number without increase in aerodynamic loads. For example, in an atmospheric cryogenic wind tunnel, Reynolds number may be increased by a factor of about 7 at low subsonic speeds and by a factor of about 5 at sonic speeds with no increase in dynamic pressure.

2. Once a tunnel size and the required Reynolds number have been established, the use of cryogenic operating temperatures greatly reduces the required tunnel stagnation pressure and, therefore, greatly reduces both the dynamic pressure and tunnel drive power.

3. In a cryogenic tunnel with independent control of temperature, pressure, and Mach number, it is possible to determine independently the effect of Reynolds number, aeroelastic distortion, and Mach number on the aerodynamic characteristics of the model.

4. Whereas most types of tunnels could operate with advantage at cryogenic temperatures, the continuous-flow fan-driven tunnel is particularly well suited to take full advantage of operating at cryogenic temperatures.

5. The saturation boundary is well defined and therefore any possible effects of liquefaction of the test gas can be easily avoided provided that the maximum local Mach number on the model is known.

6. For stagnation pressures up to about 5 atm, the isentropic expansion and the normal shock relations calculated from the real-gas properties of nitrogen differ by a maximum of about 0.4 percent (depending on test conditions) from the corresponding relations calculated from ideal diatomic gas properties and ideal-gas equations. For most purposes it would be satisfactory to adopt ideal-gas equations in the analysis of wind-tunnel data taken in a cryogenic nitrogen tunnel at any stagnation pressure up to about 5 atm.

7. Cooling by injecting liquid nitrogen directly into the tunnel circuit is practical. Test temperature is easily controlled and good temperature distribution obtained by using a simple nitrogen injection system.

8. Conventional strain-gage balances can be used for model testing. A satisfactory arrangement is to maintain the strain-gage balance at ambient temperatures by heating.

9. There is good agreement between theoretical predictions and experimental measurements of the development of laminar boundary layers at cryogenic temperatures.

Langley Research Center,
National Aeronautics and Space Administration,
Hampton, Va., September 24, 1974.

APPENDIX A

CRYOGENIC OPERATION OF VARIOUS TYPES OF NONFAN-DRIVEN TUNNELS

As previously noted in the body of this paper, the benefits of cryogenic operation can be realized with most types of tunnels, with the obvious exception of the hypersonic tunnel. Brief comments are given in appendix A concerning the application of the cryogenic concept to several types of nonfan-driven tunnels.

THE CRYOGENIC LUDWIEG TUBE TUNNEL

Theory of Operation

The operating principle of what has come to be known as the Ludwieg tube tunnel was first suggested by Prof. H. Ludwieg in 1955. The Ludwieg tube tunnel in its simplest form consists of a long supply tube separated from a nozzle and test section by a diaphragm. When the diaphragm is broken, a rearward-facing centered rarefaction fan propagates down the supply tube setting the gas in motion and lowering both the pressure and temperature of the gas.

In reference 25 several useful relationships describing flow conditions are presented for Ludwieg tube tunnels. These relations assumed that the flow in the supply tube is one dimensional and isentropic and that the test gas acts as a perfect gas.

Constant stagnation conditions exist at the entrance to the nozzle during the time required for the head of the incident wave to travel to the closed end of the supply tube, reflect, and return to the nozzle. This time is given by

$$t = \frac{2L}{a_s\left(1 + M_1\right)}\left(1 + \frac{\gamma - 1}{2} M_1\right)^{\frac{\gamma+1}{2(\gamma-1)}} \tag{A1}$$

where t is the time of constant stagnation conditions, a_s is the speed of sound at the initial supply-tube conditions, L is the length of the supply tube, M_1 is the Mach number of the gas leaving the supply tube during the steady run period, and γ is the ratio of specific heats. The stagnation conditions are given by

$$\frac{p_t}{p_s} = \frac{\left(1 + \frac{\gamma - 1}{2} M_1{}^2\right)^{\frac{\gamma}{\gamma-1}}}{\left(1 + \frac{\gamma - 1}{2} M_1\right)^{\frac{2\gamma}{\gamma-1}}} \tag{A2}$$

$$\frac{T_t}{T_s} = \frac{1 + \frac{\gamma - 1}{2} M_1^2}{\left(1 + \frac{\gamma - 1}{2} M_1\right)^2} \tag{A3}$$

where p_t and T_t are stagnation pressure and stagnation temperature, respectively, in the nozzel during the steady run period, p_s is the initial supply-tube pressure, and T_s is the initial supply-tube temperature.

Equations (A1), (A2), and (A3) show that the period of steady flow and the stagnation conditions depend only on the initial storage pressure and temperature in the supply tube, the length of the tube, the ratio of specific heats of the test gas, and the Mach number in the supply tube. This Mach number is, in turn, a function of the ratio of supply-tube cross-sectional area to the nozzle throat area.

If we assume the test gas to be an ideal diatomic gas ($\gamma = 1.4$), equations (A1) to (A3) become

$$t = \frac{2L}{a_s\left(1 + M_1\right)}\left(1 + 0.2M_1\right)^3 \tag{A4}$$

$$\frac{p_t}{p_s} = \frac{\left(1 + 0.2M_1^2\right)^{3.5}}{\left(1 + 0.2M_1\right)^7} \tag{A5}$$

and

$$\frac{T_t}{T_s} = \frac{1 + 0.2M_1^2}{\left(1 + 0.2M_1\right)^2} \tag{A6}$$

Benefits of Cryogenic Operation

In order to illustrate the benefits of cryogenic operation of a Ludwieg tube tunnel, the above equations have been used to determine the time of constant stagnation conditions and the required storage temperature for a range of operating temperatures for a hypothetical Ludwieg tube tunnel using nitrogen as the test gas. The following conditions are assumed:

Square test section, m (ft)	3 (9.84)
Reference chord, $\bar{c}$, m (ft)	0.3 (0.984)
Free-stream Mach number, M_∞	1.00

M_1 . . . . . 0.40
T_t/T_s 0.885
p_t/p_s 0.651
L, m (ft) 500 (1640)
p_t, atm 2.52
p_s, atm 3.87

The lowest stagnation temperature is chosen so that $R_{\bar{c}} = 50 \times 10^6$ (where $R_{\bar{c}}$ is Reynolds number based on reference chord) and the saturation boundary is reached at a Mach number of 1.40. The results are given in table A1.

TABLE A1.- LUDWIEG TUBE TUNNEL USING NITROGEN AS TEST GAS

T_s, K	T_t, K	t, sec	$R_{\bar{c}}$	$\frac{t}{t_{105\,K}}$	$\frac{R_{\bar{c}}}{R_{\bar{c},105\,K}}$
118.7	105.0	4.04	50.0×10^6	1	1
239.0	211.5	2.85	18.1	.71	.36
293.2	259.4	2.57	13.7	.64	.27

The increase in both Reynolds number and the time of constant stagnation conditions as temperature is reduced clearly shows the advantages of cryogenic operation. For example, for the same $R_{\bar{c}}$ and t as in the ambient-temperature Ludwieg tube tunnel, the cryogenic tunnel would require a supply tube that is about 64 percent as long and a test section that is about 27 percent as large in linear dimension.

An analysis presented in reference 7 considers the benefits of cooling a transonic Ludwieg tube tunnel to 239 K (-30° F) and predicts a potential savings of slightly over 30 percent on capital investment for a given Reynolds number. As can be seen in table A1, a storage temperature of 239 K does increase both $R_{\bar{c}}$ and t over ambient-temperature conditions. However, the selected temperature of 239 K apparently comes nowhere near to the realization of the full potential of cryogenic operation.

Operating with nitrogen as the test gas permits the use of slightly lower temperatures than operating with air because of the lower saturation temperature of nitrogen for a given pressure. However, the use of an air-nitrogen mixture might in many cases be a more practical choice of test gas. For example, one very simple method of charging the supply tube with cryogenic gas would be to inject liquid nitrogen directly into the supply tube with the usual compressed air so that the evaporated nitrogen becomes a part of the supply gas. Also, because of the efficiency of this direct method of cooling,

the cost of cooling should be less than the cost of cooling by less direct methods such as the use of nitrogen-air heat exchangers.

The combined effect of the reduction of supply tube volume resulting from cryogenic operation and the use of the direct method of cooling would be to considerably reduce the recharging time. For example, for the same pressure, Mach number, Reynolds number, and run time, and with equal investment in compressors, a cryogenic Ludwieg tube tunnel using the direct method of cooling can make nearly 13 times as many runs as an ambient Ludwieg tube tunnel during the same period of time.

THE CRYOGENIC EVANS CLEAN TUNNEL

Theory of Operation

The Evans clean tunnel (ECT) is under study in England as a possible high Reynolds number wind tunnel. In this type of intermittent wind tunnel, the settling chamber of the conventional tunnel is extended to form a long tube. Air is allowed to settle in this tube before the start of a run. During the run it is pushed through the test section by a piston moving along the tube. The air is than decelerated in a conventional diffuser and returned through a closed circuit to the upstream side of the piston. Opening a valve at the end of the diffuser produces an expansion wave which, by suitable timing, cancels the compression wave due to the acceleration of the piston so that uniform flow is maintained during the travel of the piston along the tube. Thus, virtually all of the air originally contained in the tube passes through the test section at constant stagnation pressure. A complete discussion of the principle of the ECT concept can be found in reference 6.

Benefits of Cryogenic Operation

The use of low temperatures in an ECT driven tunnel results in significant increases in Reynolds number and run time. For sonic testing in a hypothetical ECT we can assume a normal (ambient) operation stagnation pressure of 3 atm and stagnation temperature of 300 K (80° F). If stagnation pressure is held constant, the stagnation temperature can be reduced to 107 K (-267° F) for testing in nitrogen while reaching the saturation boundary at a maximum local Mach number of 1.40. The reduction in temperature increases Reynolds number by a factor of 4.32 and increases run time by a factor of 1.71. Piston velocity is reduced by 42 percent.

An alternative approach to the exploitation of low temperatures with the ECT might be to achieve the same Reynolds number and run time as in the normal-temperature ECT. In this case, the diameter and the length of the cryogenic ECT would be 23 and 58 percent, respectively, of that for the normal-temperature ECT. These figures are comparable with those for the cryogenic Ludwieg tube tunnel.

THE CRYOGENIC BLOWDOWN TUNNEL

The cryogenic mode of operation appears applicable to the blowdown tunnel. Prior to a run, the model would have to be precooled to the desired operating temperature.

One possible method of testing would be to pass dry air from a high pressure supply through a precooled metal heat exchanger having sufficient thermal inertia to insure that the temperature of the air remains relatively constant in the test section during a run. A second and more efficient method of operating a cryogenic blowdown tunnel would be to store air at ambient temperature T_s, precool the test section and model, and during a run hold a constant test temperature by injecting and evaporating liquid nitrogen in the region of the settling chamber. In this case the test-section mass flow is given by

$$\dot{m}_{TS} = \dot{m}_a + \dot{m}_{LN_2} \tag{A7}$$

where

$\dot{m}$ mass flow rate

TS test section

a air

LN_2 liquid nitrogen

The energy balance in the mixing process requires that

$$\dot{m}_a C_p \Delta T = \dot{m}_{LN_2} \beta \tag{A8}$$

where C_p is the specific heat of air, β is the cooling capacity of LN_2 (see fig. 26), and

$$\Delta T = T_s - T_t$$

Solving equations (A7) and (A8) for $\dot{m}_{LN_2}$ gives

$$\dot{m}_{LN_2} = \frac{\dot{m}_{TS} C_p \Delta T}{\beta + C_p \Delta T} \tag{A9}$$

In order to illustrate this second method of cryogenic operation of a blowdown tunnel, equations (A7) to (A9) have been used to determine the mass flow rates of both the

air from storage and the liquid nitrogen used as coolant for a hypothetical blowdown tunnel over a range of operating temperatures. Reynolds number based on $\bar{c}$ has been calculated for each temperature. The following conditions are assumed: 3- by 3-m (9.84- by 9.84-ft) test section, $\bar{c}$ = 0.3 m (0.984 ft), M = 1.00, p_t = 2.7 atm, and T_s = 288 K. The lowest stagnation temperature is chosen so that $R_{\bar{c}} = 50 \times 10^6$ and the saturation boundary of the air-nitrogen mixture is reached at a Mach number of 1.40. The results are given in table A2.

TABLE A2.- BLOWDOWN TUNNEL USING AIR-NITROGEN MIXTURE AS TEST GAS

T_t, K	Mass flow rate, kg/sec			$R_{\bar{c}}$	$\frac{R_{\bar{c}}}{R_{\bar{c},110\,K}}$
	Test section	Air	LN_2		
110	9502	5276	4226	50.0×10^6	1
150	8042	5278	2764	31.6	.63
200	6935	5429	1506	21.0	.42
250	6192	5623	569	15.4	.31
288	5765	5765	(*)	12.8	.26

*No cooling required.

As can be seen, cryogenic operation results in a large increase in Reynolds number. However, the flow rate of liquid nitrogen is relatively high, comprising about 44 percent of the total mass flow through the test section at the lowest temperature.

As an example of some of the changes to tunnel design that would result from cryogenic operation, a comparison can be made between a normal-temperature blowdown tunnel and an equivalent fully cryogenic tunnel operating at the same Reynolds number, stagnation pressure (2.7 atm), and Mach number (1.00). The test section of the cryogenic tunnel would be only 25 percent of the size of that for the normal tunnel; and when operating from the same size air storage bottles, the cryogenic tunnel could run over 17 times as long.

THE CRYOGENIC INDUCED-FLOW TUNNEL

The cryogenic mode of operation could also be used to advantage with a closed-circuit induced-flow tunnel. In order to maintain a constant test temperature, the temperature of the inducing gas must be cooled to match that of the tunnel circuit.

One method of testing in a cryogenic induced-flow tunnel with air would be to use the same scheme suggested for the cryogenic blowdown tunnel in which air would pass from the high pressure supply through a precooled metal heat exchanger. A second possible method for testing in air would be to evaporate suitable proportions of liquid oxygen and liquid nitrogen within the inducing airstream.

As was the case for the cryogenic blowdown tunnel, the most efficient method of cryogenic operation might well be to use an air-nitrogen mixture resulting from the injection and evaporation of liquid nitrogen in a mixing section between the high pressure air storage and the injector.

Assume that air is delivered to the mixing section at a temperature T_s where the proper amount of liquid nitrogen is combined with the air so that the air-nitrogen mixture reaches the injector at the operating temperature T_t. If the ratio of injector mass flow rate $\dot{m}_i$ to test-section mass flow rate $\dot{m}_{TS}$ is χ, it can be shown in a manner identical to that used for the cryogenic blowdown tunnel that

$$\chi\dot{m}_{TS} = \dot{m}_i = \dot{m}_a + \dot{m}_{LN_2} \tag{A10}$$

and that

$$\dot{m}_{LN_2} = \frac{\chi\dot{m}_{TS}C_p\Delta T}{\beta + C_p\Delta T} \tag{A11}$$

If the same example were to be used for the injector tunnel as was used in the previous section for the blowdown tunnel, the mass flow rates of air and liquid nitrogen would simply be multiplied by the factor χ. Based on results obtained in a pilot transonic injector tunnel recently built at the Langley Research Center, realistic values of χ range from about 0.17 to 0.20 for Mach 1.00 operation. Thus, for $\chi = 0.20$, the injector mass flow rate would be 20 percent of the test-section mass flow rate and the mass flow rates of air and liquid nitrogen required from storage would be only 20 percent of the values needed in the blowdown tunnel. The values of $R_{\bar{c}}$ would, of course, remain unchanged. Therefore, the comments concerning the benefits of cryogenic operation made for the blowdown tunnel apply also to the injector tunnel.

APPENDIX B

SOME AERODYNAMIC ASPECTS OF FAN AND TUNNEL MATCHING

The flow variables which the drive fan must accommodate in the conventional tunnel comprise, at the most, independent variation of test-section Mach number and stagnation pressure. In the case of the pressurized cryogenic wind tunnel the existence of the additional independent variable, temperature, has prompted consideration of the matching of fan characteristics with those of the tunnel.

TUNNEL CHARACTERISTICS

The increase of total temperature of the test gas as it passes through the fan, ΔT, is given by

$$\Delta T = \frac{\text{Power to fan}}{\text{Fan mass flow rate} \times C_p}$$

where C_p is the specific heat of the test gas. In terms of test-section flow quantities,

$$\Delta T = \frac{\eta_1 q}{\rho C_p}$$

from which

$$\frac{\Delta T}{T_{t,1}} = \frac{\eta_1 M^2 \frac{\gamma - 1}{2}}{1 + \frac{\gamma - 1}{2} M^2} \tag{B1}$$

where $T_{t,1}$ is the total temperature of the gas at the fan inlet and η_1 is a tunnel power coefficient defined by

$$\eta_1 = \frac{\text{Drive power at fan}}{qVA}$$

and A is the test-section flow area. It is assumed that there is no significant flow of heat to or from the tunnel circuit between the contraction and the fan inlet; hence $T_{t,1}$ is identical to the stagnation temperature in the test section T_t.

Fan efficiency η_f may be defined as

$$\eta_f = \frac{\Delta T'}{\Delta T} \tag{B2}$$

where $\Delta T'$ is the ideal total temperature rise across the fan, the temperature rise that would accompany an isentropic compression of the test gas through the total pressure rise developed by the fan. The relationship between fan total pressure rise Δp and ideal total temperature rise is

$$1 + \frac{\Delta p}{p_{t,1}} = \left(1 + \frac{\Delta T'}{T_t}\right)^{\frac{\gamma}{\gamma-1}} \tag{B3}$$

where $p_{t,1}$ is the stagnation pressure at the fan inlet. Combining equations (B1), (B2), and (B3) gives

$$1 + \frac{\Delta p}{p_{t,1}} = \left(1 + \frac{\eta_f \eta_1 M^2 \frac{\gamma - 1}{2}}{1 + \frac{\gamma - 1}{2} M^2}\right)^{\frac{\gamma}{\gamma-1}}$$

For constant γ and for η_1 and η_f functions of M, we may write simply

$$\frac{\Delta p}{p_{t,1}} = f_1(M) \tag{B4}$$

It is assumed that the mass flow rates through the fan and test section are equal. Therefore, in terms of flow values in the test section the mass flow rate is given by

$$\dot{m} = pAM\sqrt{\frac{\gamma}{\mathcal{R}T}} \tag{B5}$$

where p and T are the static pressure and temperature, respectively, in the test section. Equation (B5) may be rewritten

$$\frac{\sqrt{\mathcal{R}T_t}}{Ap_{t,1}} = M\sqrt{\gamma}\left(1 + \frac{\gamma - 1}{2} M^2\right)^{-\frac{\gamma+1}{2(\gamma-1)}} \tag{B6}$$

but, for a given test gas and size of tunnel, the shorter but no longer dimensionless form of equation (B6) may be used; that is,

$$\dot{m}\frac{\sqrt{T_t}}{p_{t,1}} = f_2(M) \tag{B7}$$

FAN CHARACTERISTICS

The pressure rise across a fan and the fan efficiency are functions of several variables which at least include inlet total temperature T_t, inlet total pressure $p_{t,1}$, fan

tip speed v, and mass flow rate through the fan $\dot{m}$. By invoking dimensional analysis, it may be shown that any nondimensional measure of performance is a function of the two groupings $\dot{m}\frac{\sqrt{T_t}}{p_{t,1}}$ and $\frac{v}{\sqrt{T_t}}$. For a particular fan size and geometry, these two parameters can be recognized as indicators of the axial and tangential components, respectively, of Mach number relative to a fan blade section. Thus, their ratio and resultant determine the angle of attack and Mach number of flow past a blade section. For convenience, we may substitute the fan rotational speed N for tip speed v.

A conveniently nondimensionalized form of pressure rise is $\Delta p/p_{t,1}$, which can be written as

$$\frac{\Delta p}{p_{t,1}} = f_3\left(\frac{\dot{m}\sqrt{T_t}}{p_{t,1}}, \frac{N}{\sqrt{T_t}}\right)$$

and, similarly, the fan efficiency η_f can be written as

$$\eta_f = f_4\left(\frac{\dot{m}\sqrt{T_t}}{p_{t,1}}, \frac{N}{\sqrt{T_t}}\right)$$

The forms of function f_3 and f_4 depend upon the details of fan design. However, certain characteristics are common to all fans. For example, there are combinations of flow conditions which cause the fan to stall, or to operate at low efficiency. A sketch of typical fan characteristics is given in figure B1 where functions f_3 and f_4 are shown superimposed. Diagrams of this type are general because they take into account all tunnel operating variables affecting the fan. Laid on the sketch is a typical tunnel characteristic, an operating line given by equation (B7).

CHOICE OF FAN

The fan may be chosen by arranging a suitable match of fan to tunnel in the usual manner at, for example, 1 atm and normal temperature. Because the operating line is fixed in position relative to the fan characteristics, the matching of the tunnel flow and pressure rise requirements with the capabilities of the fan will be as good at any other combination of pressure and temperature. Hence, the existence of the additional variable temperature does not affect the aerodynamic behavior of the fan.

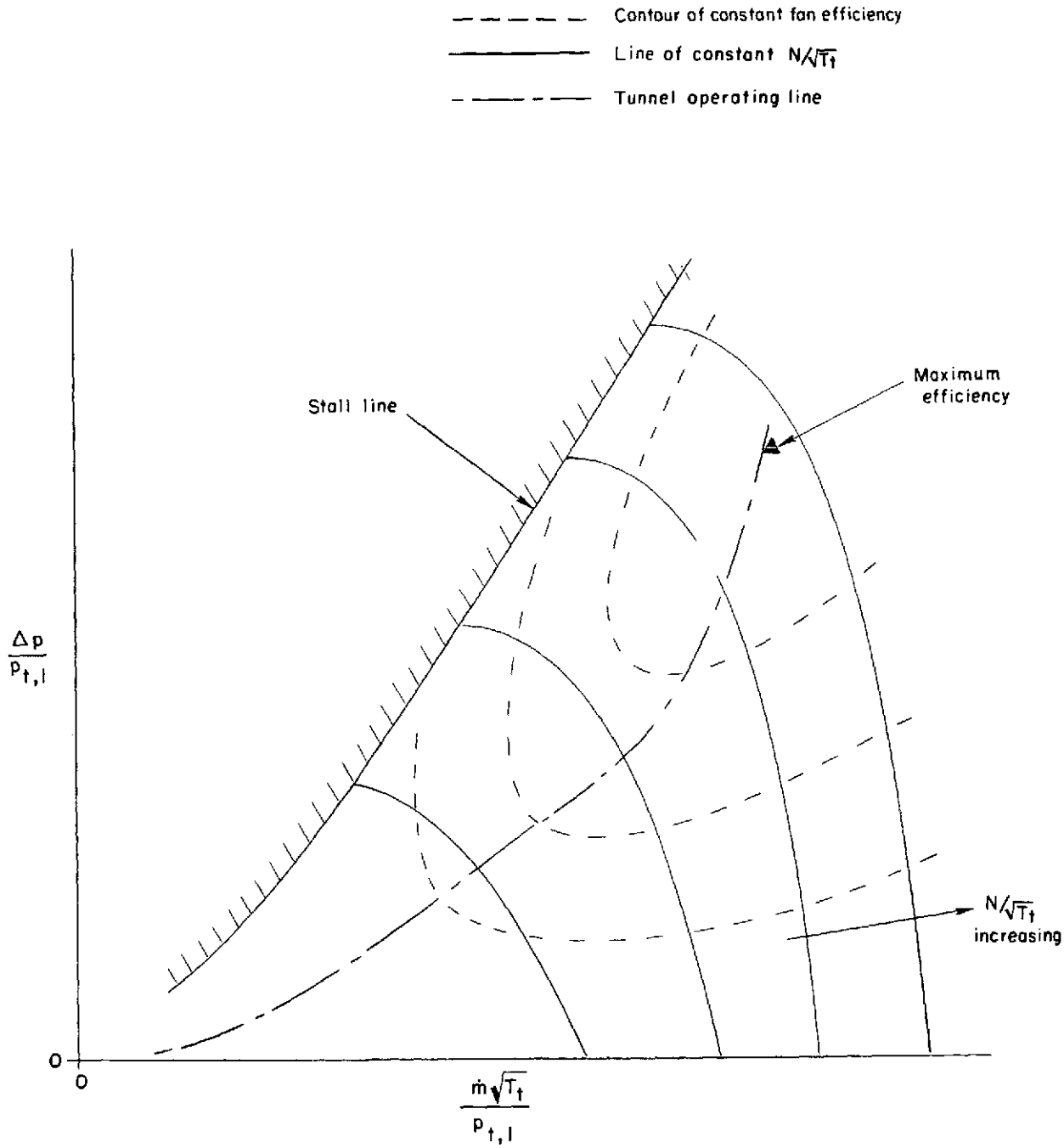

Figure B1.- Sketch of typical fan characteristics.

REFERENCES

1. Heppe, Richard R.; O'Laughlin, B. D.; and Celniker, Leo: New Aeronautical Facilities – We Need Them Now. Astronaut. & Aeronaut., vol. 6, no. 3, Mar. 1968, pp. 42-54.

2. Poisson-Quinton, Philippe: From Wind Tunnel to Flight, the Role of the Laboratory in Aerospace Design. J. Aircraft, vol. 5, no. 3, May-June 1968, pp. 193-214.

3. Baals, Donald D.; and Stokes, George M.: A Facility Concept for High Reynolds Number Testing at Transonic Speeds. Facilities and Techniques for Aerodynamic Testing at Transonic Speeds and High Reynolds Number, AGARD CP No.83, Aug. 1971, pp. 28-1 – 28-12.

4. Evans, J. Y. G.; and Taylor C. R.: Some Factors Relevant to the Simulation of Full-Scale Flows in Model Tests and to the Specification of New High-Reynolds-Number Transonic Tunnels. Facilities and Techniques for Aerodynamic Testing at Transonic Speeds and High Reynolds Number, AGARD CP No.83, Aug. 1971, pp. 31-1 – 31-13.

5. Igoe, William B.; and Baals, Donald D.: Reynolds Number Requirements for Valid Testing at Transonic Speeds. Facilities and Techniques for Aerodynamic Testing at Transonic Speeds and High Reynolds Number, AGARD CP No.83, Aug. 1971, pp. 5-1 – 5-4.

6. Evans, J. Y. G.: A Scheme for a Quiet Transonic Flow Suitable for Model Testing at High Reynolds Number. Facilities and Techniques for Aerodynamic Testing at Transonic Speeds and High Reynolds Number, AGARD CP No.83, Aug. 1971, pp. 35-1 – 35-5.

7. Whitfield, Jack D.; Schueler, C. J.; and Starr, Rogers F.: High Reynolds Number Transonic Wind Tunnels – Blowdown or Ludwieg Tube? Facilities and Techniques for Aerodynamic Testing at Transonic Speeds and High Reynolds Number, AGARD CP No.83, Aug. 1971, pp. 29-1 – 29-17.

8. Pozniak, O. M.: Investigation Into the Use of Freon 12 as a Working Medium in a High-Speed Wind-Tunnel. Note No. 72, Coll. Aeronaut., Cranfield (Engl.), Nov. 1957.

9. Treon, Stuart L.; Hofstetter, William R.; and Abbott, Frank T., Jr.: On the Use of Freon-12 for Increasing Reynolds Number in Wind-Tunnel Testing of Three-Dimensional Aircraft Models at Subcritical and Supercritical Mach Numbers. Facilities and Techniques for Aerodynamic Testing at Transonic Speeds and High Reynolds Number, AGARD CP No.83, Aug. 1971, pp. 27-1 – 27-8.

10. AGARD Fluid Dynamics Panel Hirt Group: AGARD Study of High Reynolds Number Wind Tunnel Requirements for the North Atlantic Treaty Organization Nations. Facilities and Techniques for Aerodynamic Testing at Transonic Speeds and High Reynolds Number, AGARD CP No.83, Aug. 1971, pp. 32-1 – 32-9.

11. Smelt, R.: Power Economy in High-Speed Wind Tunnels by Choice of Working Fluid and Temperature. Rep. No. Aero. 2081, Brit. R.A.E., Aug. 1945.

12. Rush, C. K.: A Low Temperature Centrifugal Compressor Test Rig. Mech. Eng. Rep. MD-48 (NRC-7776), Nat. Res. Counc. Can. (Ottawa), Nov. 1963.

13. Goodyer, Michael J.; and Kilgore, Robert A.: The High Reynolds Number Cryogenic Wind Tunnel. AIAA Paper No. 72-995, Sept. 1972.

14. Mechtly, E. A.: The International System of Units – Physical Constants and Conversion Factors (Second Revision). NASA SP-7012, 1973.

15. Chapman, Dean R.: Some Possibilities of Using Gas Mixtures Other Than Air in Aerodynamic Research. NACA Rep. 1259, 1956. (Supersedes NACA TN 3226.)

16. Hilsenrath, Joseph; Beckett, Charles W.; et al.: Tables of Thermal Properties of Gases. NBS Circ. 564, U.S. Dept. Com., 1955.

17. Pankhurst, R. C.; and Holder, D. W.: Wind-Tunnel Technique. Sir Isaac Pitman & Sons, Ltd. (London), 1965.

18. Jacobsen, Richard T.: The Thermodynamic Properties of Nitrogen From 65 to 2000 K With Pressures to 10,000 Atmospheres. Ph. D. Thesis, Washington State Univ., 1972. (Available as NASA CR-128526.)

19. Schlichting, Hermann (J. Kestin, transl.): Boundary Layer Theory. McGraw-Hill Book Co., Inc., 1955, p. 206.

20. Jones, J. Lloyd, Jr.: Problems of Flow Simulation in Wind Tunnels. AIAA Paper No. 69-660, June 1969.

21. Barron, Randall: Cryogenic Systems. McGraw-Hill Book Co., c.1966.

22. Jacobs, R. B.: Liquid Requirements for the Cool-Down of Cryogenic Equipment. Advances in Cryogenic Engineering, Volume 8, K. D. Timmerhaus, ed., Plenum Press, 1963, pp. 529-535.

23. MiniLaWs Working Group: A Review of Current Research Aimed at the Design and Operation of Large Windtunnels. AGARD-AR-68, Mar. 1974.

24. Anon.: Second International Symposium on Electro-Magnetic Suspension. Dep. Aeronaut. & Astronaut., Univ. of Southampton, July 1971.

25. Davis, John W.: A Shock Tube Technique for Producing Subsonic, Transonic, and Supersonic Flows With Extremely High Reynolds Numbers. AIAA Paper No. 68-18, Jan. 1968.

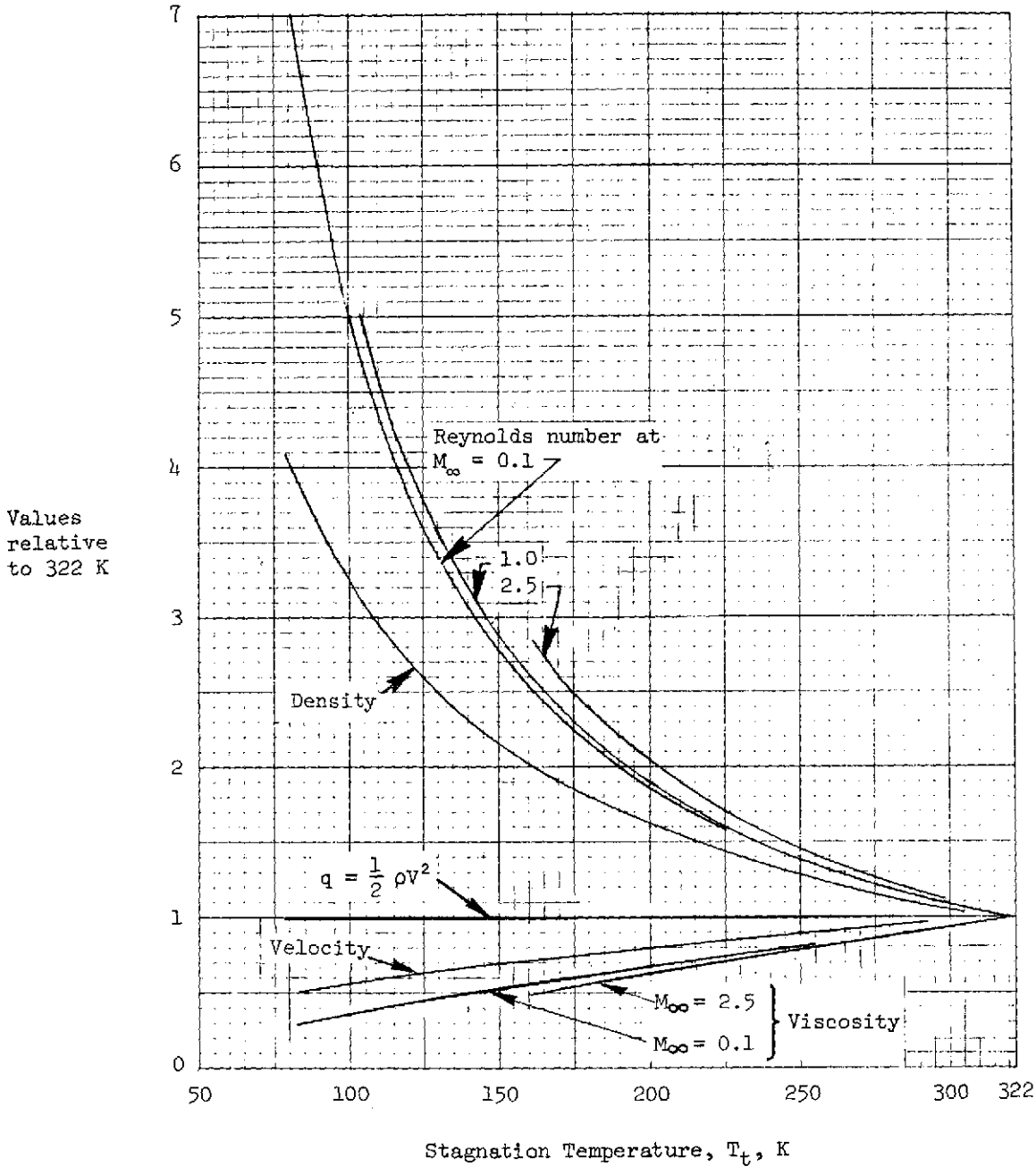

Figure 1.- Variation of test-section flow parameters relative to values at 322 K with stagnation temperature in air. Constant values of stagnation pressure, tunnel size, and Mach number. (Values of viscosity obtained from ref. 16.)

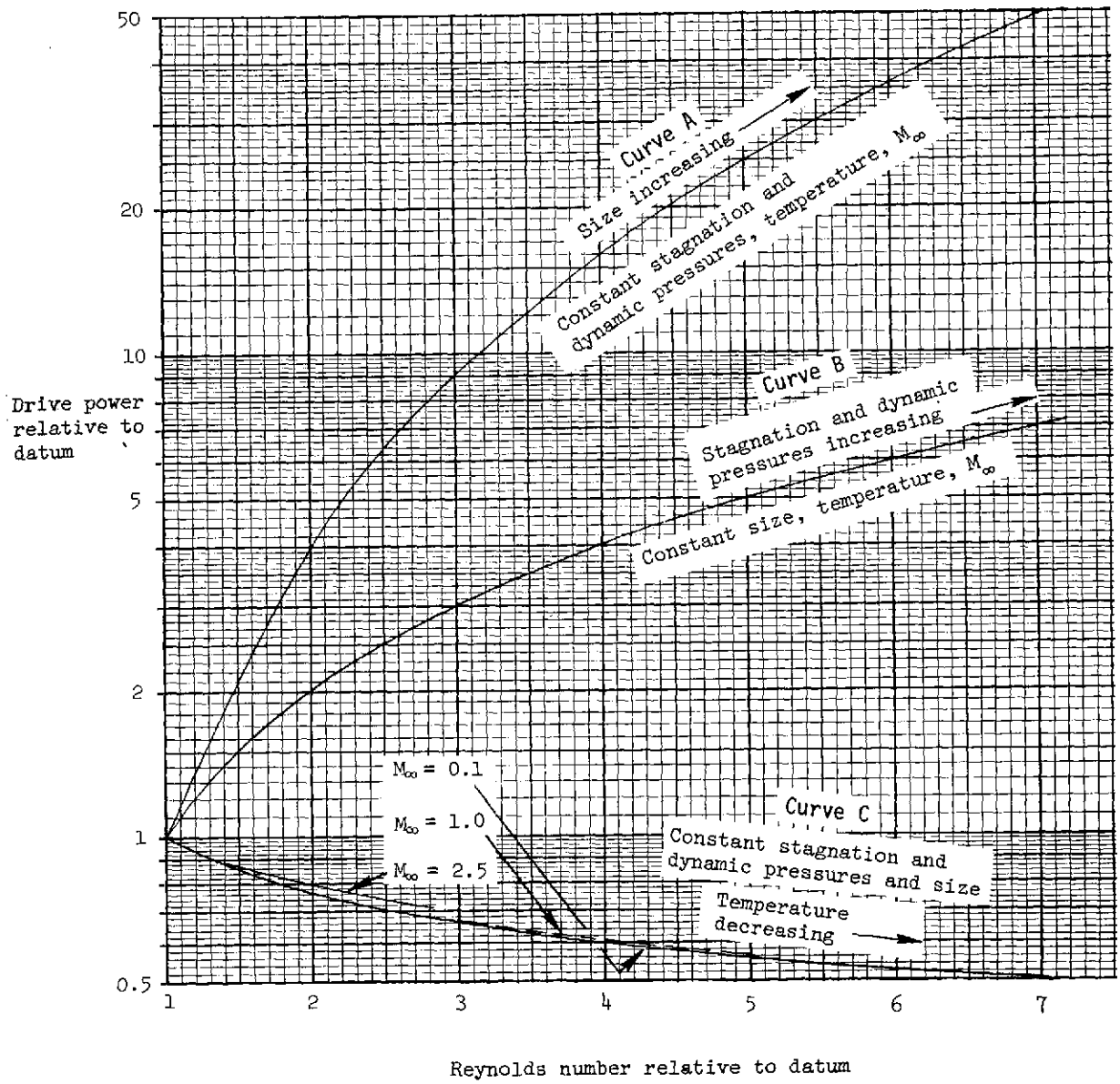

Figure 2.- Variation of drive power relative to 322 K for three methods of increasing Reynolds number in air.

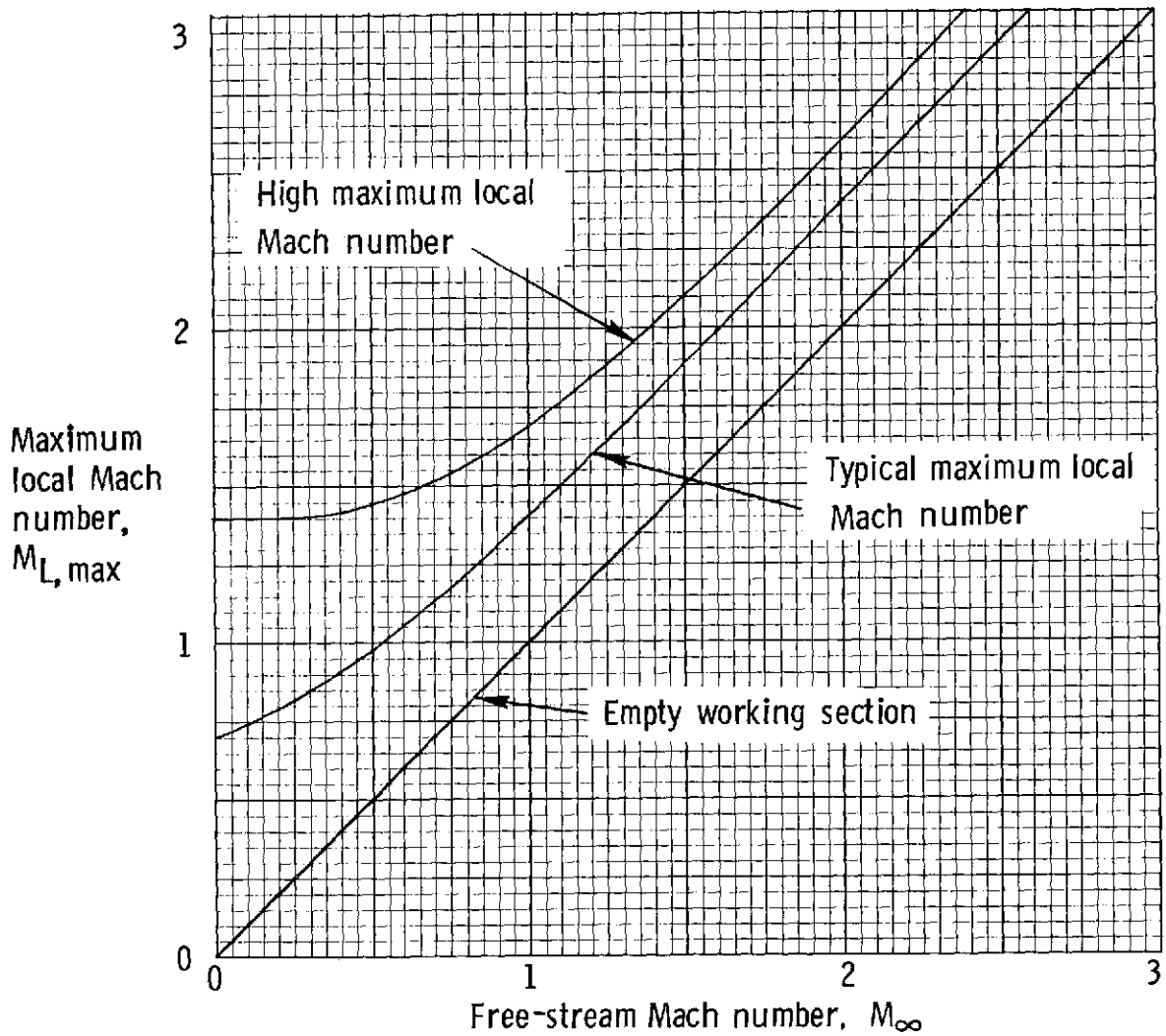

Figure 3.- Assumed maximum local Mach number as a function of free-stream Mach number.

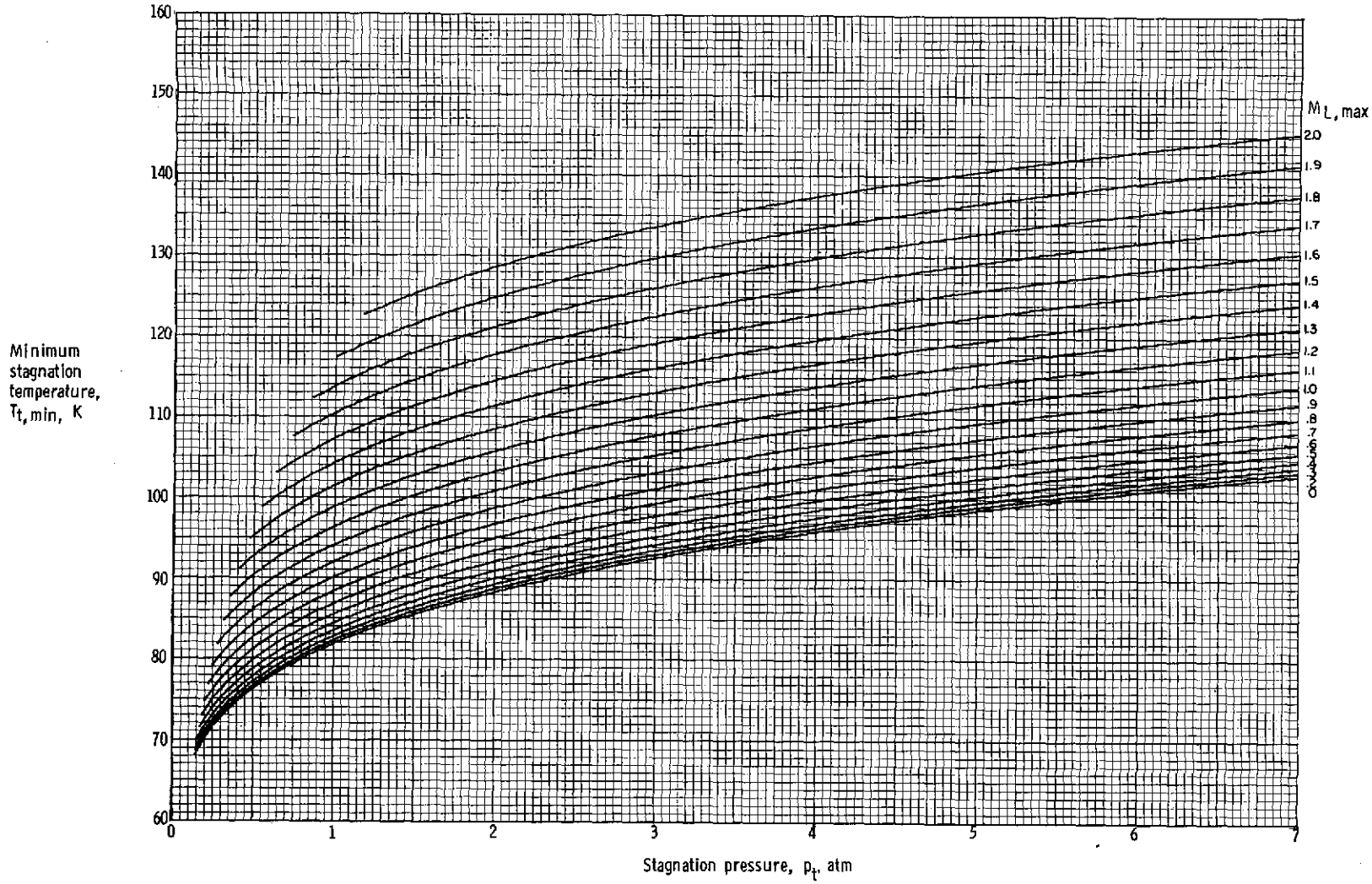

Figure 4.- Variation of minimum stagnation temperature $T_{t,min}$ with stagnation pressure and maximum local Mach number for testing in air.

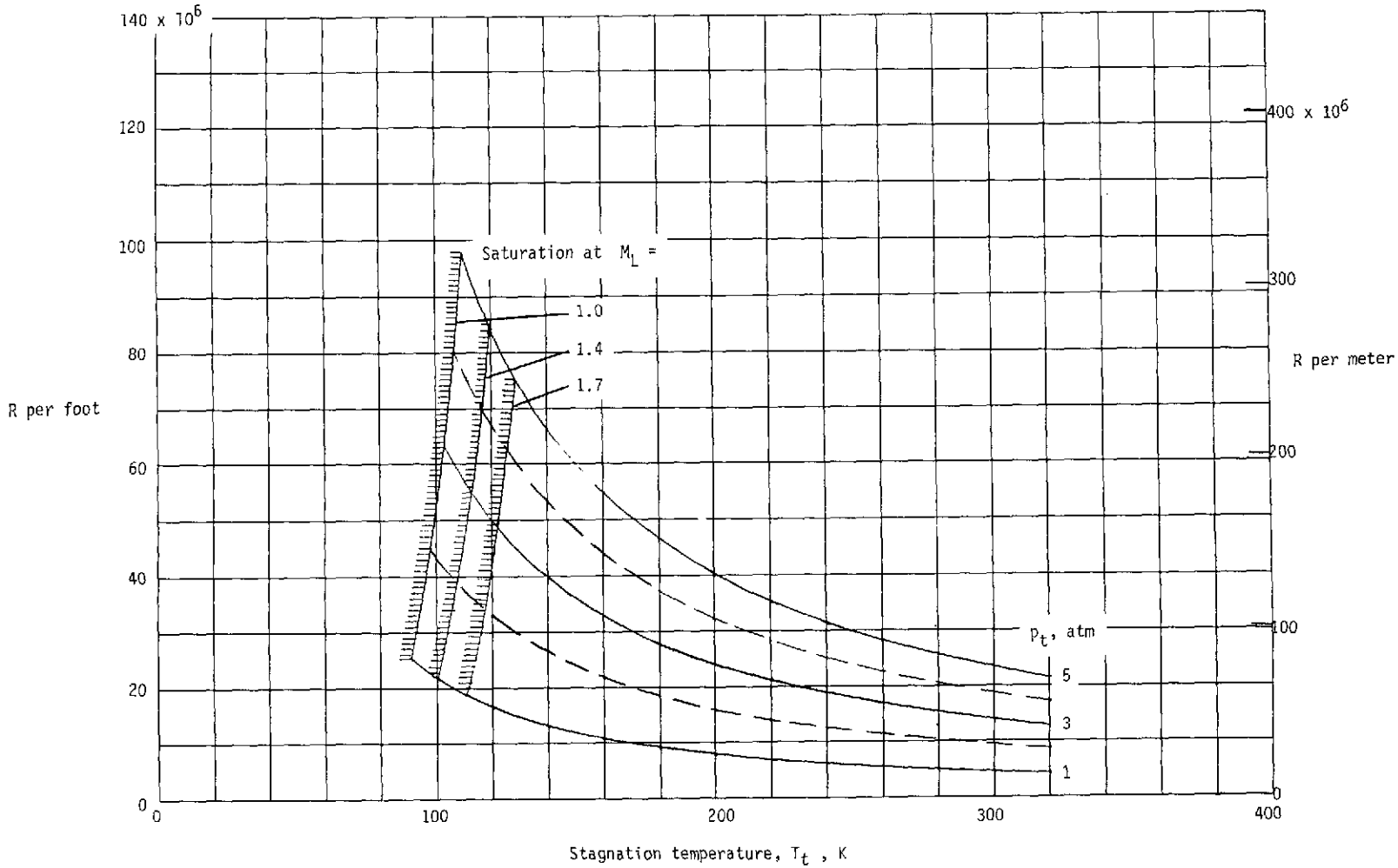

Figure 5.- Restrictions imposed on stagnation temperature and Reynolds number due to saturation as a function of stagnation pressure and maximum local Mach number. $M_\infty = 1.00$ in air.

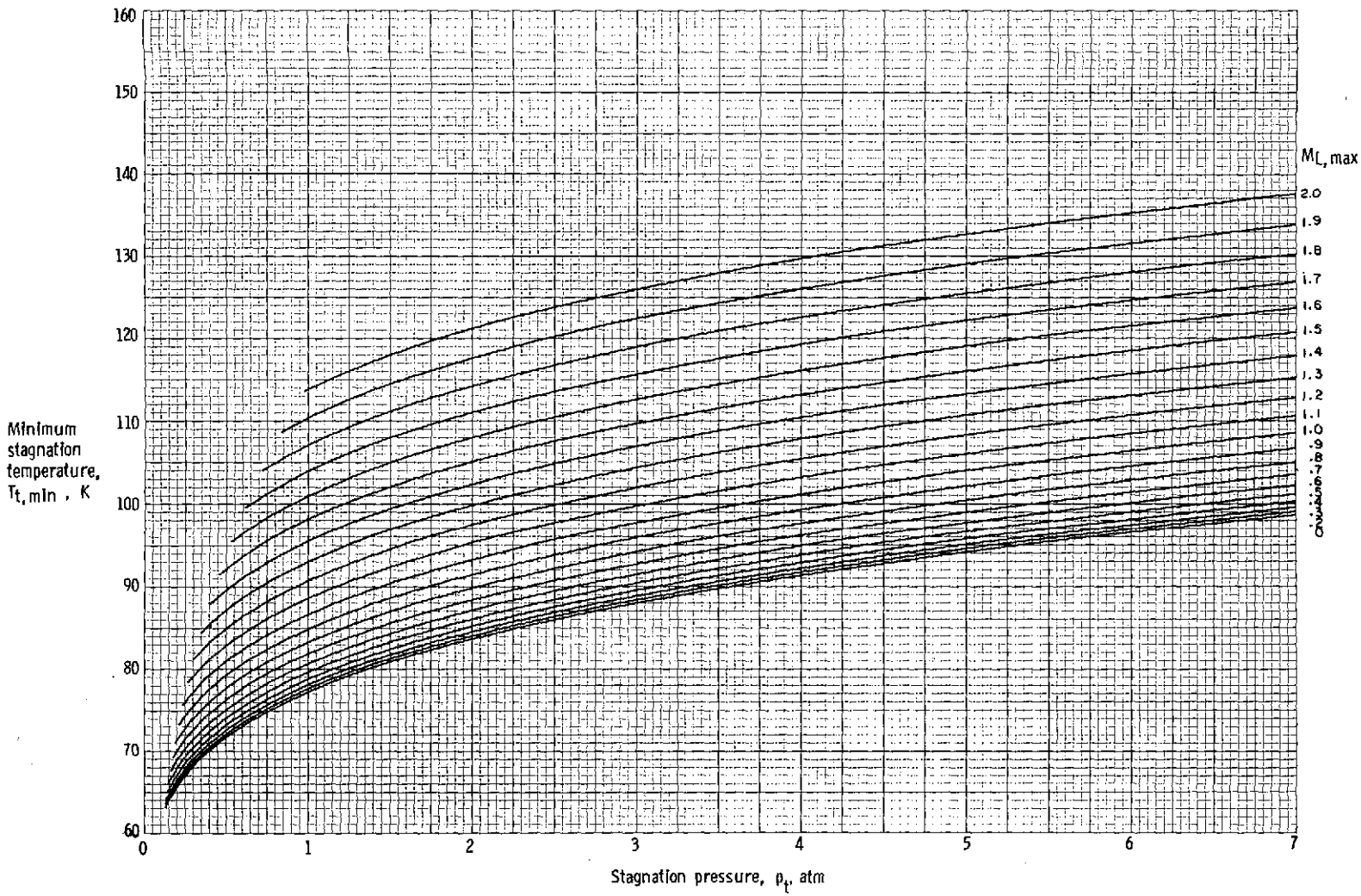

Figure 6.- Variation of minimum stagnation temperature $T_{t,min}$ with stagnation pressure and maximum local Mach number for testing in nitrogen.

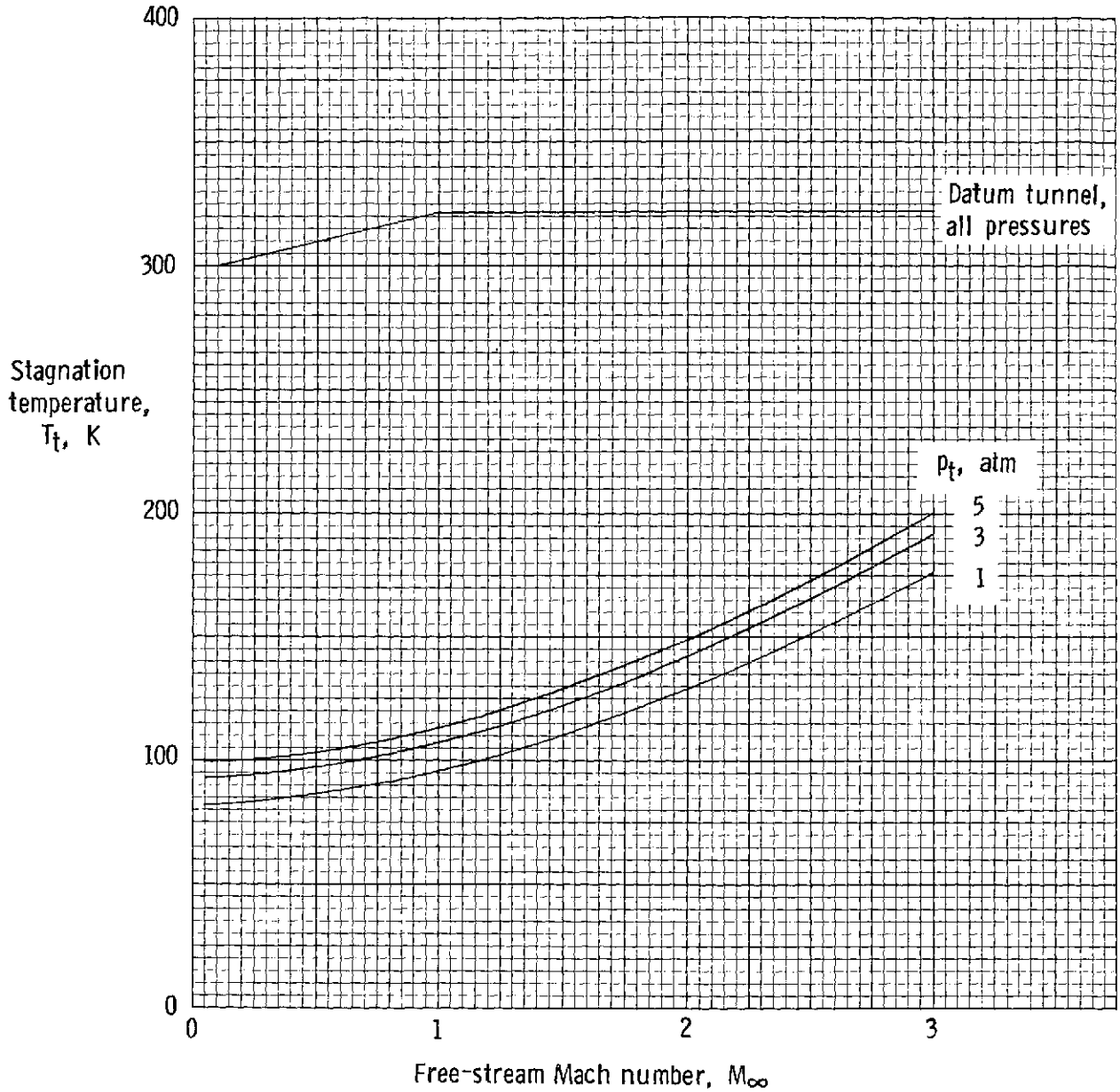

Figure 7.- Assumed stagnation temperature in datum tunnel and minimum stagnation temperature in cryogenic nitrogen tunnel as a function of free-stream Mach number and stagnation pressure.

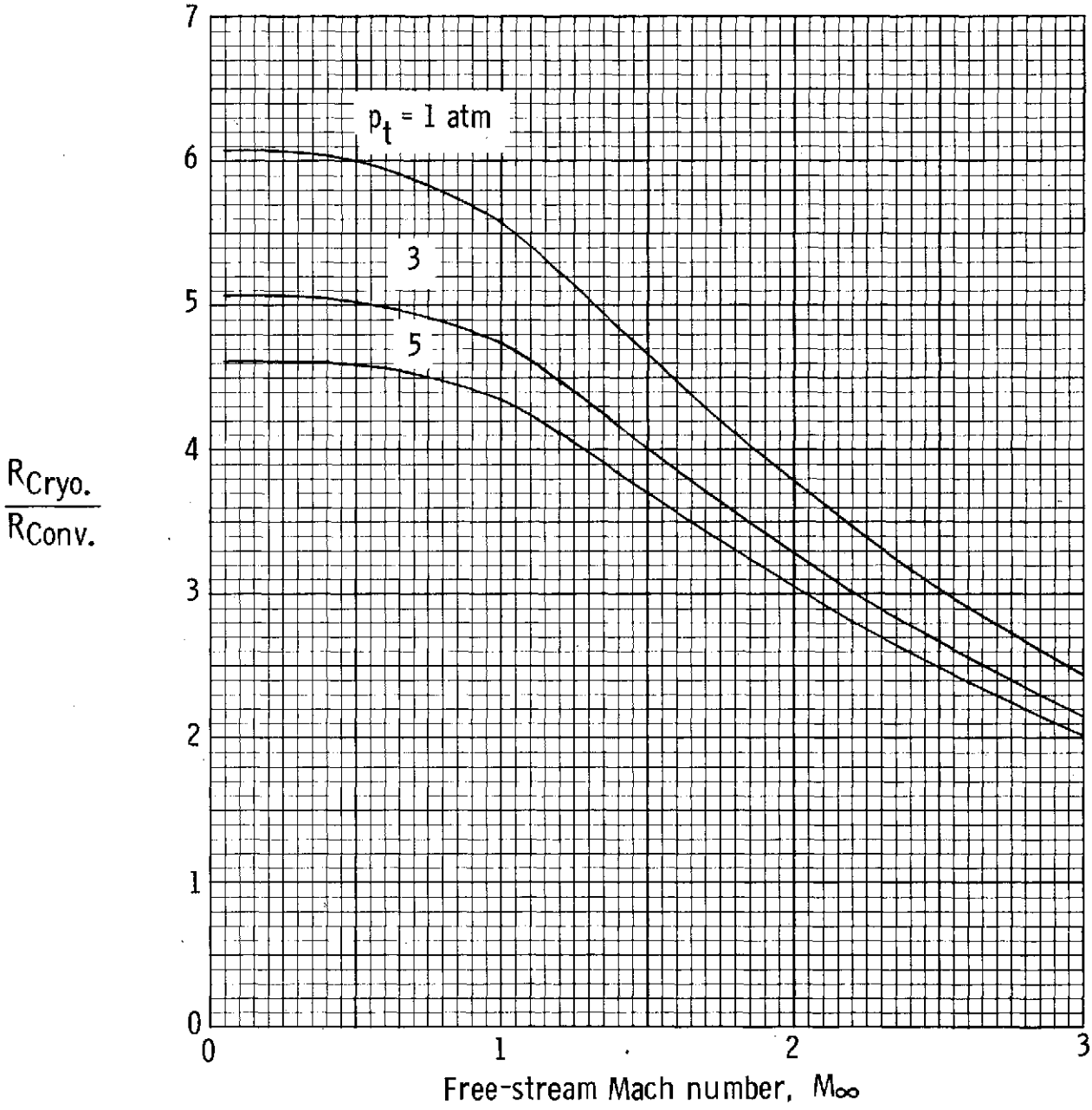

Figure 8.- Reynolds number in cryogenic nitrogen tunnel relative to Reynolds number in conventional tunnel of same size as a function of free-stream Mach number and stagnation pressure.

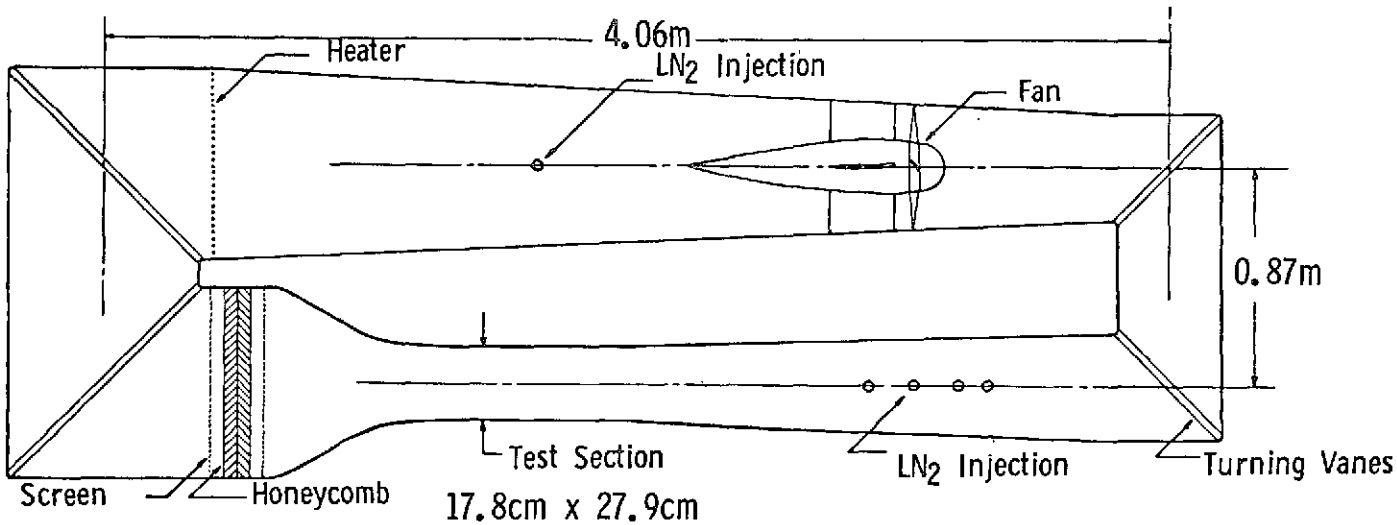

Figure 9.- Low-speed cryogenic tunnel circuit.

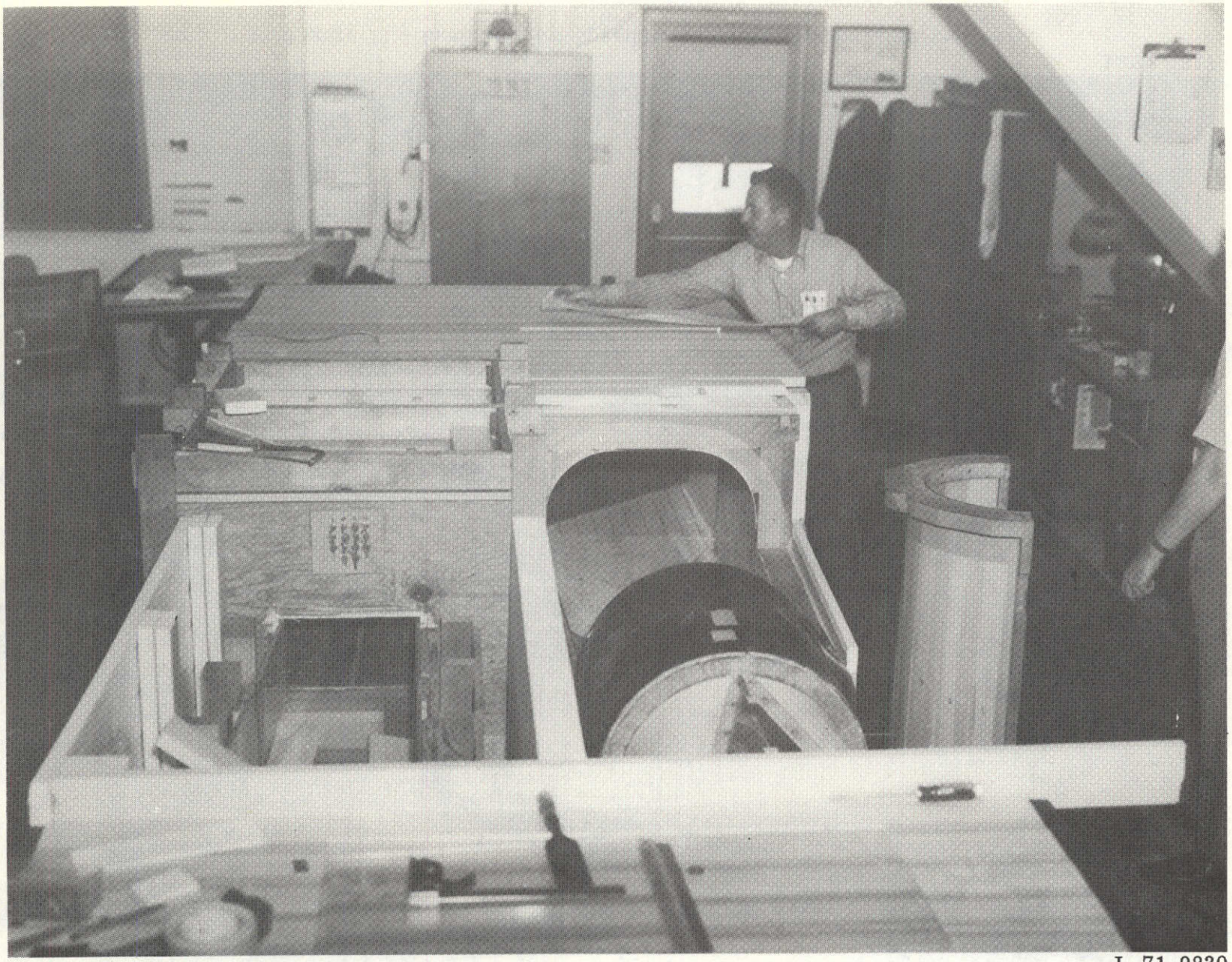

L-71-9830

Figure 10.- Low-speed tunnel being insulated.

L-72-1537

Figure 11.- Insulated low-speed tunnel and test apparatus.

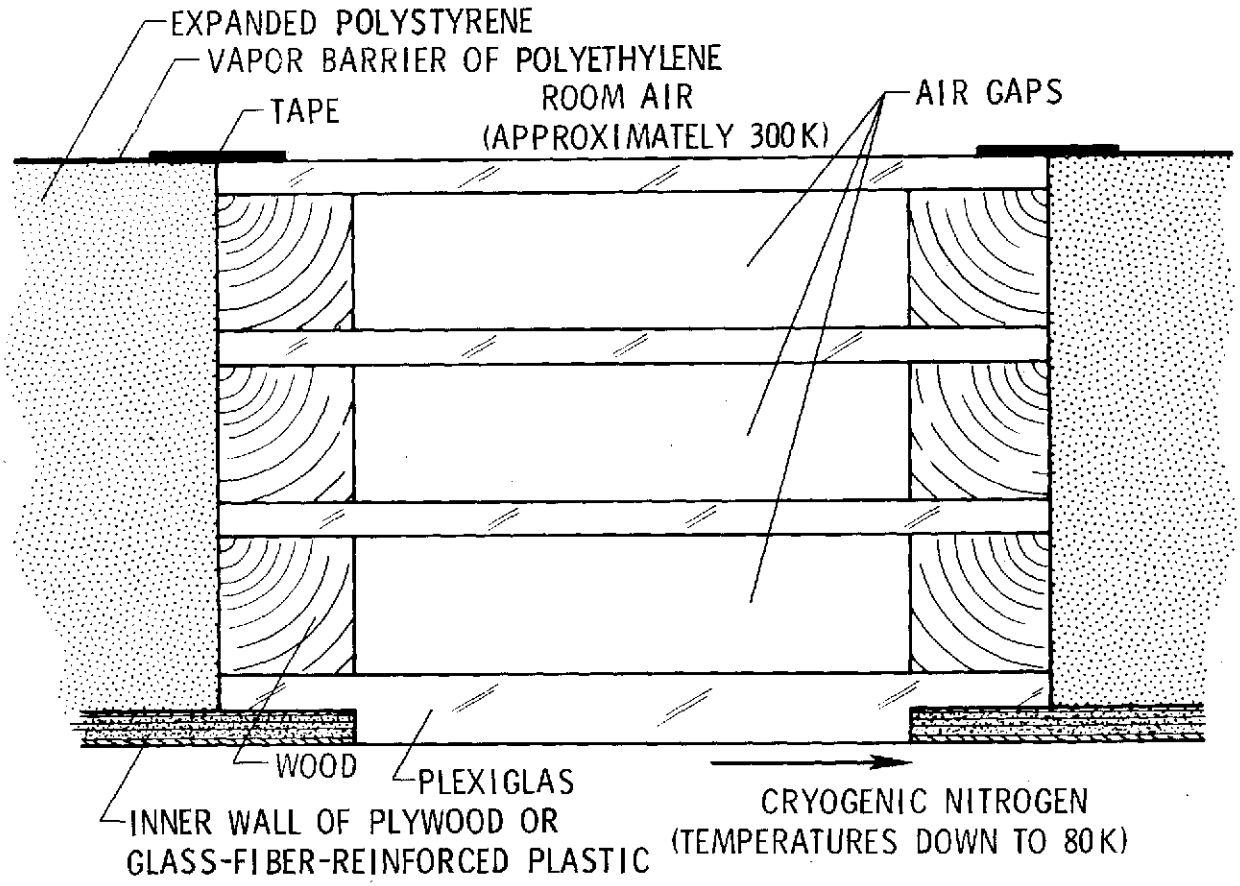

Figure 12.- Sketch of typical section of insulation and viewing port.

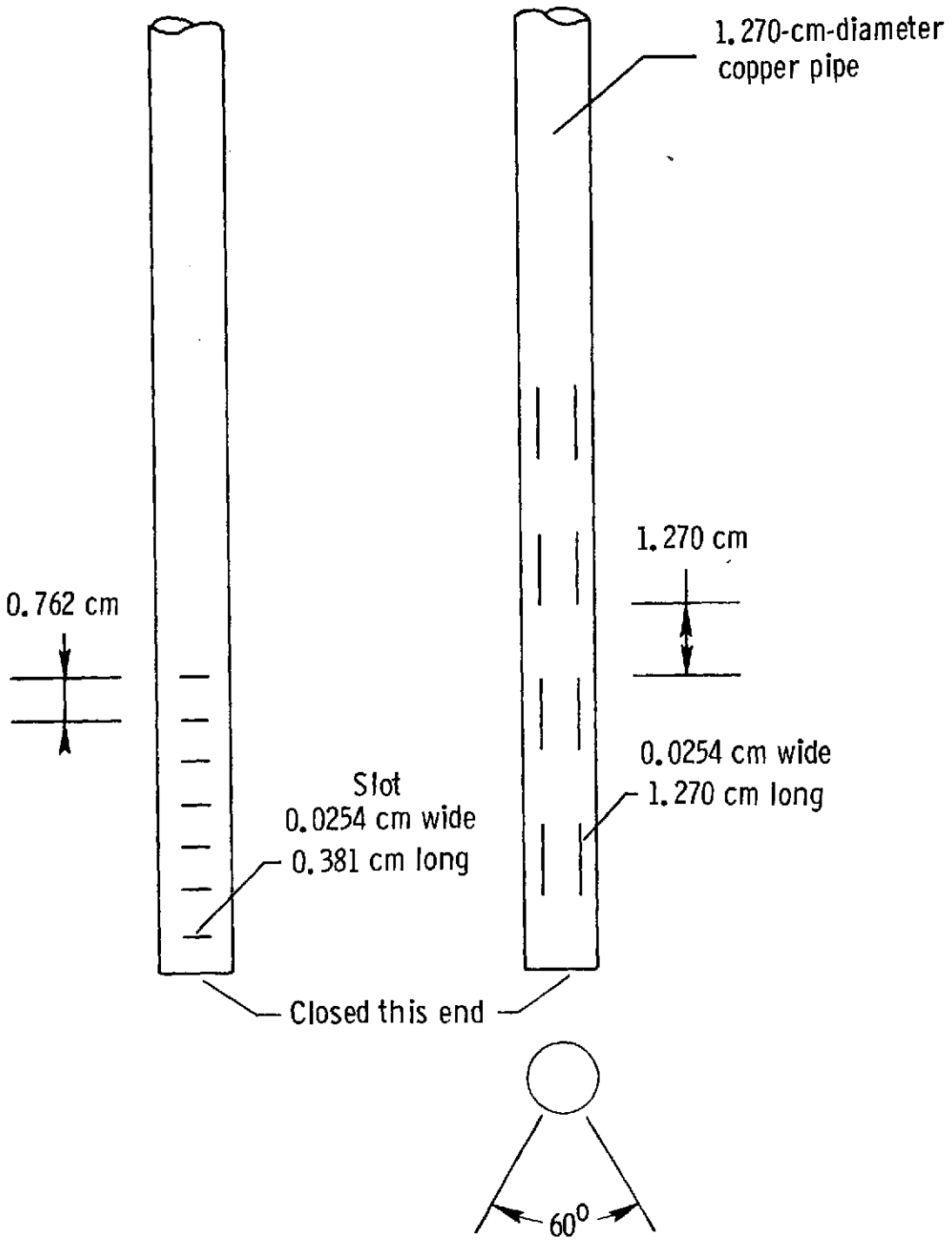

Figure 13.- Liquid-nitrogen injection spray bars.

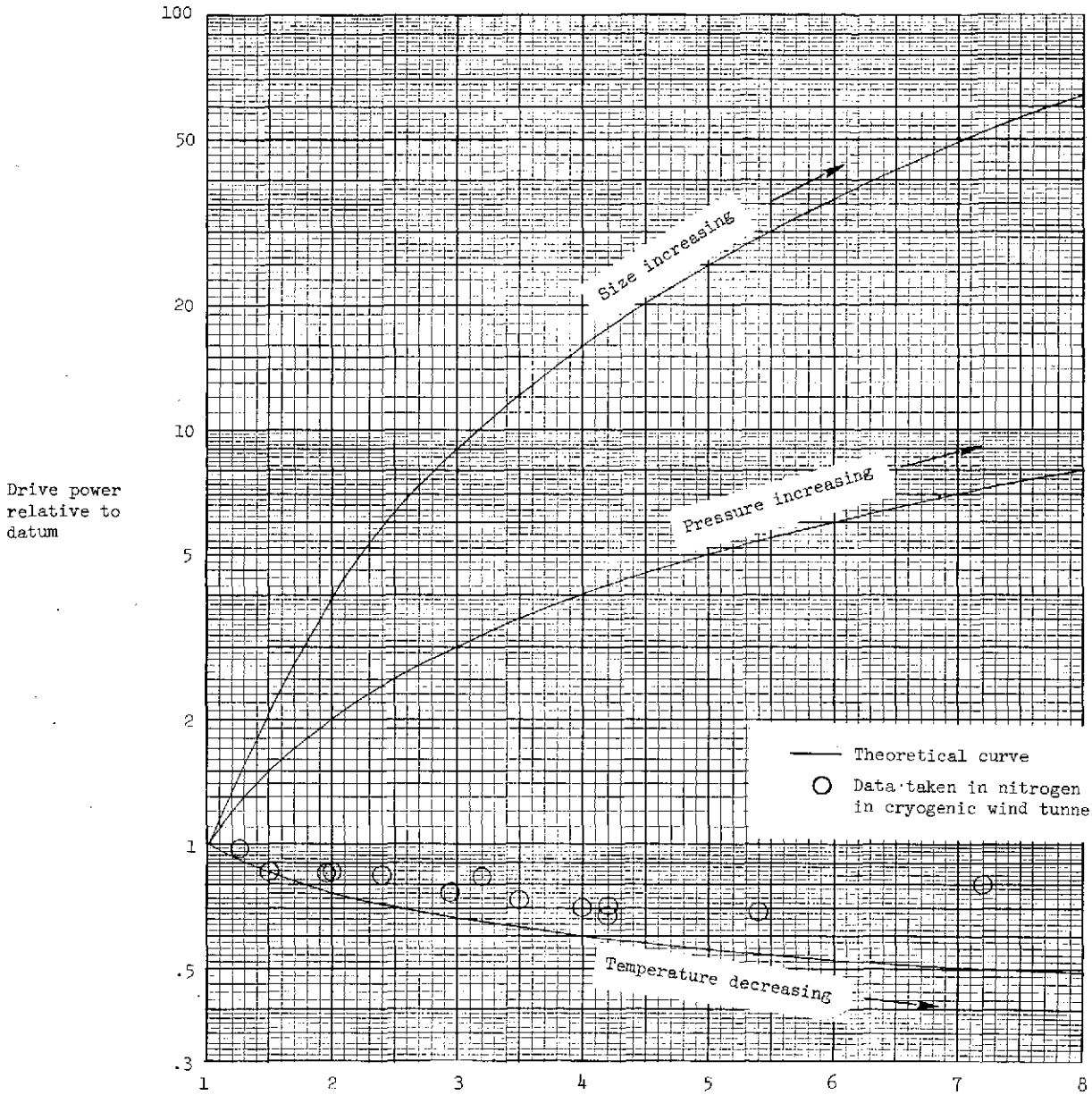

Figure 14.- Theoretical variation of drive power for three methods of increasing Reynolds number and measured variation of drive power at $M_\infty \approx 0.1$ for low-speed cryogenic tunnel.

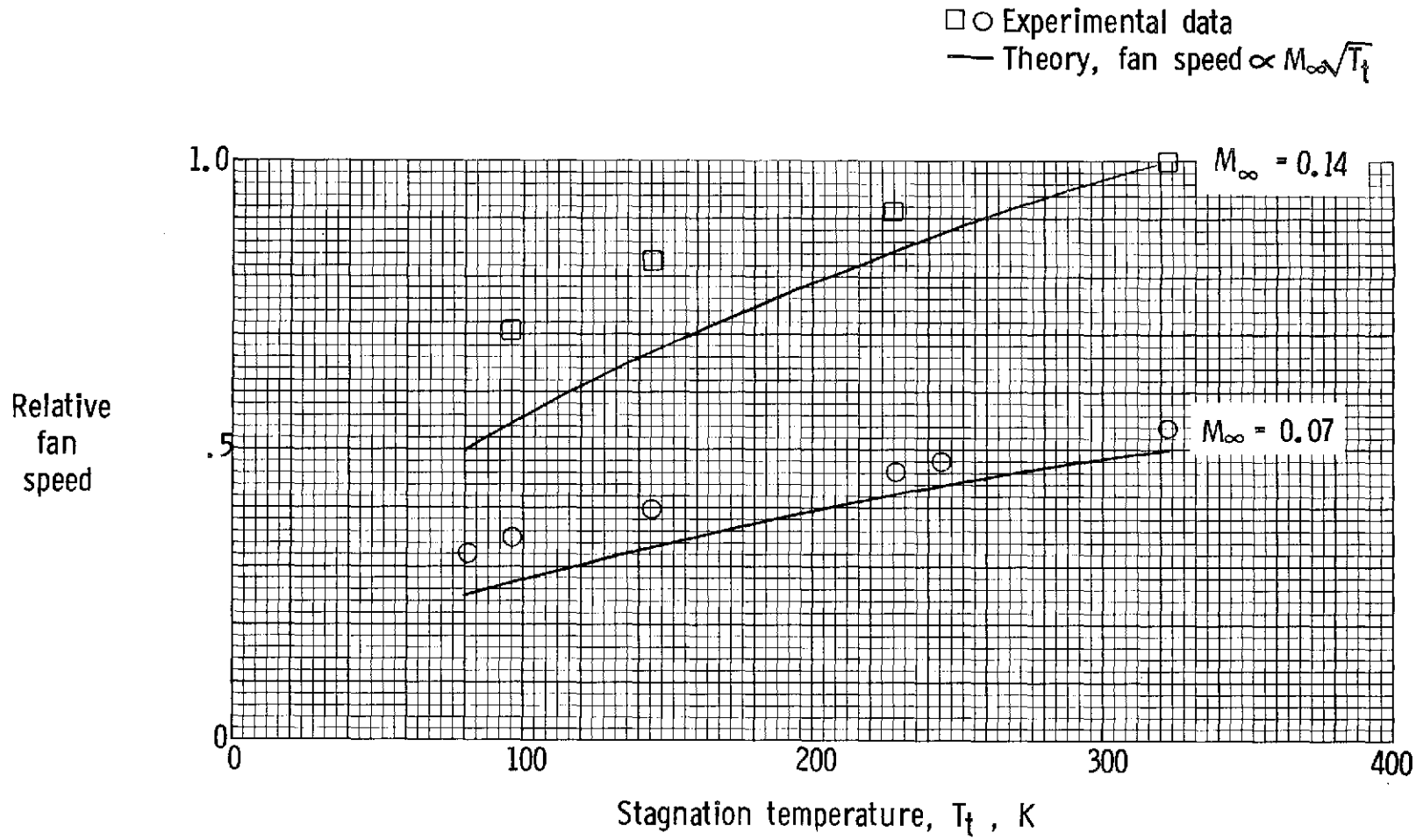

Figure 15.- Theoretical and measured variation of fan speed relative to maximum fan speed with stagnation temperature in low-speed cryogenic tunnel.

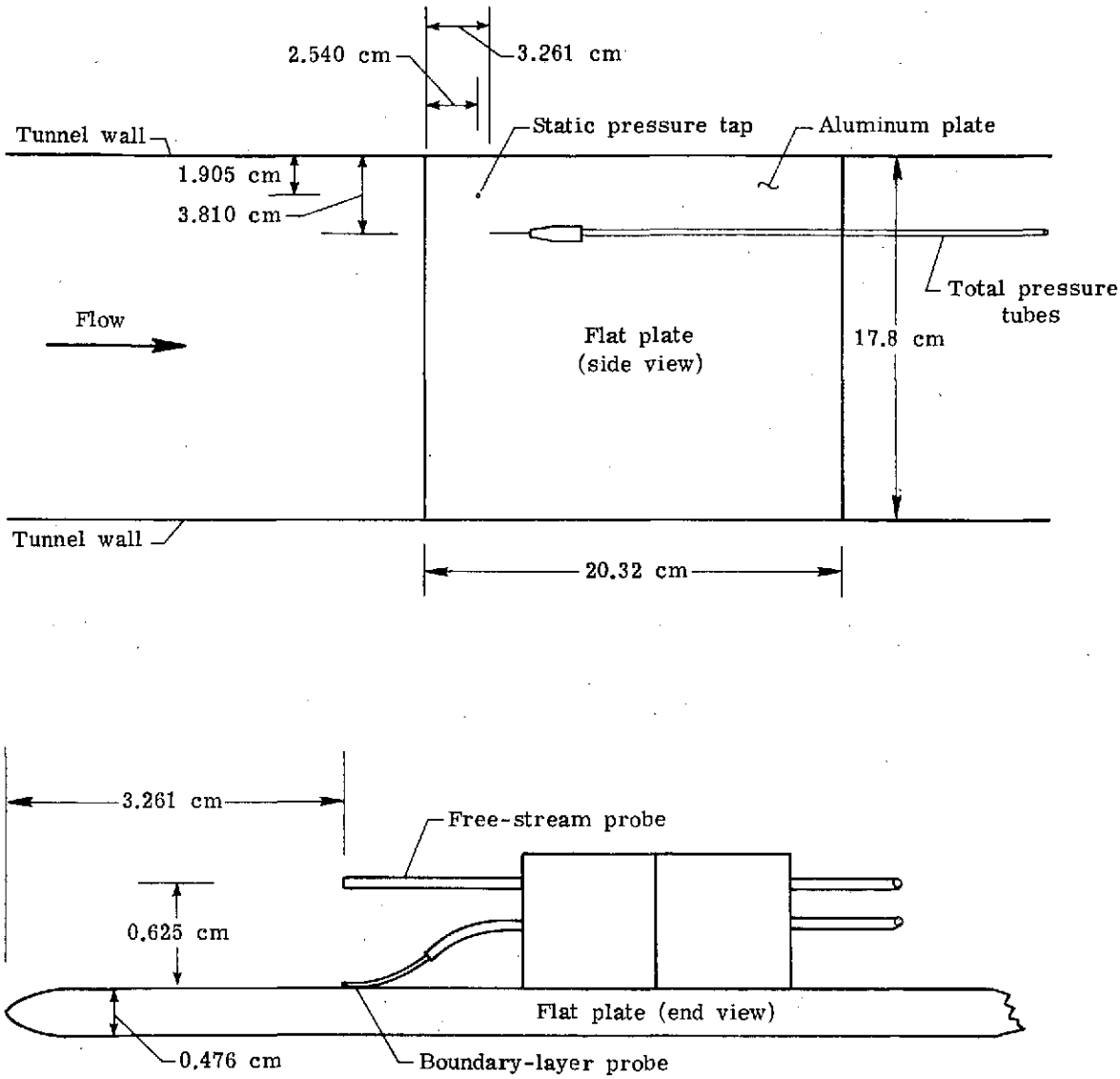

Figure 16.- Sketch of plate and probes used in boundary-layer experiment.

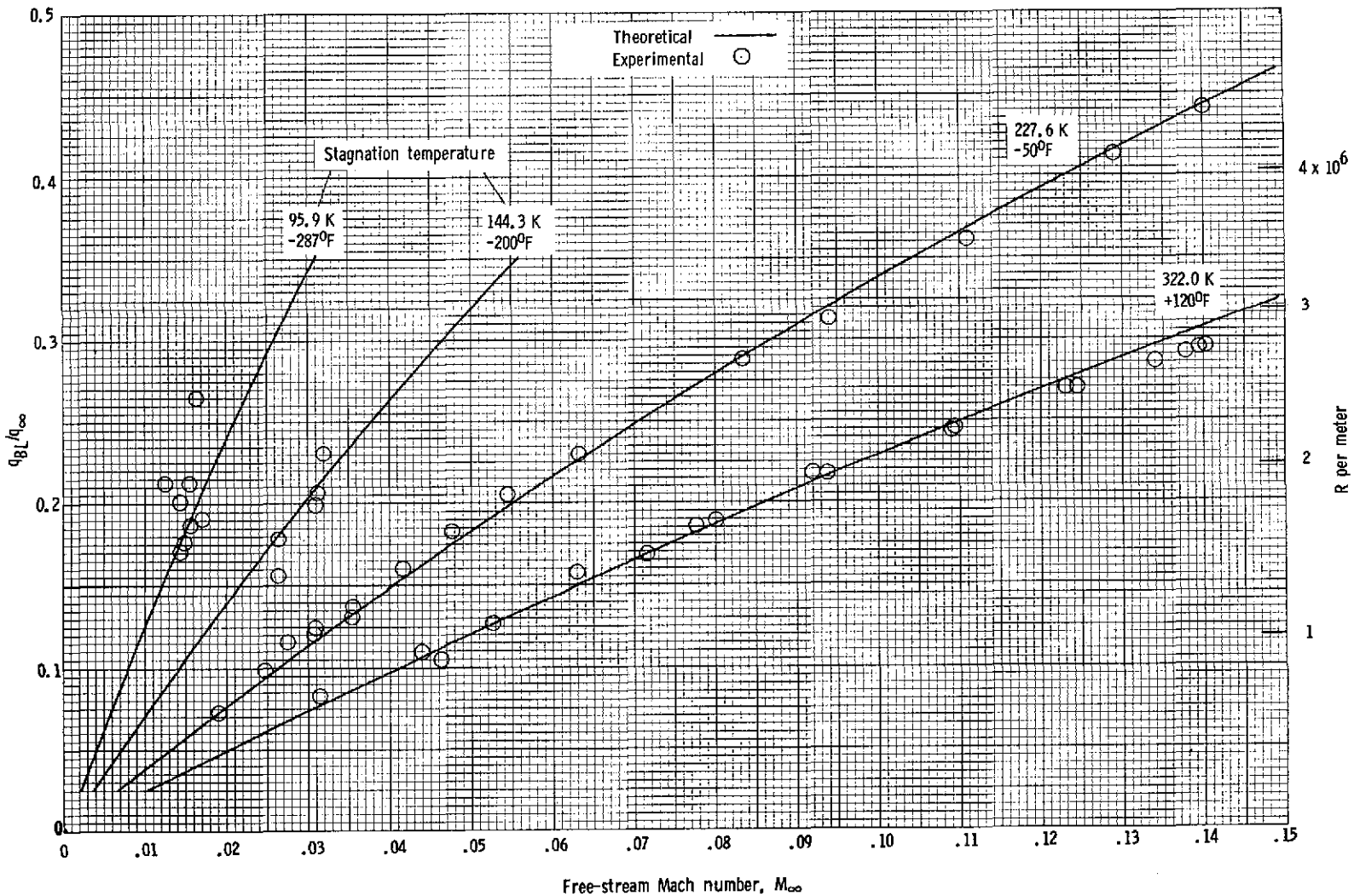

Figure 17.- Theoretical and measured variation of the ratio of dynamic pressure in a laminar boundary layer to free-stream dynamic pressure as a function of Mach number and stagnation temperature.

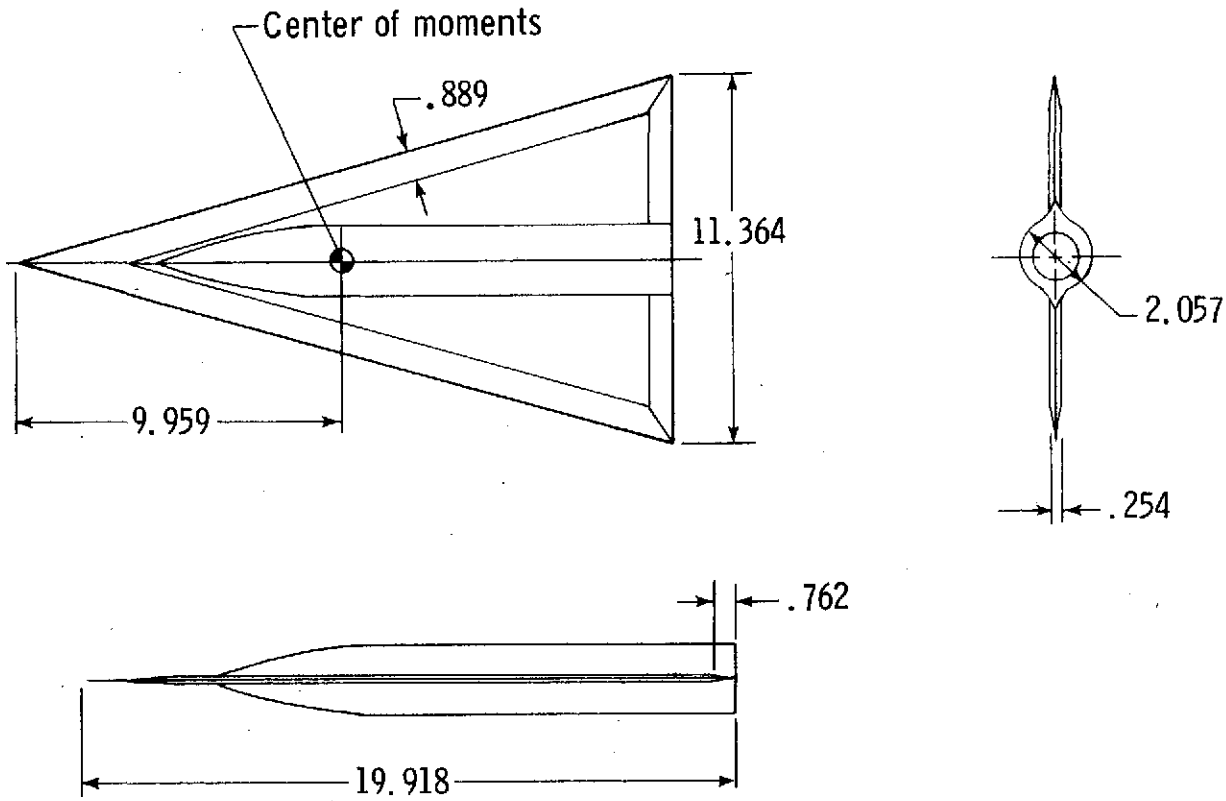

Figure 18.- 74° delta-wing model tested in low-speed cryogenic tunnel. Dimensions in centimeters.

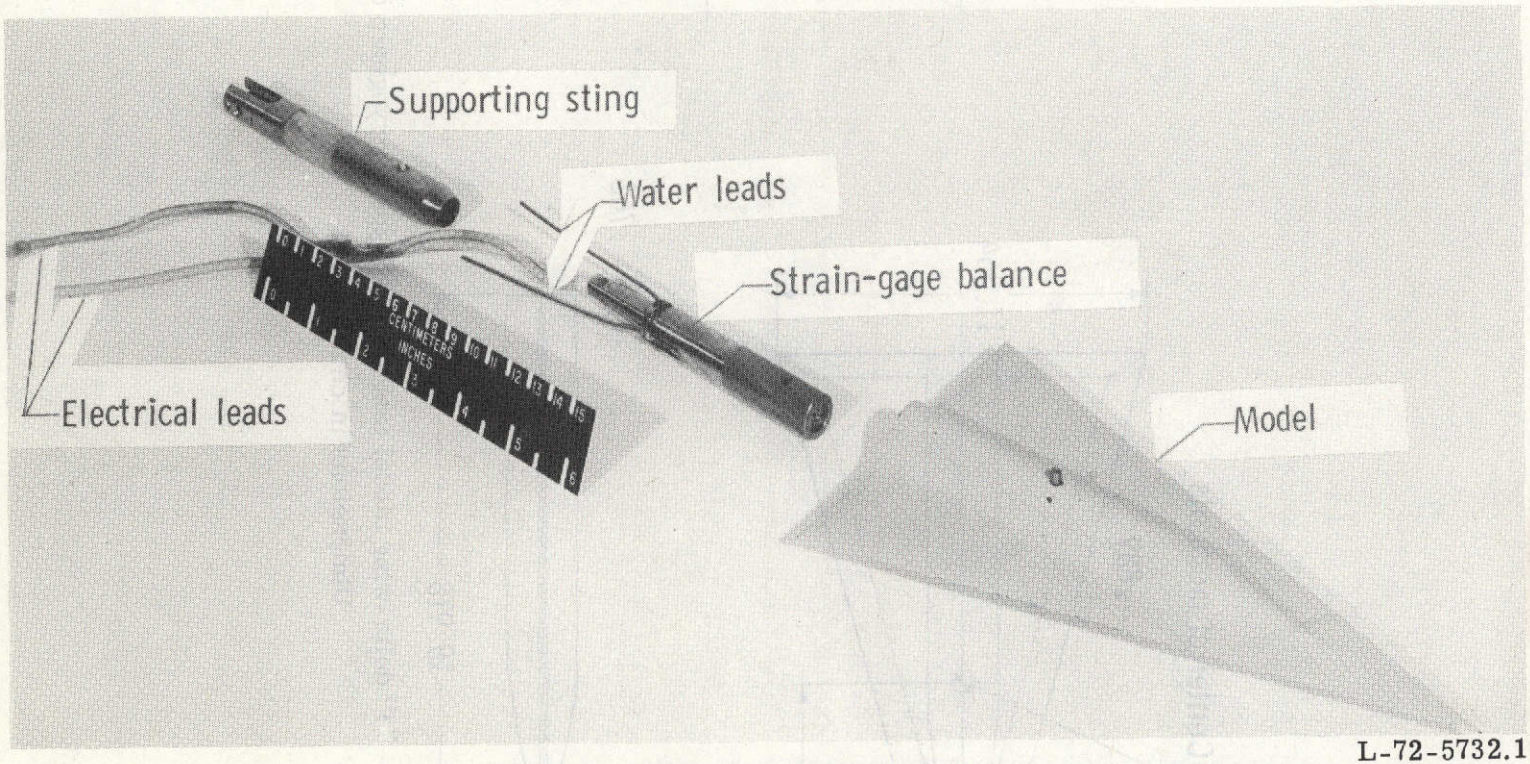

L-72-5732.1

Figure 19.- 74° delta-wing model, strain-gage balance, and supporting sting.

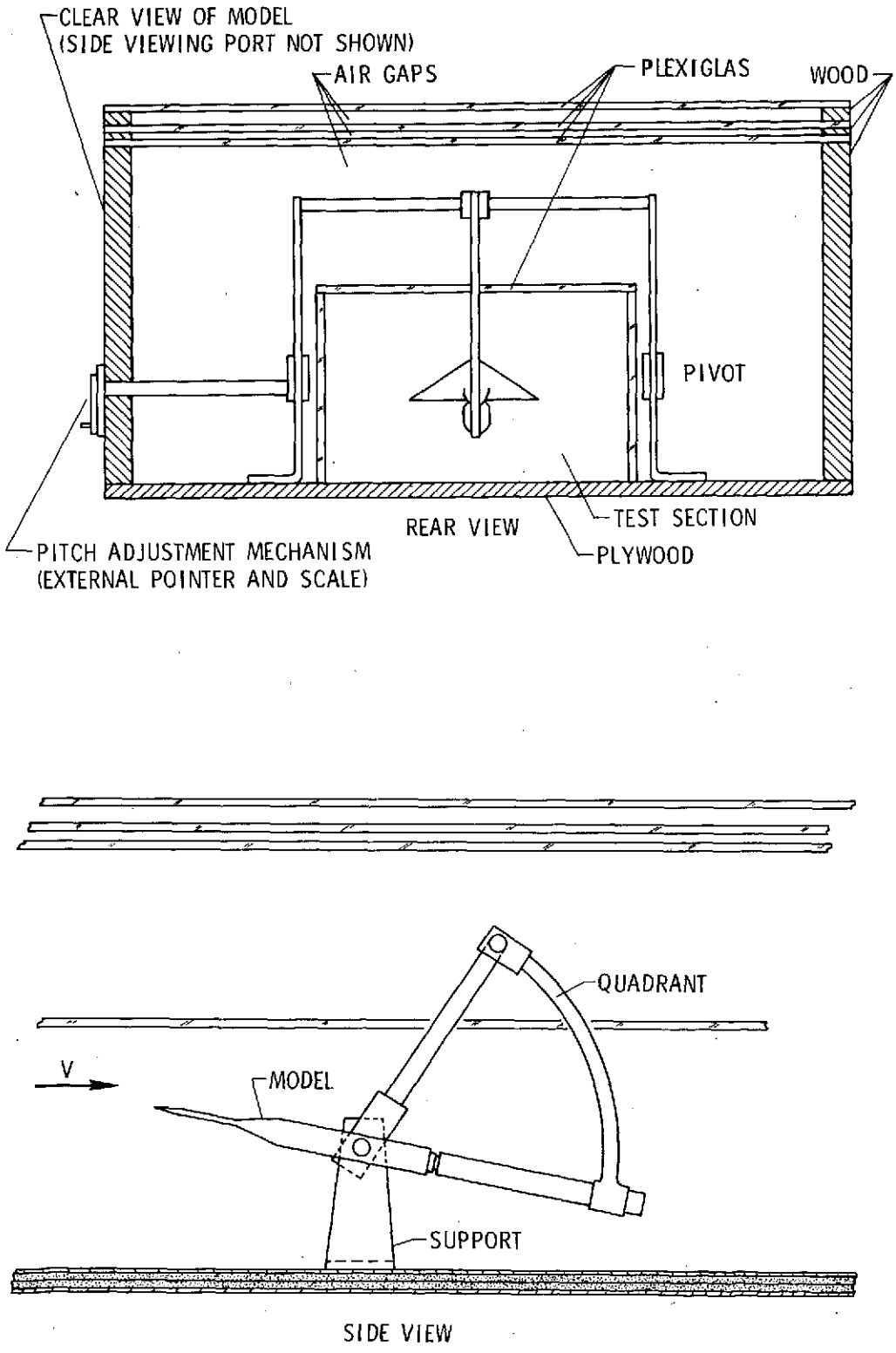

Figure 20.- Model support mechanism used in low-speed cryogenic tunnel.

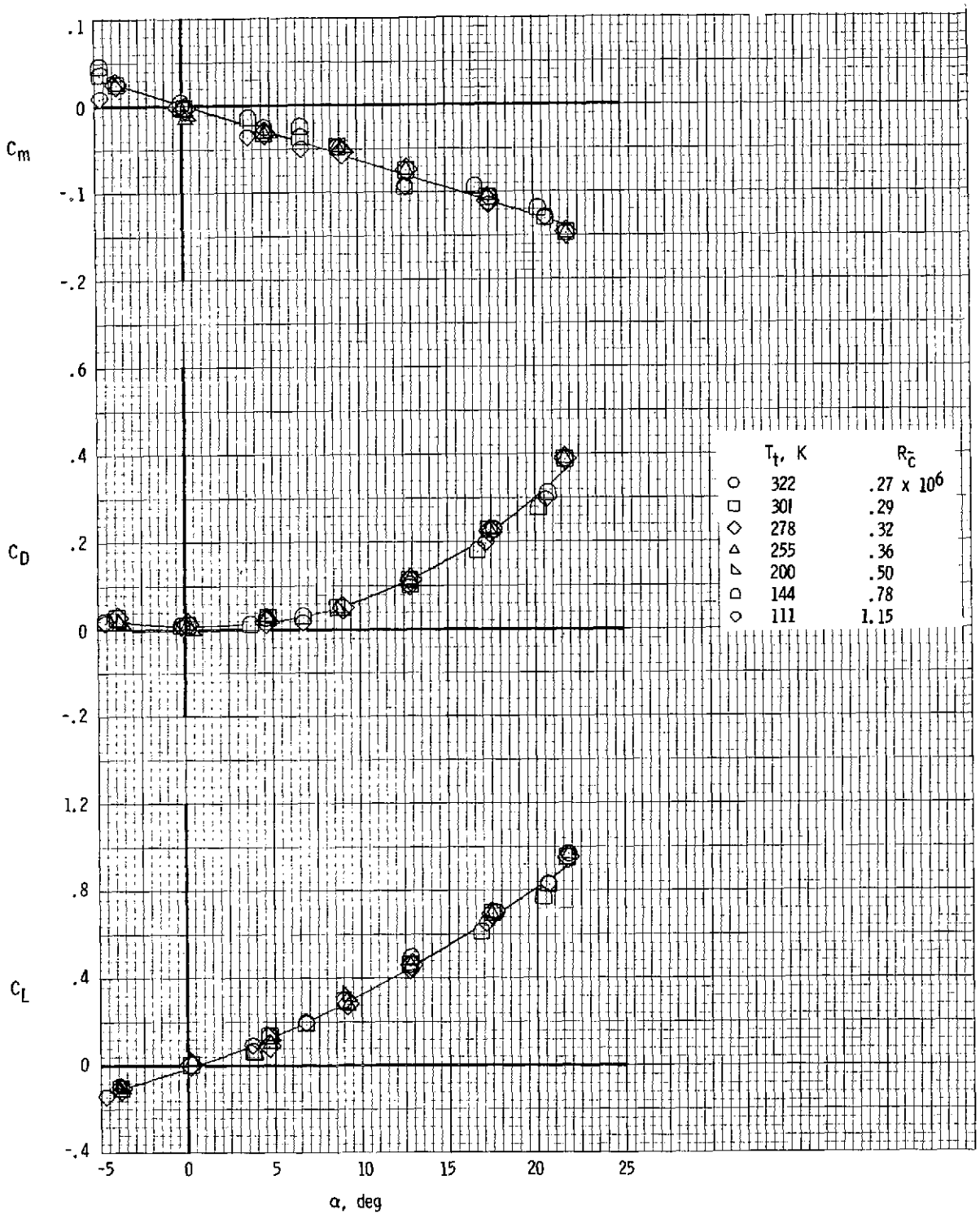

Figure 21.- Aerodynamic data obtained in low-speed cryogenic tunnel on sharp leading-edge 74° delta-wing model.

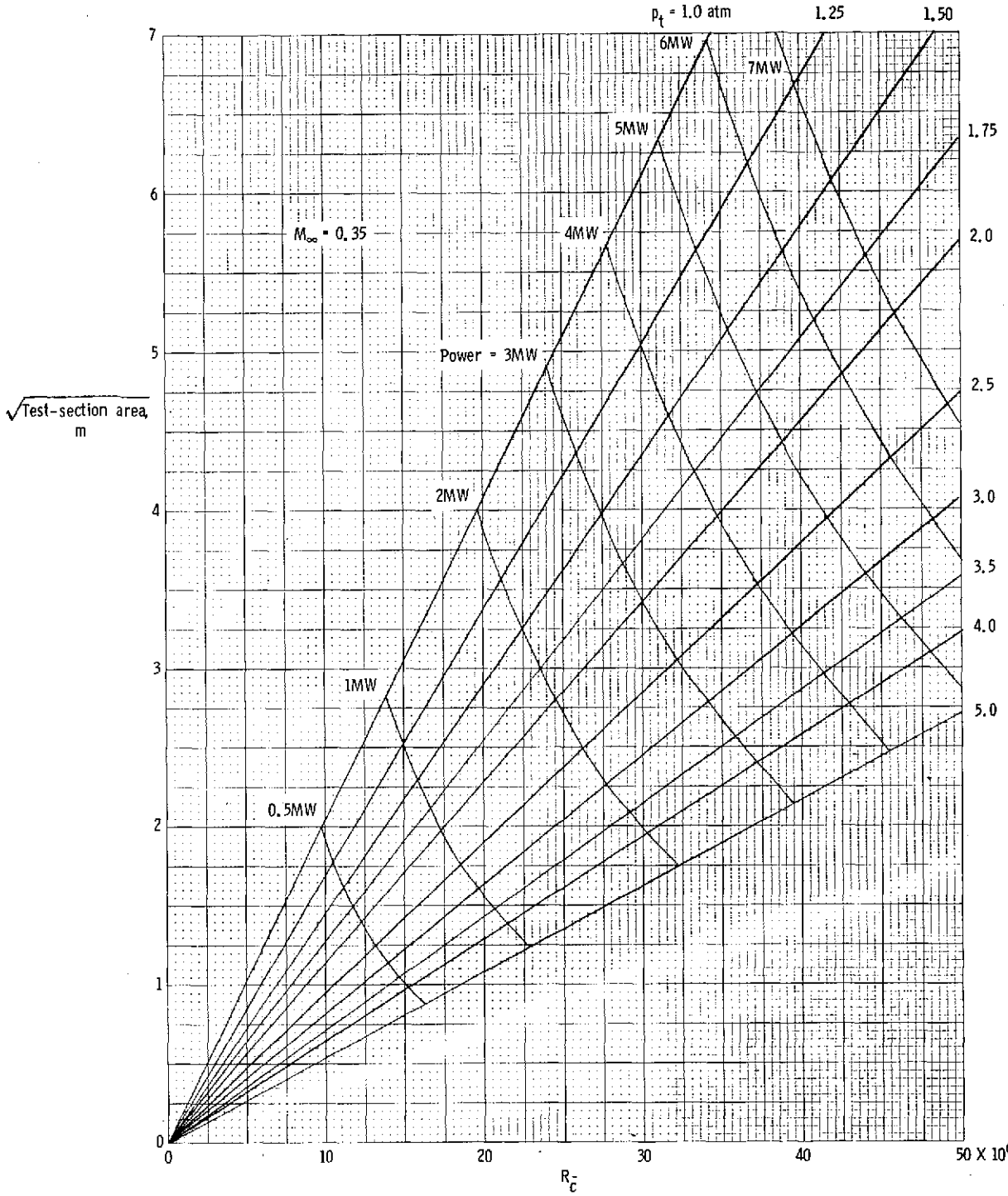

(a) $M_{L,max} = 0.35$.

Figure 22.- Performance chart for cryogenic nitrogen tunnel showing relationship between tunnel size, stagnation pressure, drive power, and Reynolds number for a free-stream Mach number of 0.35. $\bar{c} = 0.1\sqrt{\text{Test-section area}}$.

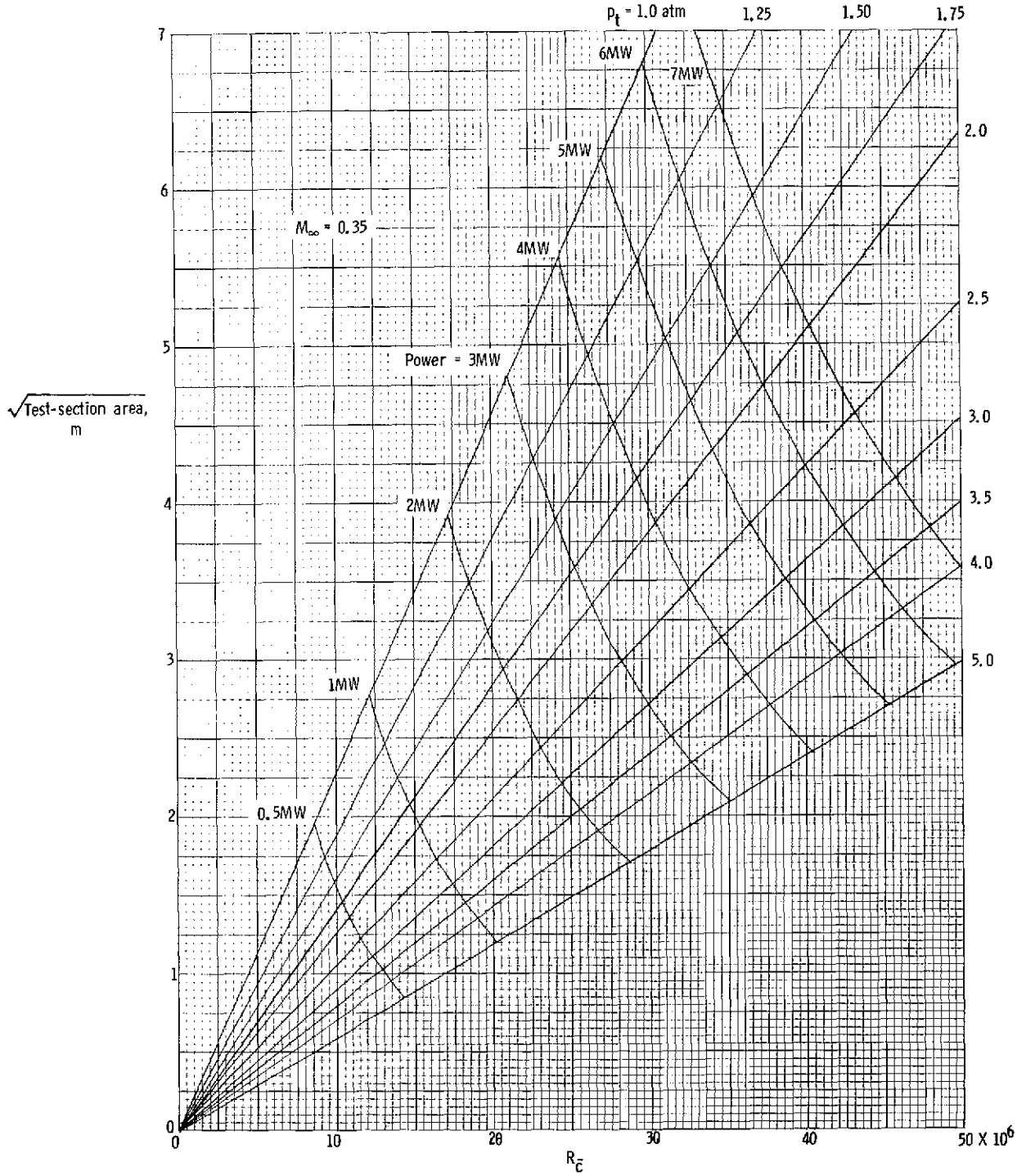

(b) $M_{L,max} = 0.88$.

Figure 22.- Continued.

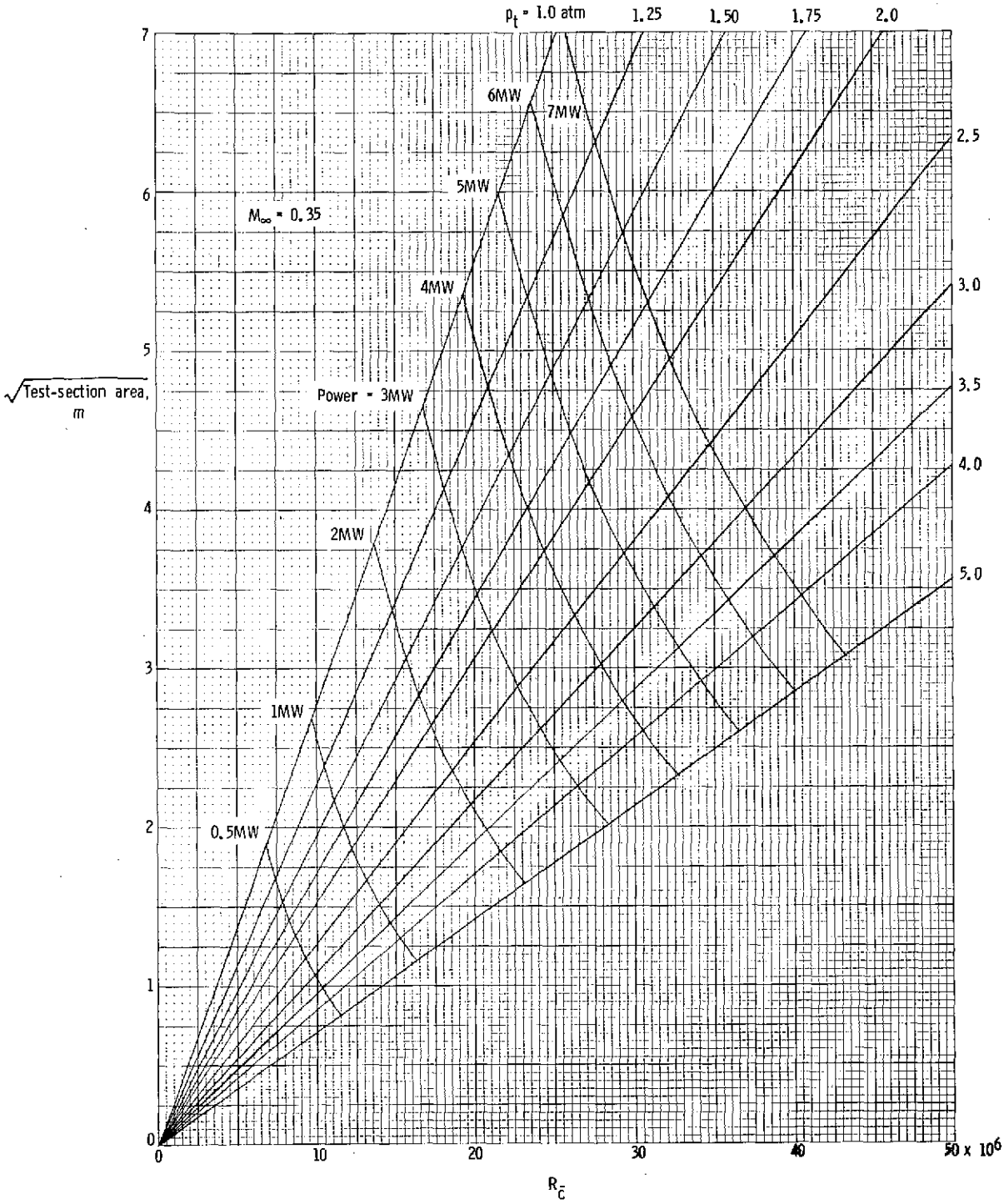

(c) $M_{L,max} = 1.42$.

Figure 22.- Concluded.

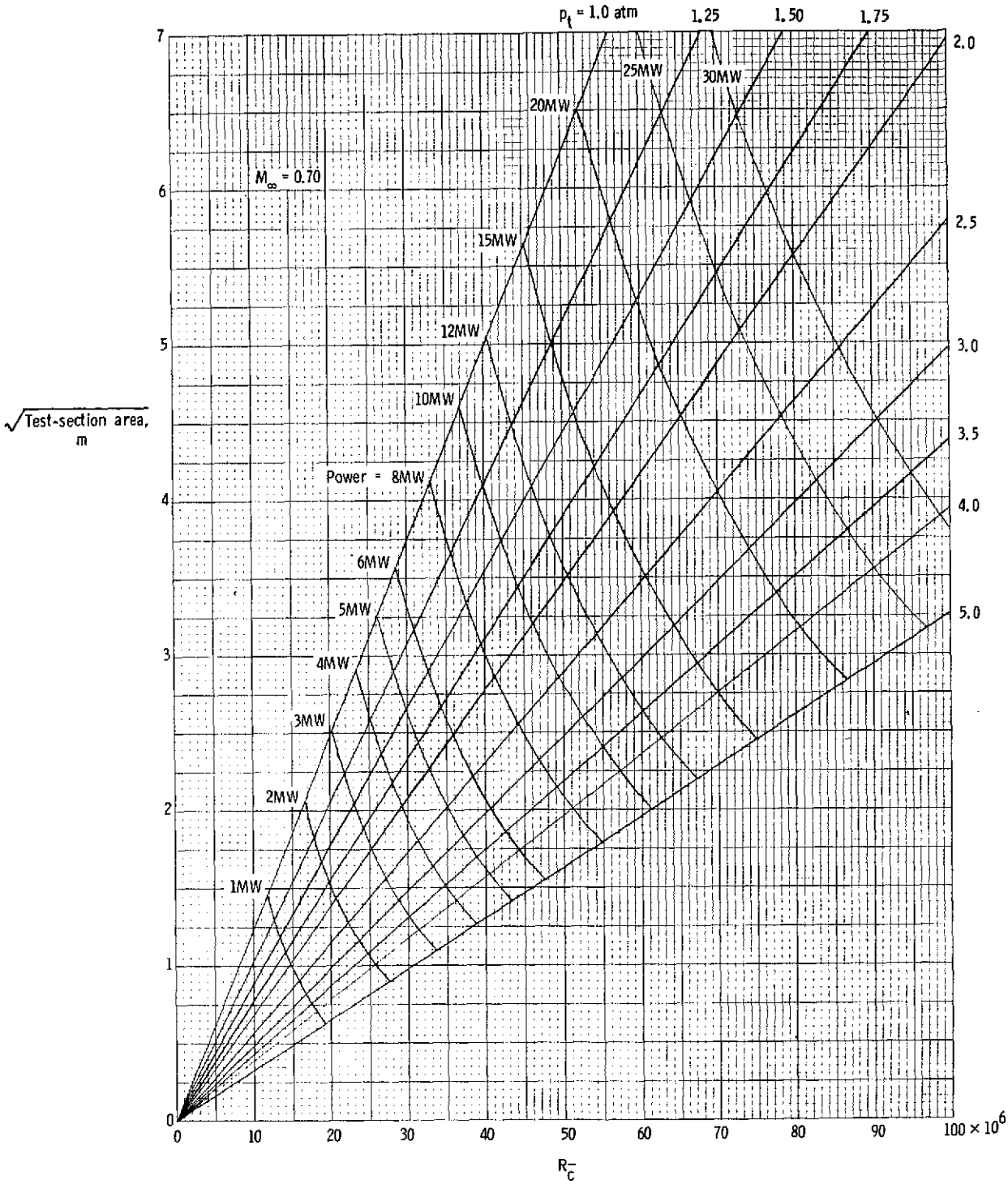

(a) $M_{L,max} = 0.70$.

Figure 23.- Performance chart for cryogenic nitrogen tunnel showing relationship between tunnel size, stagnation pressure, drive power, and Reynolds number for a free-stream Mach number of 0.70. $\bar{c} = 0.1\sqrt{\text{Test-section area}}$.

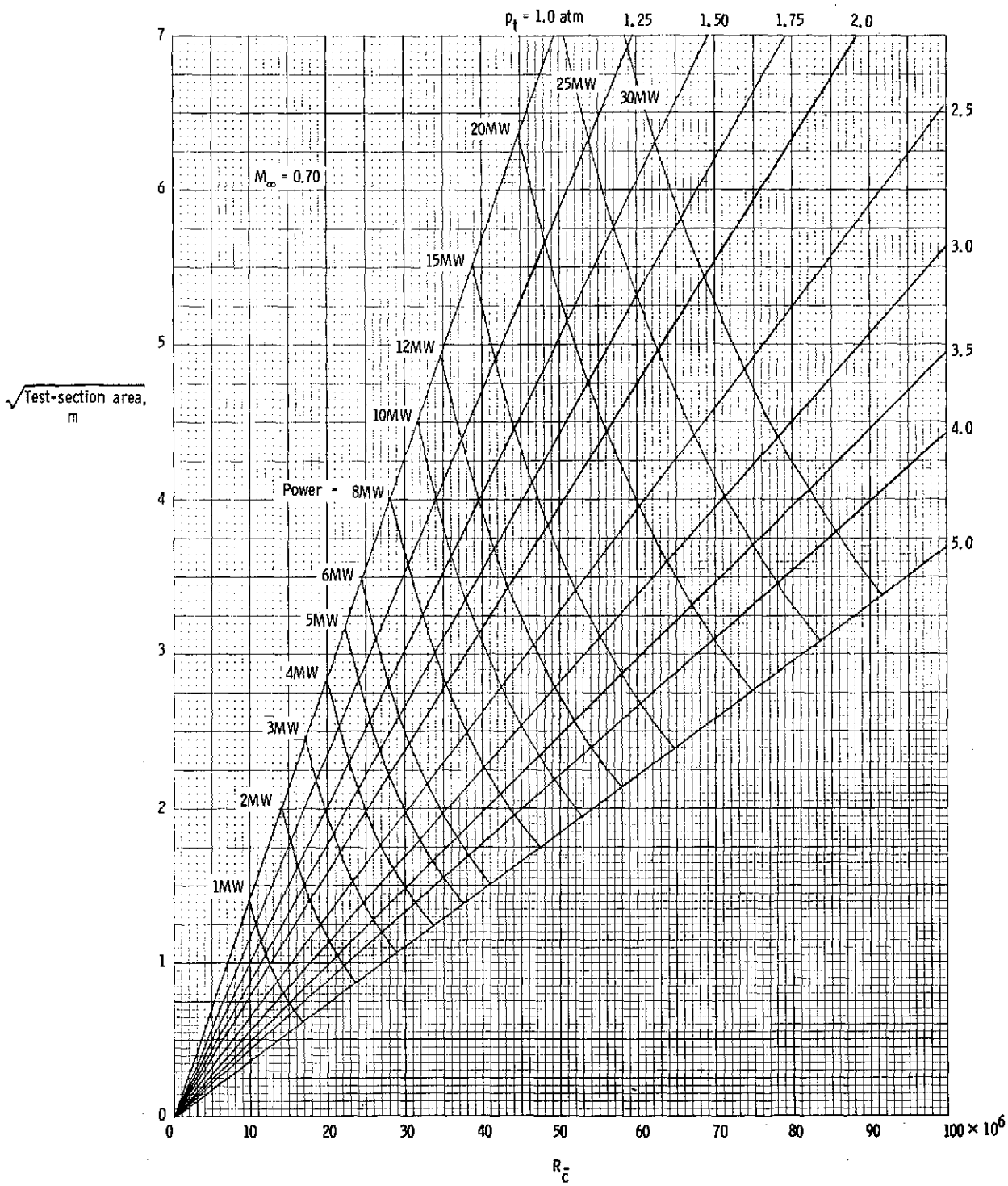

(b) $M_{L,max} = 1.14$.

Figure 23.- Continued.

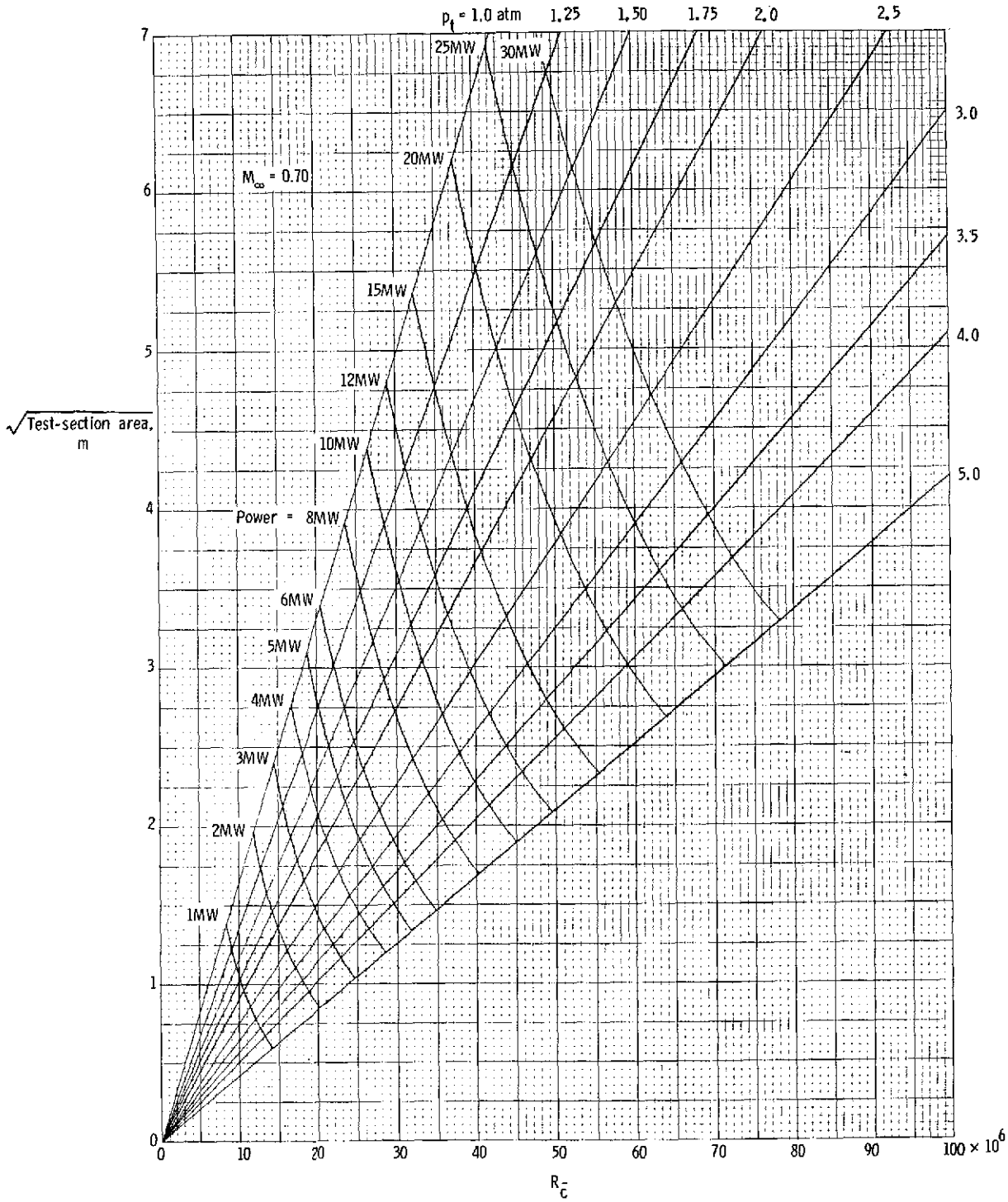

(c) $M_{L,max} = 1.52$.

Figure 23.- Concluded.

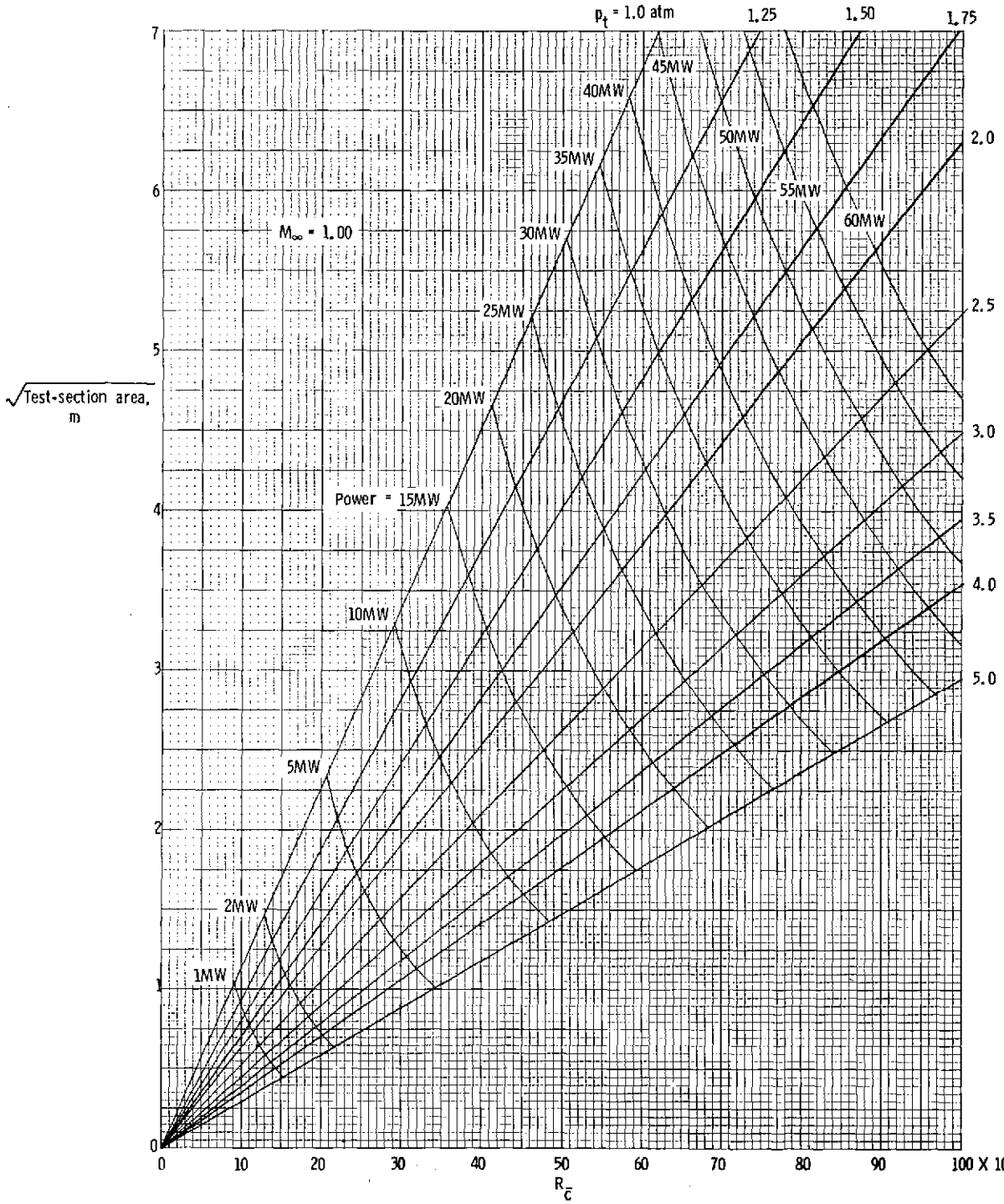

(a) $M_{L,max} = 1.00$.

Figure 24.- Performance chart for cryogenic nitrogen tunnel showing relationship between tunnel size, stagnation pressure, drive power, and Reynolds number for a free-stream Mach number of 1.00. $\bar{c} = 0.1\sqrt{\text{Test-section area}}$.

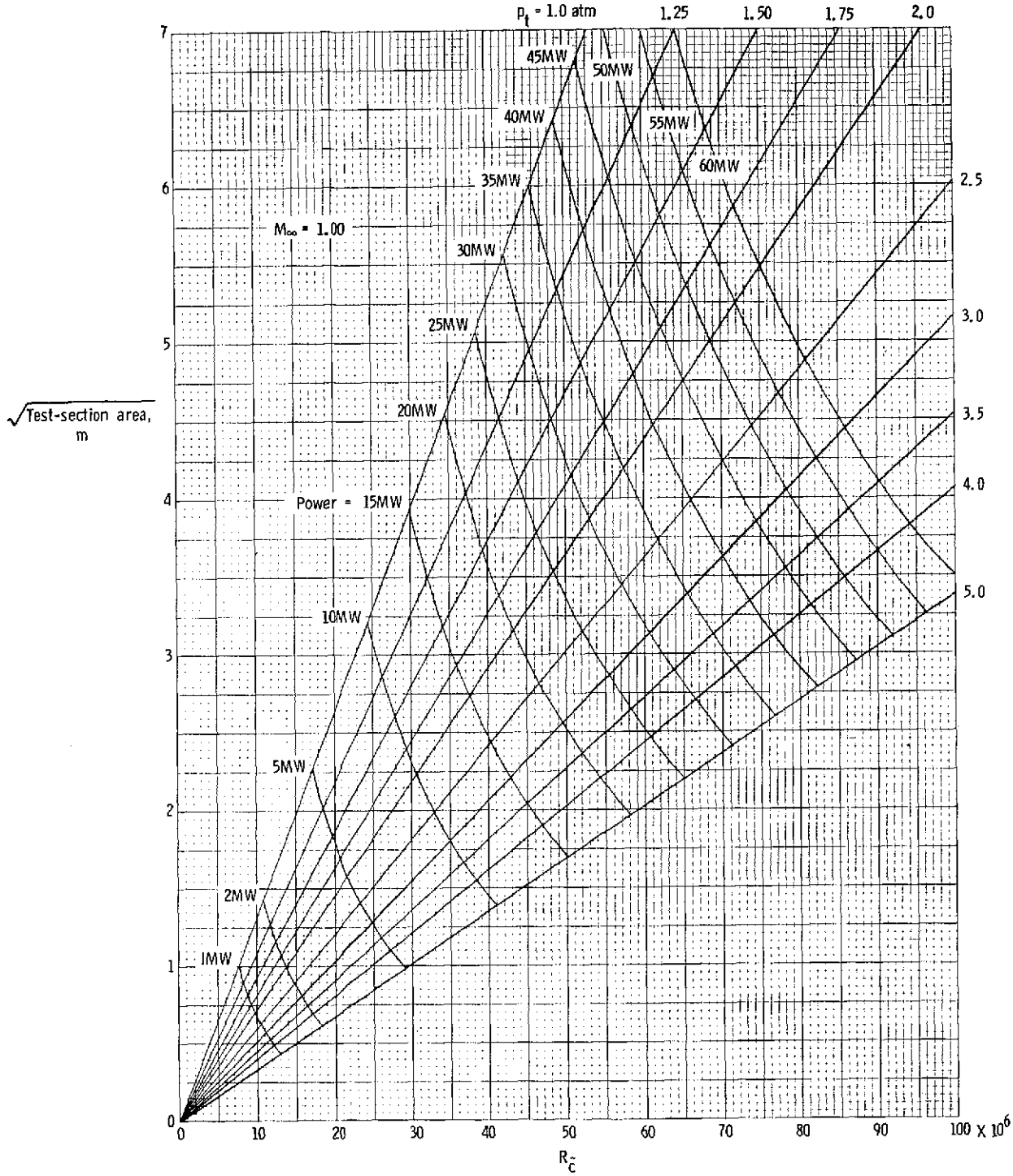

(b) $M_{L,max} = 1.40$.

Figure 24.- Continued.

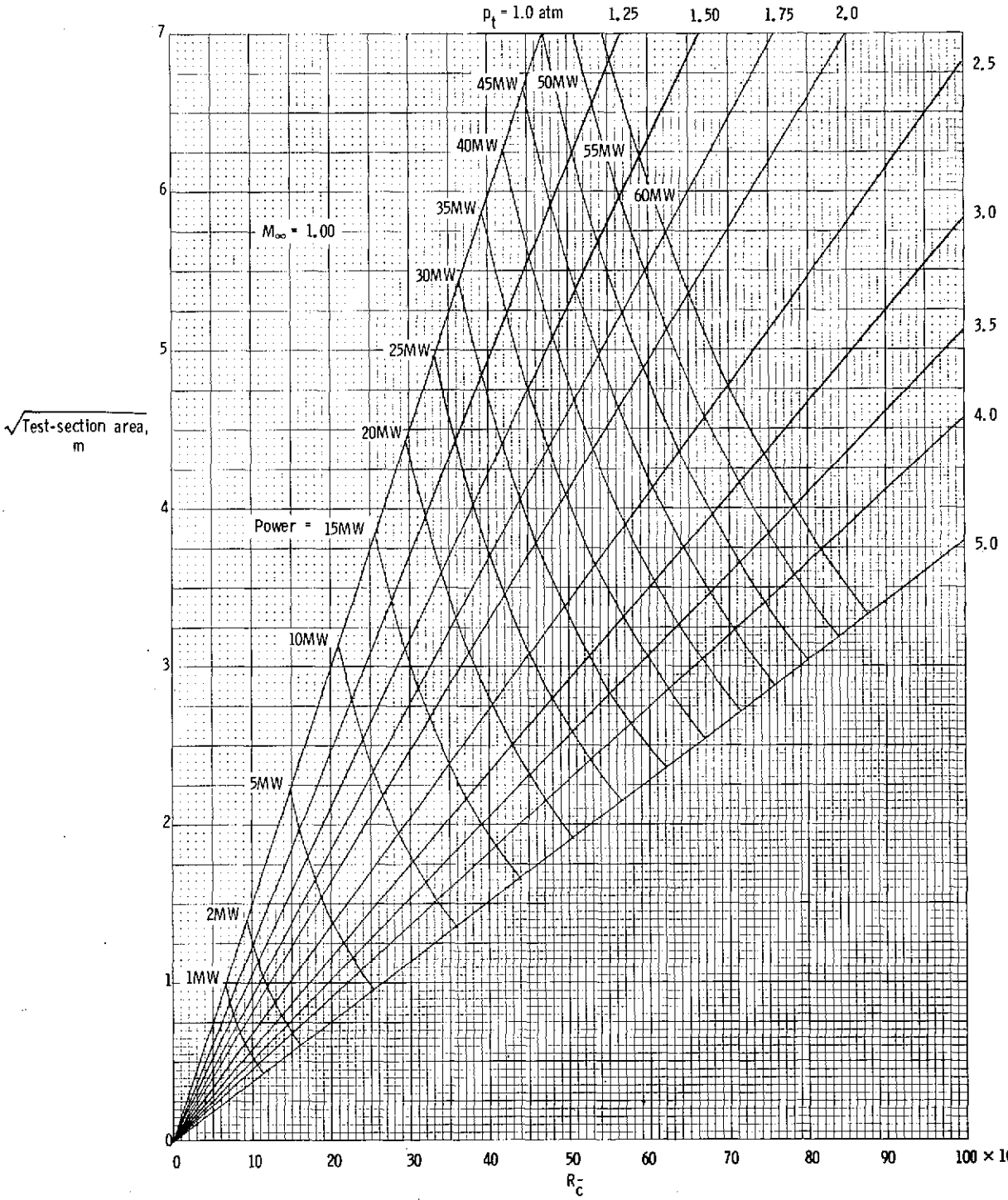

(c) $M_{L,max} = 1.70$.

Figure 24.- Concluded.

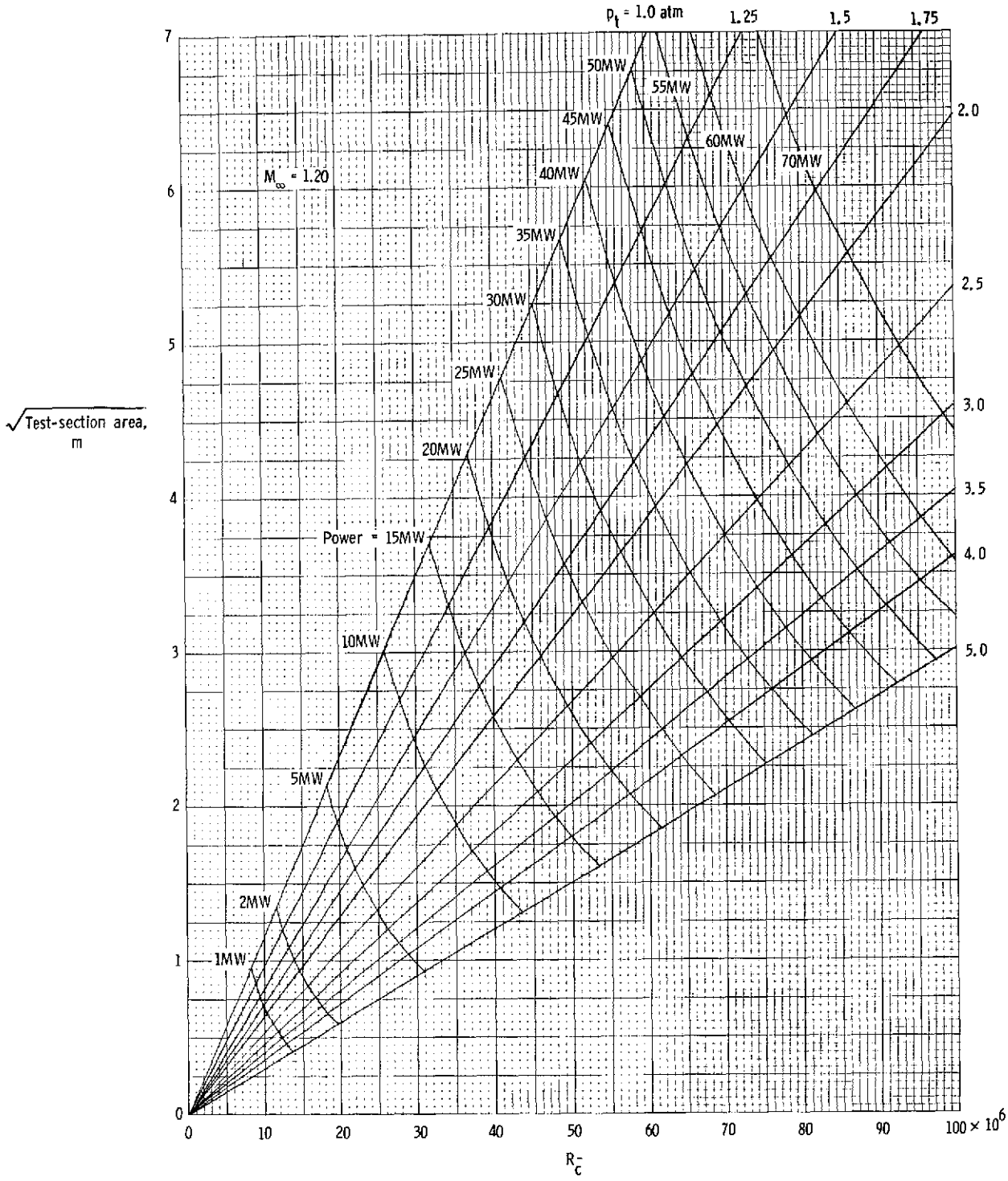

(a) $M_{L,max}$ = 1.20.

Figure 25.- Performance chart for cryogenic nitrogen tunnel showing relationship between tunnel size, stagnation pressure, drive power, and Reynolds number for a free-stream Mach number of 1.20. $\bar{c} = 0.1\sqrt{\text{Test-section area}}$.

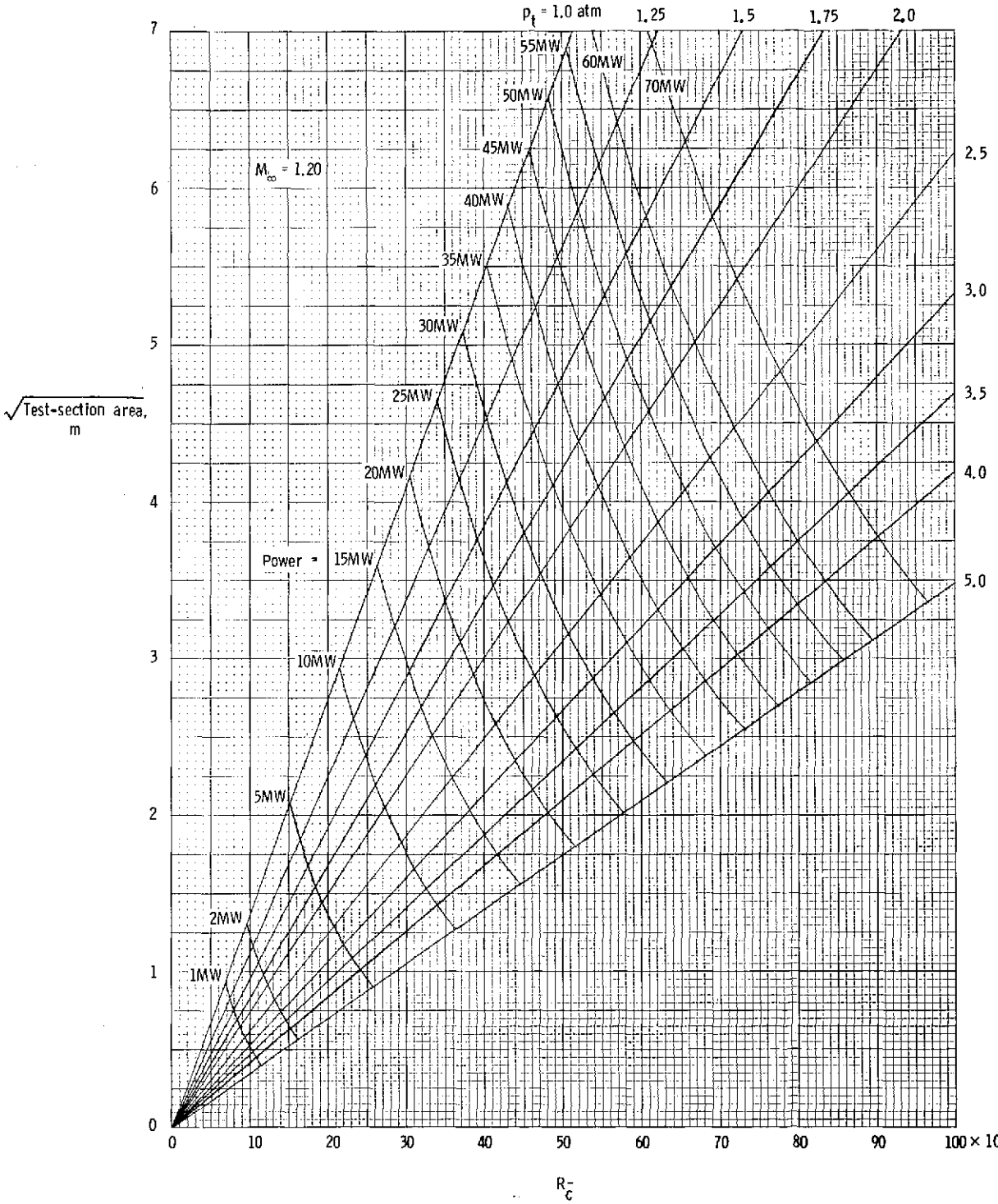

(b) $M_{L,max} = 1.59$.

Figure 25.- Continued.

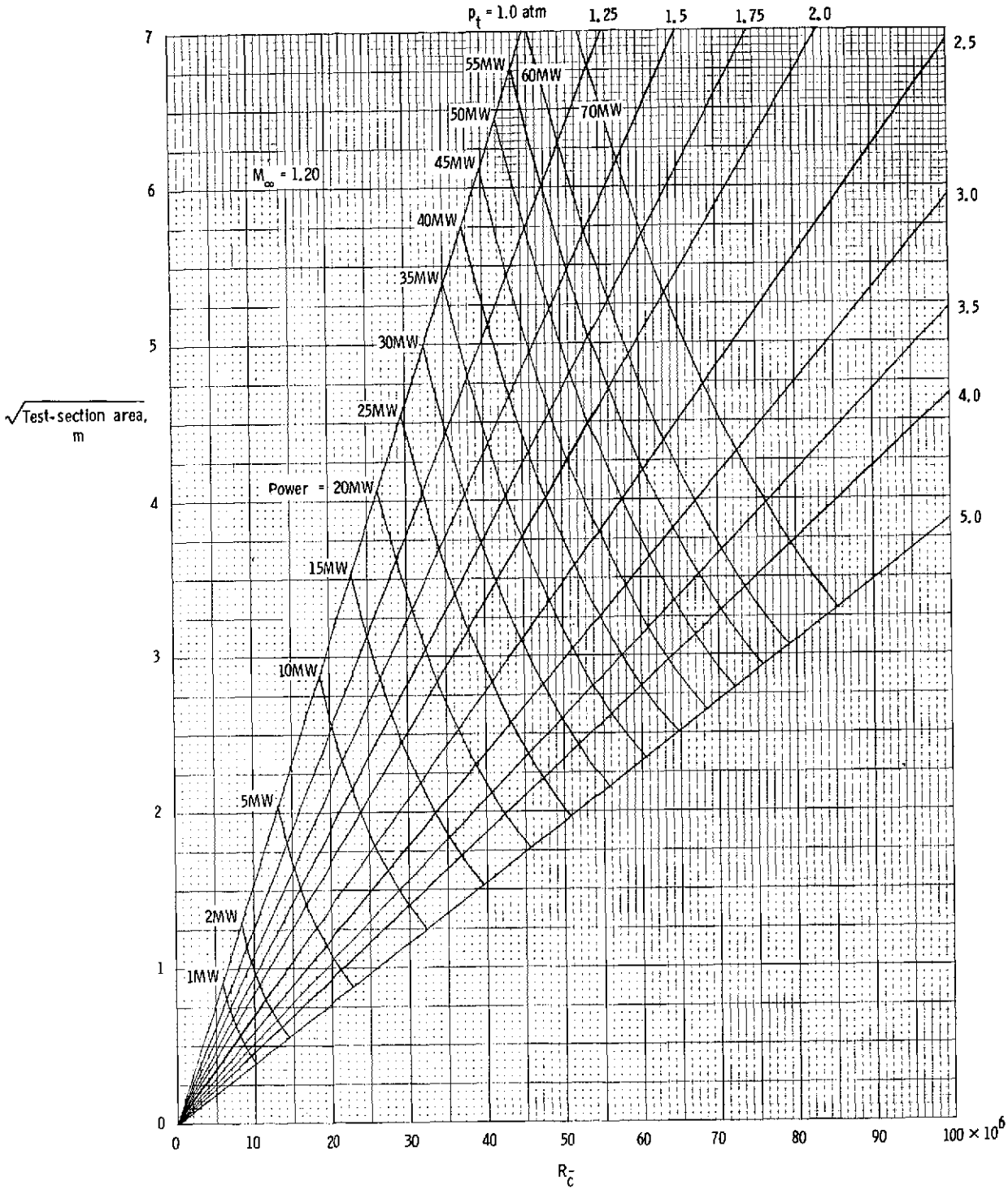

(c) $M_{L,max} = 1.85$.

Figure 25.- Concluded.

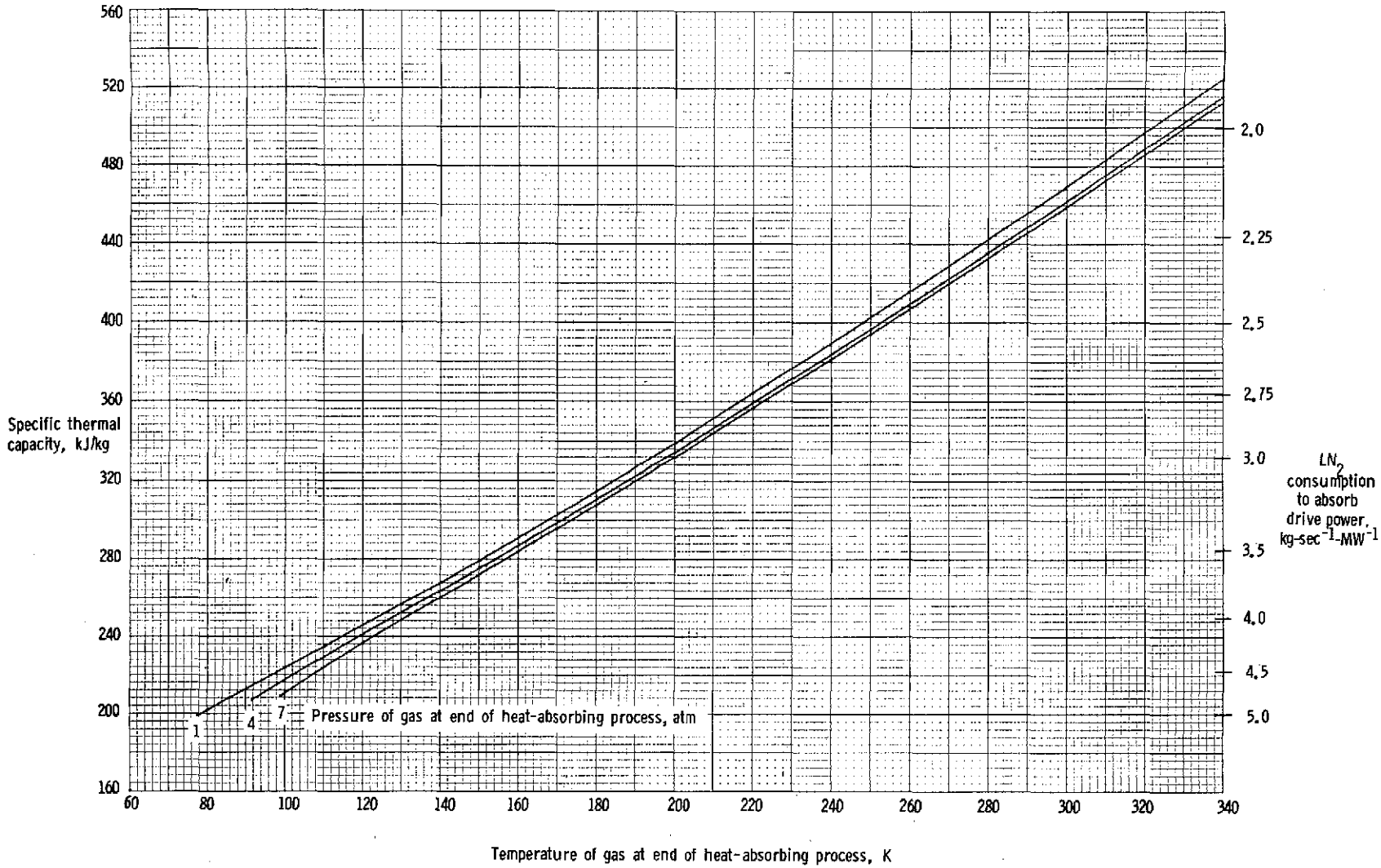

Figure 26.- Heat-absorbing capacity of liquid nitrogen. Liquid initially at a pressure of 1 atm and a temperature of 77.347 K.

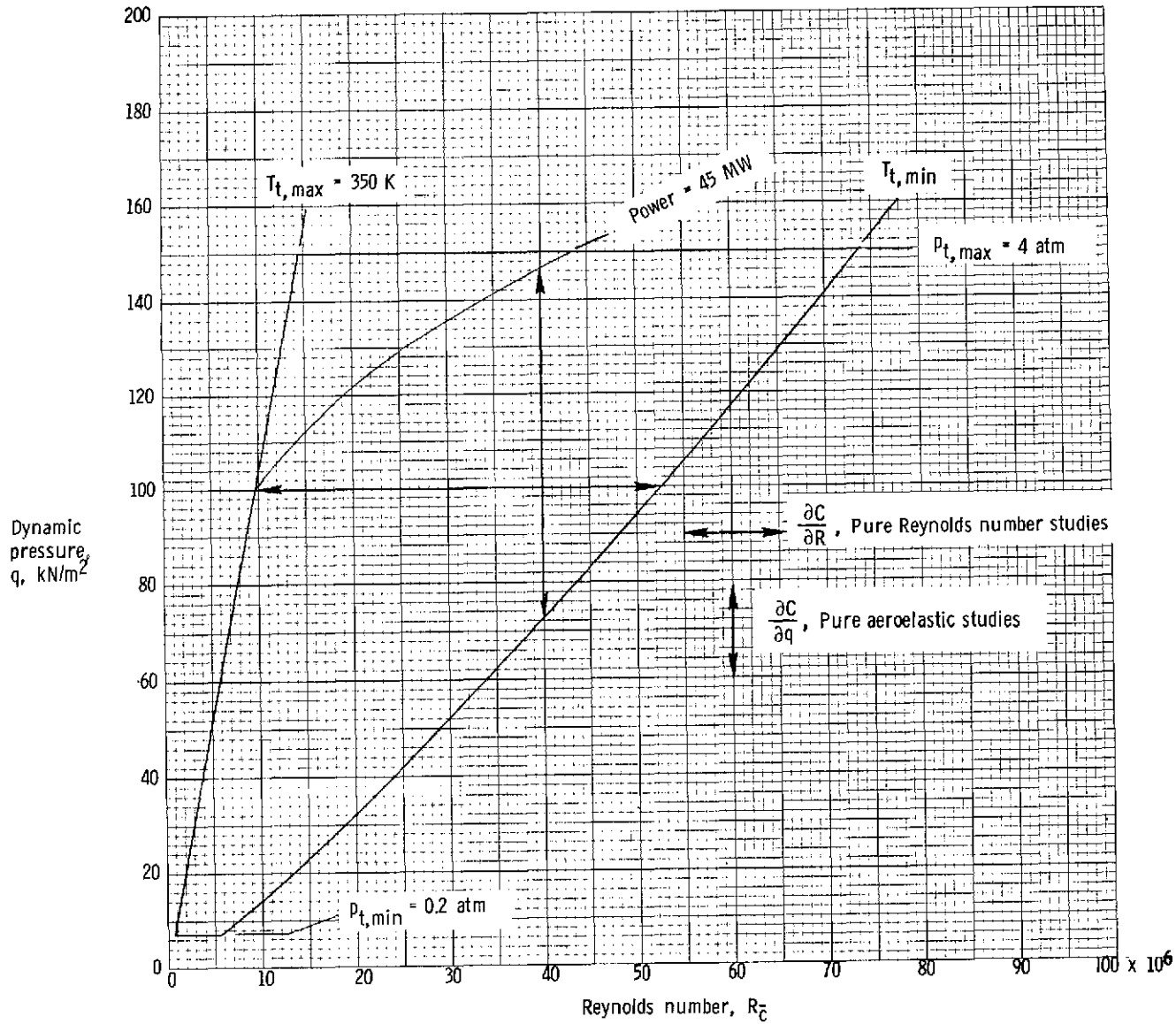

Figure 27.- Constant Mach number operating envelope for a cryogenic nitrogen tunnel having a 3- by 3-m test section. $M_\infty = 1.00$.

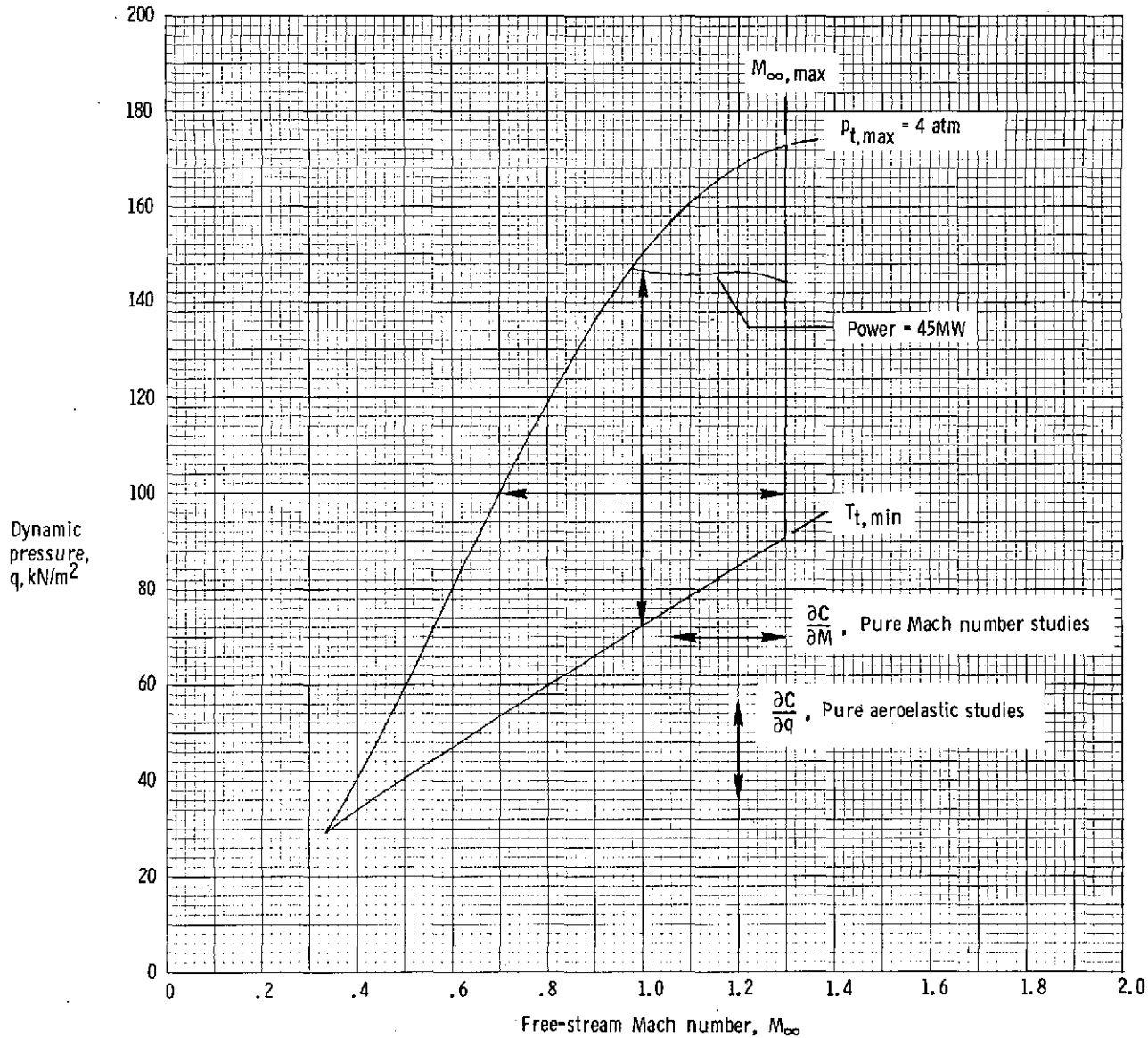

Figure 28.- Constant Reynolds number operating envelope for a cryogenic nitrogen tunnel having a 3- by 3-m test section. $R_{\bar{c}} = 40 \times 10^6$.

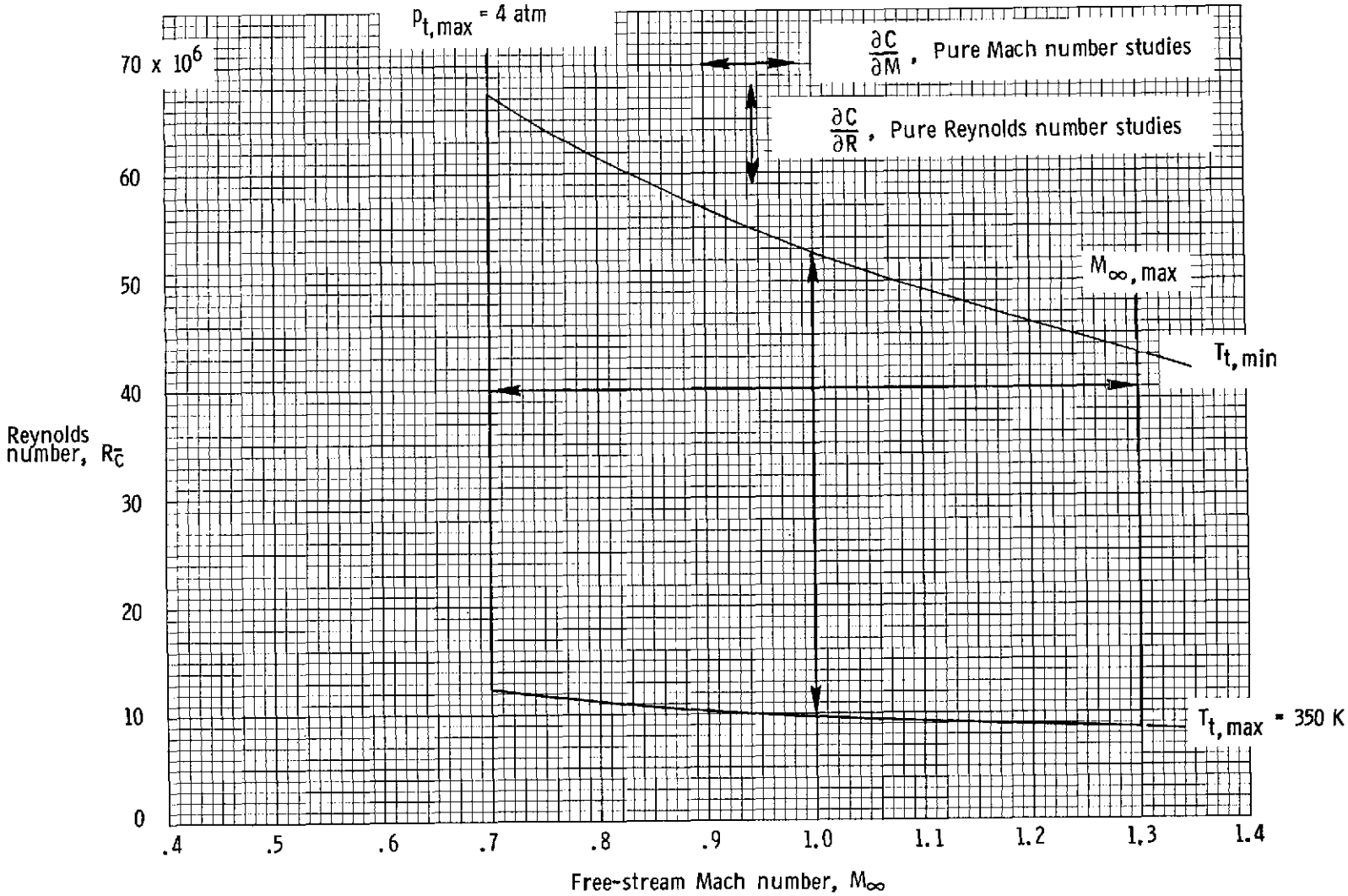

Figure 29.- Constant dynamic pressure operating envelope for a cryogenic nitrogen tunnel having a 3- by 3-m test section. q = 100 kN/m^2.

NASA-Langley, 1974